Electronic Supplementary Material (ESI) for Dalton Transactions.
This journal is © The Royal Society of Chemistry 2023

Iron(II) Complexes of 2,6-*Bis*(imidazo[1,2-a]pyridin-2-yl)pyridine and Related Ligands with Annelated Distal Heterocyclic Donors

Rafal Kulmaczewski and Malcolm A. Halcrow*,[a]

[a]*School of Chemistry, University of Leeds, Woodhouse Lane, Leeds LS2 9JT, United Kingdom.*
E-mail: m.a.halcrow@leeds.ac.uk

Supporting Information

		Page
Experimental details		S4
Scheme S1	Synthesis of the new ligands L^2 and L^3.	S4
Figure S1	^{1}H and ^{13}C NMR spectra of L^1.	S5
Figure S2	^{1}H NMR spectrum of L^2.	S6
Figure S3	^{1}H and ^{13}C NMR spectra of L^3.	S7
Figure S4	^{1}H and ^{13}C NMR spectra of L^4.	S8
Crystallographic procedures and refinement details		S9
Table S1	Experimental data for the crystal structure determinations.	S11
Definitions of the structural parameters discussed in the paper		S13
Scheme S2	Angles used in the definitions of the coordination distortion parameters Σ and Θ.	S13
Scheme S3	The parameters θ and ϕ, used to discuss the structures of **1**-**4**.	S13
Figure S5	The asymmetric unit of **1[BF$_4$]$_2$**·MeCN.	S14
Figure S6	The asymmetric unit of **1[BF$_4$]$_2$**·*m*MeNO$_2$.	S15
Figure S7	The asymmetric unit of **1[BF$_4$]$_{1.6}$[SiF$_6$]$_{0.2}$**·1.7MeNO$_2$·0.3Et$_2$O.	S16
Figure S8	The asymmetric unit of **1[BF$_4$]$_2$**·1.5MeOH.	S17
Table S2	Selected bond lengths and angles in the solvate crystals of **1[BF$_4$]$_2$**	S18
Figure S9	Packing diagram of **1[BF$_4$]$_2$**·MeCN.	S19
Figure S10	Space-filling plot of the intermolecular C–H$\cdots\pi$ contact which is proposed to inhibit SCO in solvates of **1[BF$_4$]$_2$**.	S20
Figure S11	A "terpyridine embrace" layer in the lattice of **1[BF$_4$]$_{1.6}$[SiF$_6$]$_{0.2}$**·1.7MeNO$_2$·-0.3Et$_2$O.	S21
Table S3	Intermolecular interactions in the crystal structure of **1[BF$_4$]$_{1.6}$[SiF$_6$]$_{0.2}$**·1.7MeNO$_2$·-0.3Et$_2$O.	S22
Figure S12	Packing diagram of **1[BF$_4$]$_{1.6}$[SiF$_6$]$_{0.2}$**·1.7MeNO$_2$·0.3Et$_2$O.	S23
Figure S13	Alternative packing diagram of **1[BF$_4$]$_{1.6}$[SiF$_6$]$_{0.2}$**·1.7MeNO$_2$·0.3Et$_2$O.	S24
Figure S14	Packing diagram of **1[BF$_4$]$_2$**·1.5MeOH.	S25
Figure S15	X-ray powder diffraction data from the solvate materials of **1[BF$_4$]$_2$**.	S26
Figure S16	Magnetic susceptibility data from the solvate materials of **1[BF$_4$]$_2$**.	S27
Figure S17	The asymmetric unit of **2[BF$_4$]$_2$**·1.5MeCN.	S28
Figure S18	The asymmetric unit of **2[BF$_4$]$_2$**·Me$_2$CO.	S29
Figure S19	The asymmetric unit of **2[BF$_4$]$_2$**·3.5MeNO$_2$·0.5Et$_2$O.	S30
Table S4	Selected bond lengths and angles in the solvate crystals of **2[BF$_4$]$_2$**	S31
Figure S20	Intermolecular contacts in the lattice of **2[BF$_4$]$_2$**·1.5MeCN.	S32
Figure S21	Intermolecular contacts in the lattice of **2[BF$_4$]$_2$**·3.5MeNO$_2$·0.5Et$_2$O.	S33
Table S5	Intermolecular interactions in the solvate crystals of **2[BF$_4$]$_2$**.	S34
Figure S22	Packing diagram of **2[BF$_4$]$_2$**·1.5MeCN.	S35
Figure S23	Packing diagram of **2[BF$_4$]$_2$**·3.5MeNO$_2$·0.5Et$_2$O.	S36
Figure S24	X-ray powder diffraction data from the solvate materials of **2[BF$_4$]$_2$**.	S37
		Page

Figure S25 Magnetic susceptibility data from the solvate materials of **2[BF$_4$]$_2$**. S38
Figure S26 The asymmetric unit of [FeBr(py)$_2$(L^3)]Br·0.5H$_2$O. S39
Table S6 Selected bond lengths and angles in [FeBr(py)$_2$(L^3)]Br·0.5H$_2$O. S40
Figure S27 Packing diagram of [FeBr(py)$_2$(L^3)]Br·0.5H$_2$O. S40
Figure S28 Molecule D in the refinement of **4[BF$_4$]$_2$**·1.39MeCN·0.125Et$_2$O·0.25H$_2$O. S41
Figure S29 The asymmetric unit of **4[BF$_4$]$_2$**·1.39MeCN·0.125Et$_2$O·0.25H$_2$O. S42
Table S7 Selected bond lengths and angles in **4[BF$_4$]$_2$**·1.39MeCN·0.125Et$_2$O·0.25H$_2$O. S43
Figure S30 The four unique complex molecules in **4[BF$_4$]$_2$**·1.39MeCN·0.125Et$_2$O·0.25H$_2$O. S44
Figure S31 Space-filling views of the molecules in **4[BF$_4$]$_2$**·1.39MeCN·0.125Et$_2$O·0.25H$_2$O. S45
Figure S32 Alternative space-filling views of the molecules in **4[BF$_4$]$_2$**·1.39MeCN·0.125Et$_2$O·-0.25H$_2$O. S46
Table S8 Intramolecular contacts in **4[BF$_4$]$_2$**·1.39MeCN·0.125Et$_2$O·0.25H$_2$O. S47
Figure S33 Packing diagram of **4[BF$_4$]$_2$**·1.39MeCN·0.125Et$_2$O·0.25H$_2$O. S48
Figure S34 Alternative packing diagram of **4[BF$_4$]$_2$**·1.39MeCN·0.125Et$_2$O·0.25H$_2$O. S49
Figure S35 A helical cation stack in the lattice of **4[BF$_4$]$_2$**·1.39MeCN·0.125Et$_2$O·0.25H$_2$O. S50
Table S9 Intermolecular contacts in **4[BF$_4$]$_2$**·1.39MeCN·0.125Et$_2$O·0.25H$_2$O. S51
Figure S36 Variable temperature magnetic susceptibility data for **4[BF$_4$]$_2$**. S51
Figure S37 ^{1}H NMR spectra of **1[BF$_4$]$_2$** and **2[BF$_4$]$_2$**. S52
Figure S38 ^{1}H NMR spectrum of a mixture of Fe[BF$_4$]$_2$·6H$_2$O and 2 equiv *L*^{3} in CD$_3$CN. S53
Figure S39 ^{1}H NMR spectrum of **4[BF$_4$]$_2$**. S54
Table S10 UV-vis absorption and emission spectrum data for the compounds in this work. S54
Figure S40 Energy-minimised structures for the organic ligands. S55
Figure S41 Frontier orbital plots for L^1. S56
Figure S42 Frontier orbital energies for the *bis*(azolyl)pyridine ligands computed in this work. S57
Table S11 Computed energies of the organic ligands, and their N-donor lone pair MOs. S58
Discussion of the free ligand DFT calculations. S58
Figure S43 Energy-minimised structures of [FeL$_2$]$^{2+}$ (L = *L*^{1}-*L*^{4}). S59
Table S12 Computed metric parameters for the complexes in this work. S61
Figure S43 Frontier orbital plots for **1**$^{2+}$. S63
Figure S45 Frontier molecular orbital energies of low-spin complexes in this work. S64
Figure S46 Comparison of the MO energies of **1**$^{2+}$, [Fe(bimpy)$_2$]$^{2+}$ and [Fe(2-bip)$_2$]$^{2+}$. S65
Discussion of the frontier orbitals in the complexes (Figures S45 and S46) S66
Figure S47 Comparison of the computed and experimental high-spin geometries of [Fe(*L*^{4})$_2$]$^{2+}$. S66
Figure S48 Energy-minimised structures of the distorted coordination geometries of high-spin **1**$^{2+}$ and **2**$^{2+}$. S67
Table S13 Computed metric parameters for the distorted coordination geometries of **1**$^{2+}$ and **2**$^{2+}$. S68
Table S14 Atomic coordinates for the DFT-minimised molecules. S69
References S100

Experimental

2,6-*Bis*(imidazo[1,2-a]pyrimidin-2-yl)pyridine (L^1)[1] and 2,6-di(quinolin-2-yl)pyridine (L^4)[2] were synthesised by the literature procedures. α,α'-Dibromo-2,6-diacetylpyridine was freshly prepared from 2,6-diacetyl-pyridine as described in ref. 1, and used immediately to make L^2 and L^3. Other reagents were purchased commercially and used as supplied.

Synthetic protocols and characterisation data for the iron complexes are given in the Experimental section of the main article.

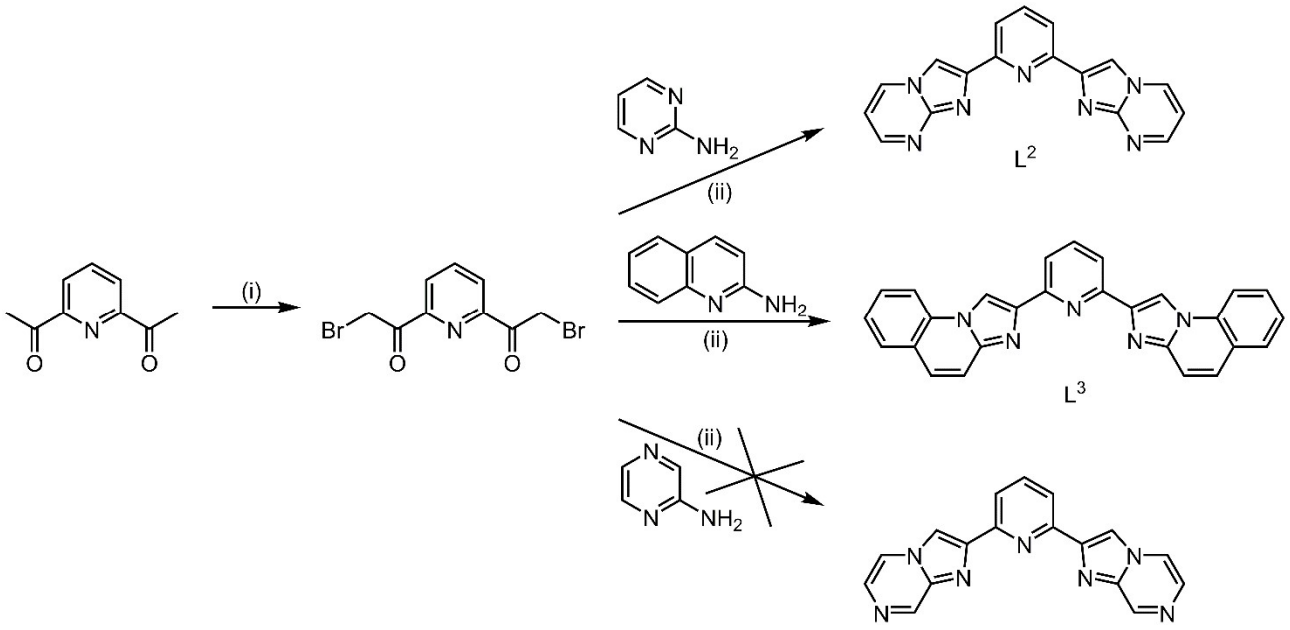

Scheme S1 Synthesis of the new ligands L^2 and L^3. The bottom reaction using aminopyrazine was also attempted, but the product was too insoluble for NMR or ES-MS characterisation or for use in complexation reactions. Reagents and conditions: (i) *N*-bromosuccinimide, *p*-toluenesulfonic acid monohydrate, acetonitrile, reflux, 16 hrs.[1] (ii) $NaHCO_3$, acetonitrile, reflux, 16 hrs.

Synthesis of 2,6-*bis*(imidazo[1,2-a]pyrimidin-2-yl)pyridine (L^2). A mixture of 2-aminopyrimidine (0.16 g, 1.6 mmol), α,α'-dibromo-2,6-diacetylpyridine (0.25 g, 0.78 mmol) and $NaHCO_3$ (0.20 g, 2.4 mol) in MeCN (5 cm^3) was heated under reflux for 16 hrs. The resultant orange-brown precipitate was cooled, then collected by filtration and washed with MeCN and water. The product is very sparingly soluble, and was analysed without further purification. Yield 0.17 g, 68 %. ES-MS *m*/*z* 157.5610 (calcd $[H_2(L^2)]^{2+}$ 157.5611), 314.1150 (calcd $[H(L^2)]^+$ 314.1149), 336.0968 (calcd $[Na(L^2)]^+$ 336.0968). ^{1}H NMR ($\{CD_3\}_2SO$) δ 7.13 (dd, 4.1 and 6.7 Hz, 2H), 8.05 (roofed m, 1H), 8.13 (roofed d, 7.1 Hz, 2H), 8.58 (s, 2H), 8.61 (dd, 2.0 and 4.1 Hz, 2H), 9.07 (dd, 2.0 and 6.7 Hz, 2H). L^2 was too insoluble to afford a ^{13}C NMR spectrum.

Synthesis of 2,6-*bis*(imidazo[1,2-a]quinolin-2-yl)pyridine (L^3). Method as for L^2, using 2-aminoquinoline (0.24 g, 1.6 mmol). The product was a sparingly soluble brown solid. Yield 0.25 g, 78 %. ES-MS *m*/*z* 206.5874 (calcd $[H_2(L^3)]^{2+}$ 206.5815), 412.1664 (calcd $[H(L^3)]^+$ 412.1557), 845.3067 (calcd $[Na(L^3)_2]^+$ 845.2866). ^{1}H NMR ($\{CD_3\}_2SO$) δ 7.62 (pseudo-t, 7.5 Hz, 2H), 7.67 (d, 9.4 Hz, 2H), 7.80 (d, 9.4 Hz, 2H), 7.83 (pseudo-t, 7.4 Hz, 2H), 7.98-8.06 (m, 5H), 8.55 (d, 8.4 Hz, 2H), 9.42 (s, 2H). ^{13}C NMR ($\{CD_3\}_2SO$) δ 111.9, 116.5, 117.4, 118.5, 123.5, 125.7, 127.2, 129.8 (2C), 132.9, 138.4, 143.9, 144.8, 152.8.

Attempted synthesis of 2,6-*bis*(imidazo[1,2-a]pyrazin-2-yl)pyridine. Method as for L^2, using aminopyrazine (0.16 g, 1.6 mmol). The reaction gave 0.10 g of brown precipitate (putative yield 41 %), which was too insoluble for NMR or ES-MS characterisation.

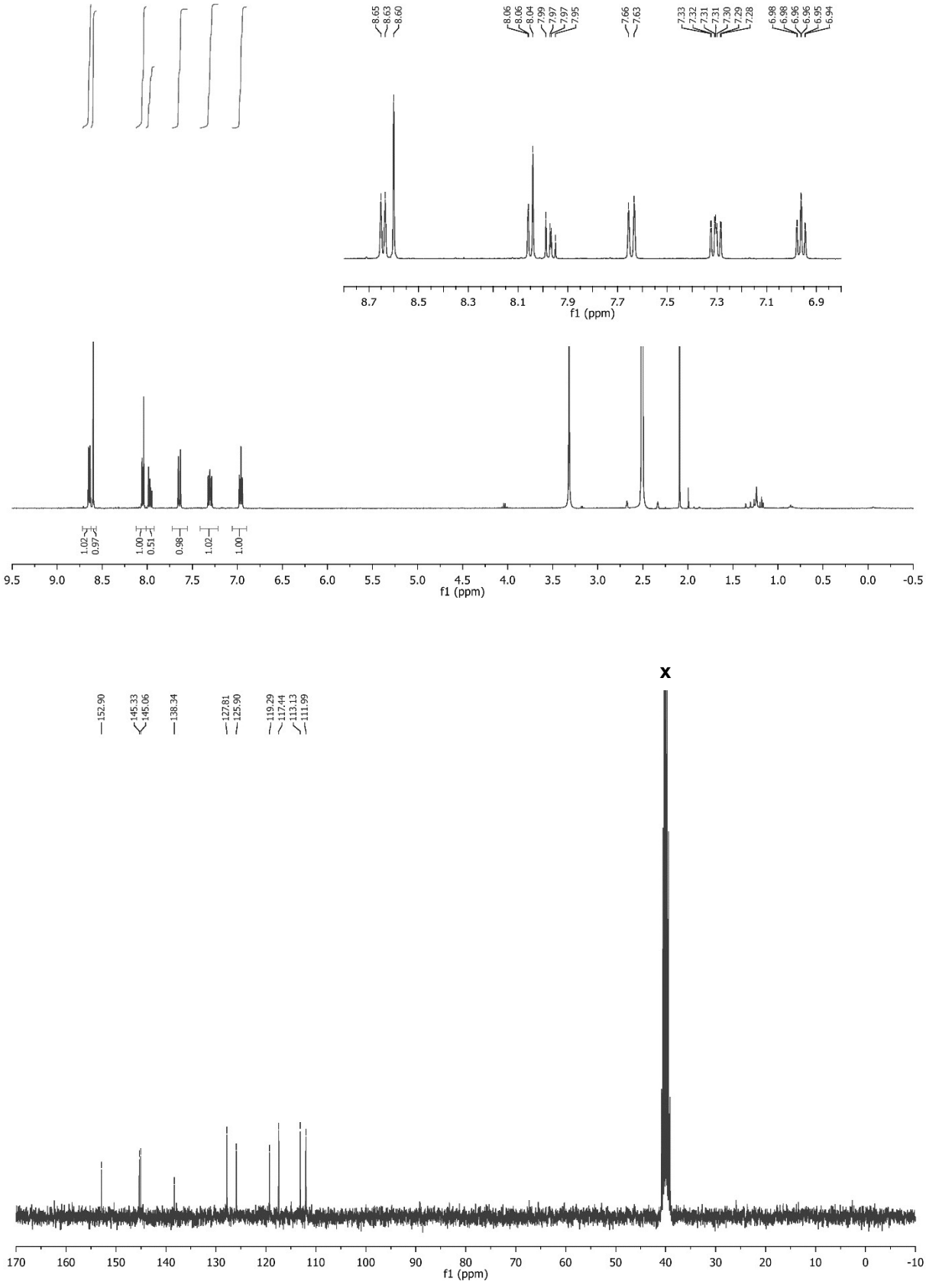

Figure S1 ^{1}H (top) and ^{13}C (bottom) NMR spectra of L^{1} ($\{CD_3\}_2SO$).[1]

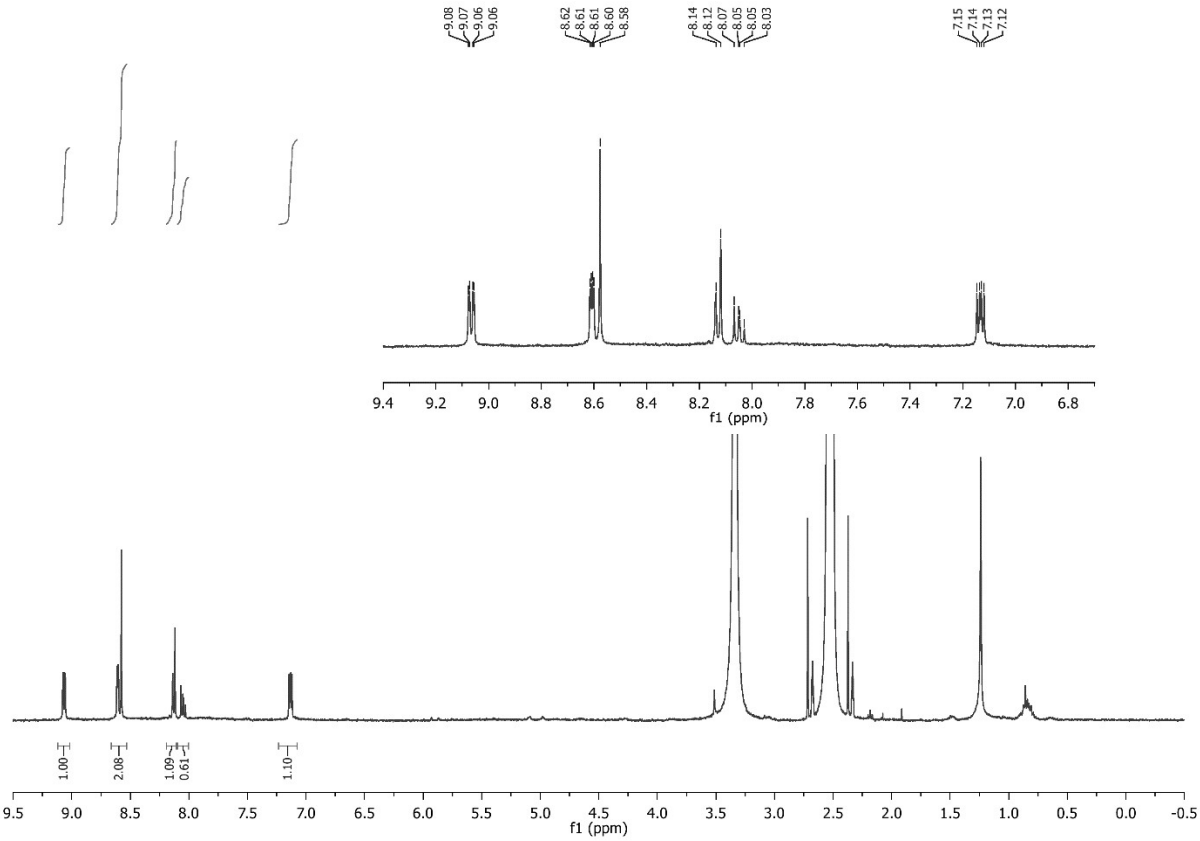

Figure S2 ^{1}H NMR spectrum of L^2 ($\{CD_3\}_2SO$).

The compound was too insoluble to afford a ^{13}C spectrum.

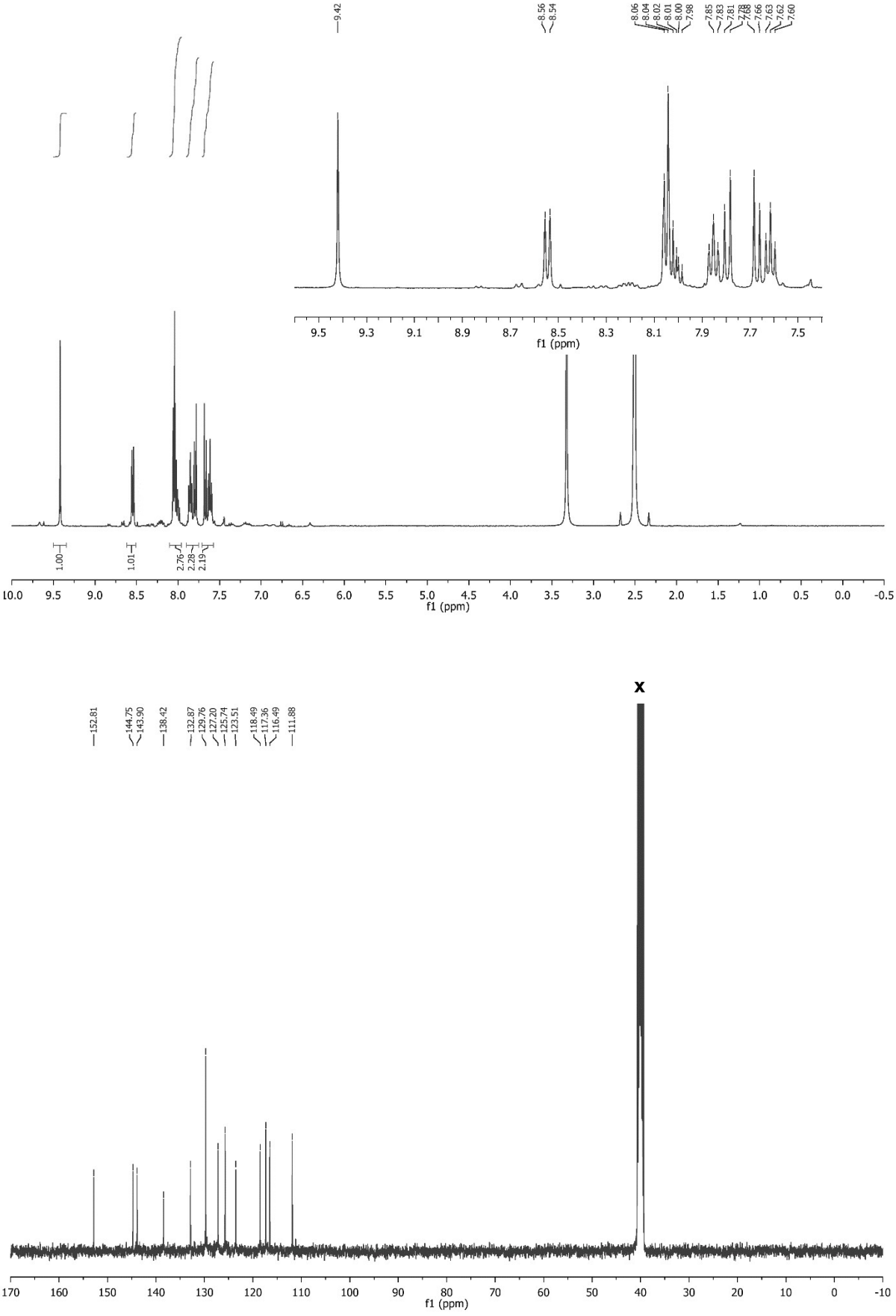

Figure S3 ^{1}H (top) and ^{13}C (bottom) NMR spectra of L^3 ($\{CD_3\}_2SO$).

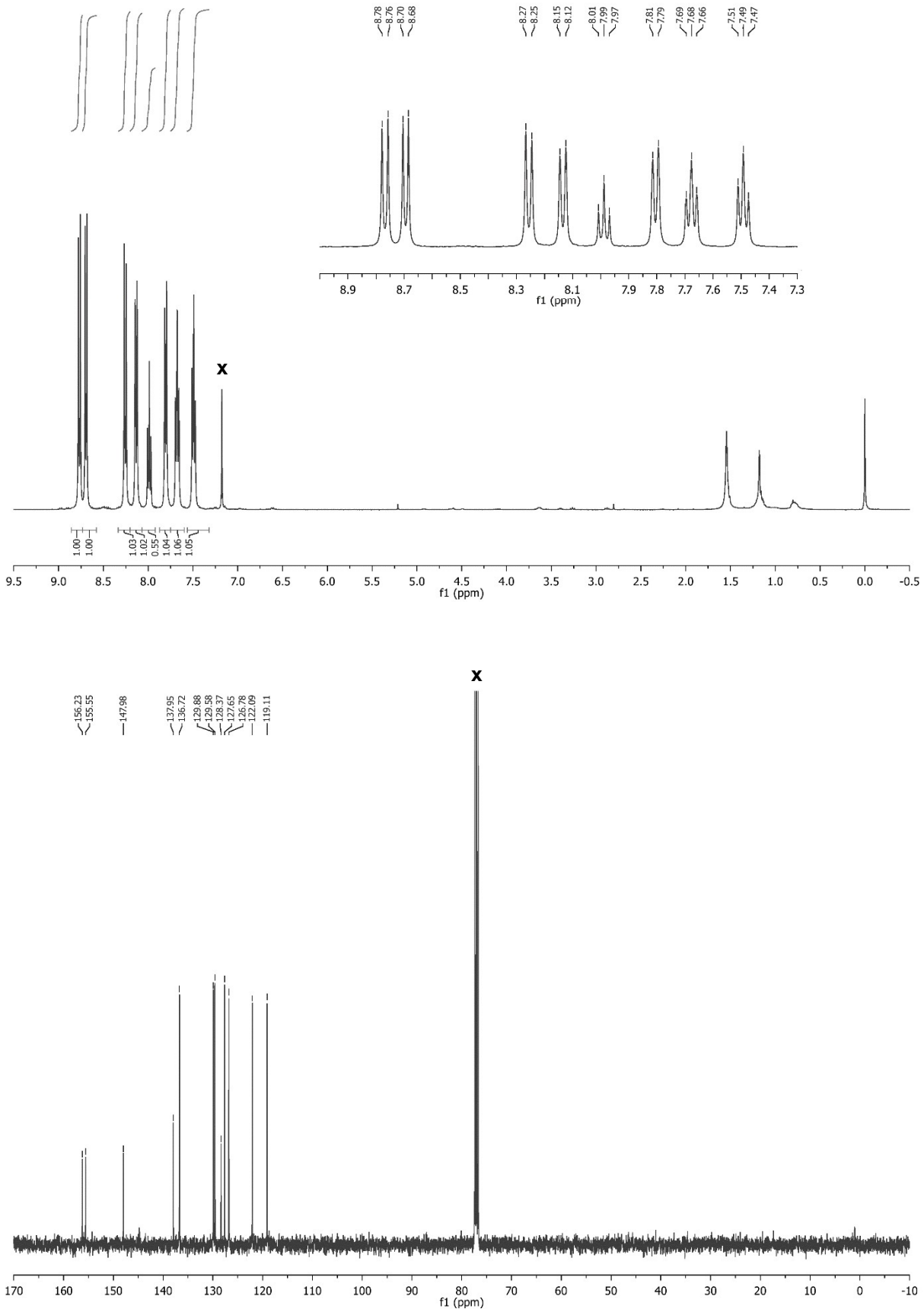

Figure S4 ^{1}H (top) and ^{13}C (bottom) NMR spectra of L^4 ($CDCl_3$).[2]

Single Crystal Structure Analyses

Experimental details of the structure determinations are given in Table S1. All the structures were solved by direct methods *(SHELX-TL*[3]), and developed by full least-squares refinement on F^2 (*SHELXL2018*[4]). Crystallographic figures were produced using *XSEED*,[5] and other publication materials were prepared with *OLEX*2.[6]

Unless otherwise stated, all fully occupied non-H atoms in the following refinements were refined anisotropically, while H atoms were placed in calculated positions and refined using a riding model. Disordered anions were treated with refined B–F and F···F distance restraints, while disordered solvent residues were modelled using fixed distance restraints.

Structure refinements of $1[BF_4]_2$·MeCN and $[Fe(L^1)_2][BF_4]_2$·*m*$MeNO_2$. The asymmetric units of these isomorphous crystals contain half a formula unit. There is: half a complex cation, with Fe(1) lying on the C_2 axis $^1/_4$, $^3/_4$, *z*; a disordered solvent site spanning the same C_2 axis; and, two BF_4^- half-anions that also span C_2 axes. The solvent was refined over two orientations, whose occupancies sum to 0.5 in the MeCN solvate or 0.4 in the $MeNO_2$ solvate; no additional, well-defined 0.1-occupied $MeNO_2$ environment was apparent in the Fourier map of the latter crystal. All the non-H atoms except the disordered solvent were refined anisotropically.

Structure refinement of $1[BF_4]_{1.6}[SiF_6]_{0.2}$·1.7$MeNO_2$·0.3$Et_2O$. There is one formula unit in the asymmetric unit of this crystal with all residues on general crystallographic sites. One anion was badly disordered, with a central atom whose U_{iso} parameter was abnormally low when refined as a fully occupied B atom. To account for that, the anion was modelled as a mixture of BF_4^- [two orientations sharing a common B atom, total occupancy 0.60] and SiF_6^{2-} [one site, occupancy 0.20]. Fixed B–F, Si–F and F···F distance restraints were applied to the disordered anion residues. In addition to one ordered nitromethane molecule, a disordered region of solvent was modelled with two partial molecules of nitromethane (occupancies 0.55 and 0.15) and one molecule of diethyl ether (0.3). SIMU U_{iso} constraints were applied to each disordered residue in this model, in addition to the distance restraints listed above. All wholly occupied non-H atoms were refined anisotropically except the disordered B atom (which was persistently non-positive definite). There are two residual Fourier peaks of 1.2-1.6 *e* Å^{-3}, which are both associated with the disordered solvent region.

Structure refinement of $1[BF_4]_2$·1.5MeOH. This crystal is an apparently perfect racemic twin, in the space group $Pna2_1$. Allowing for their different space group settings, its orthorhombic unit cell dimensions are the same as for $\mathbf{1[BF_4]_2}$·MeCN and $\mathbf{1[BF_4]_2}$·*m*$MeNO_2$, which adopt the centrosymmetric space group *Pccn*. However, attempts to refine this structure using that model were unsuccessful. A PLATON analysis[7] of this refinement (in $Pna2_1$) noted a non-crystallographic approximate inversion centre, but suggested this choice of space group was correct.

The asymmetric unit contains one complex cation and two BF_4^- anions, which are crystallographically ordered, and a disordered region of solvent that was modelled with four partial methanol environments whose occupancies sum to 1.5. The highest residual Fourier peak of +1.1 *e* Å^{-3} is associated with one of the BF_4^- ions, and may indicate a small degree of unmodelled disorder in that residue.

Structure refinements of $2[BF_4]_2$·1.5MeCN and $2[BF_4]_2$·Me_2CO. The asymmetric unit of $\mathbf{2[BF_4]_2}$·1.5MeCN contains one formula unit, including a half-molecule of acetonitrile that is disordered about the crystallographic inversion centre. Fixed distance restraints were applied to the solvent half-molecule to ensure a reasonable geometry. No other disorder is present in the model, and no other restraints were used during the refinement. All non-H atoms except the disordered solvent were refined anisotropically.

$\mathbf{2[BF_4]_2}$·Me_2CO is isomorphous with the acetonitrile solvate, but lacks the disordered solvent site near the crystallographic inversion centre. No disorder is present in that model, and no restraints were applied to the refinement.

Structure refinement of $2[BF_4]_2 \cdot 3.5MeNO_2 \cdot 0.5Et_2O$. Anion B(50)-F(54) is disordered over three sites, with occupancies of 0.40:0.40:0.20. Three of the four solvents sites in the model are also disordered, two of them with three partial nitromethane molecules (two of them sharing a common N atoms), and the other with half-occupied, overlying nitromethane and diethyl ether residues. The disordered solvent was modelled using fixed distance restraints.

Structure refinement of $[FeBr(py)_2(L^3)]Br \cdot 0.5H_2O$. The asymmetric unit contains one complex cation, one bromide anion that is disordered over two equally occupied sites; and, another Fourier peak that is not bonded to any other atom, and was modelled as half an equivalent of water. All non-H atoms except the partial water O atom were refined anisotropically. The partial water H atoms were not located in the Fourier map, but are included in the molecular weight and density calculations.

The disordered bromide ion and water half-molecule occupy a cavity surrounding a crystallographic inversion centre. Although its H atoms were not located, the partial water site is positioned to hydrogen bond to Br(7B) and Br(7A^{i}) [symmetry code: (i) $-x$, $1-y$, $1-z$].

Structure refinement of $4[BF_4]_2 \cdot 1.39MeCN \cdot 0.125Et_2O \cdot 0.25H_2O$. The asymmetric unit of this crystal contains four formula units of the compound (*ie Z'* = 4) with four complex dications, eight BF_4^- anions, six fully or part-occupied acetonitrile molecules, a disordered half-occupied diethyl ether molecule and two partial water sites whose occupancies sum to 1. All these residues are on general crystallographic sites apart from one acetonitrile half-molecule, that spans a crystallographic inversion centre.

Ligand N(28)-C(35) in cation B is disordered over two sites, whose occupancies refined to 0.61:0.39. The major disorder site was modelled without restraints, but the quinolyl groups of the minor disorder site were refined as rigid groups to ensure a sensible geometry. This ligand disorder may be connected to the occupancy of a neighbouring partial water site O(121), which is 1.92 Å from the major partial ligand atom H(53B).

Three of the BF_4^- ions are also disordered: one over two sites in a 0.70:0.30 ratio, that share a common F atom; and the other two over three equally occupied orientations where, in one case, two of the disorder sites have a common B atom. Two of the acetonitrile sites and the partial diethyl molecule were also disordered.

All fully occupied non-H atoms were refined anisotropically. The partial water H atoms were not located in the Fourier map and are not included in the model, but are accounted for in the molecular weight and density calculations.

CCDC 2288873-2288881 contain the supplementary crystallographic data for this paper (Table S1). These data can be obtained free of charge from The Cambridge Crystallographic Data Centre via www.ccdc.cam.ac.uk/data_request/cif.

Table S1 Experimental data for the crystal structure determinations in this work.

	1[BF$_4$]$_2$·MeCN	**1[BF$_4$]$_2$**·*m*MeNO$_2$ (*m* ≈ 0.8)	**1[BF$_4$]$_{1.6}$[SiF$_6$]$_{0.2}$**·1.7MeNO$_2$-·0.3Et$_2$O	**1[BF$_4$]$_2$**·1.5MeOH	**2[BF$_4$]$_2$**·1.5MeCN
molecular formula	$C_{40}H_{29}B_2F_8FeN_{11}$	$C_{38.8}H_{28.4}B_2F_8FeN_{10.8}O_{1.6}$	$C_{40.9}H_{34.1}B_{1.6}F_{7.6}FeN_{11.7}O_{3.7}Si_{0.2}$	$C_{39.5}H_{32}B_2F_8FeN_{10}O_{1.5}$	$C_{37}H_{26.5}B_2F_8FeN_{15.5}$
M_r	893.21	900.99	971.86	900.22	917.71
crystal class	orthorhombic	orthorhombic	triclinic	orthorhombic	triclinic
space group	*Pccn*	*Pccn*	$P\bar{1}$	$Pna2_1$	$P\bar{1}$
a / Å	12.4421(3)	12.3988(5)	12.7520(4)	25.2181(6)	13.0255(5)
b / Å	12.9696(3)	12.9182(4)	13.6771(4)	12.4550(2)	13.5032(6)
c / Å	25.2174(8)	25.2840(9)	13.9688(4)	12.9419(3)	13.7441(6)
α / °	–	–	79.861(2)	–	101.726(4)
β / °	–	–	78.387(3)	–	102.485(3)
γ / °	–	–	64.173(3)	–	118.470(4)
V / Å^3	4069.31(19)	4049.7(3)	2137.25(12)	4064.94(15)	1938.19(16)
Z	4	4	2	4	2
μ / mm^{-1}	3.694	3.746	3.677	3.722	3.931
D_c / gcm^{-3}	1.458	1.478	1.510	1.471	1.572
T / K	120	120	120	120	120
measured reflections	10690	10459	16955	10785	15897
independent reflections	4029	3990	8110	6058	7308
R_{int}	0.050	0.050	0.056	0.028	0.041
parameters	316	318	640	574	569
restraints	6	12	86	5	23
R_1 [$F_0 > 4\sigma(F_0)$][a]	0.077	0.059	0.071	0.050	0.055
wR_2, all data[b]	0.228	0.183	0.200	0.145	0.154
goodness of fit	1.076	1.054	1.102	1.062	1.064
$\Delta\rho_{min/max}$ / *e*Å^{-3}	−0.45/0.90	−0.47/0.76	−0.64/1.63	−0.45/1.11	−0.62/0.88
Flack parameter	–	–	–	0.498(7)	–
CCDC	2288873	2288874	2288875	2288876	2288877

[a] $R = \Sigma[\,|F_o| - |F_c|\,] / \Sigma|F_o|$ [b] $wR = [\Sigma w(F_o^2 - F_c^2) \;/\; \Sigma wF_o^4]^{1/2}$

Table S1 continued

	2[BF$_4$]$_2$·Me$_2$CO	**2[BF$_4$]$_2$**·3.5MeNO$_2$-·0.5Et$_2$O	[FeBr(py)$_2$(L^3)]Br·0.5H$_2$O	**4[BF$_4$]$_2$**·1.39MeCN-·0.125Et$_2$O·0.25H$_2$O
molecular formula	$C_{37}H_{28}B_2F_8FeN_{14}O$	$C_{39.5}H_{37.5}B_2F_8FeN_{17.5}O_{7.5}$	$C_{37}H_{28}Br_2FeN_7O_{0.5}$	$C_{49.28}H_{35.93}B_2F_8FeN_{7.39}O_{0.38}$
M_r	914.20	1106.84	978.17	967.16
crystal class	triclinic	triclinic	monoclinic	monoclinic
space group	$P\bar{1}$	$P\bar{1}$	$P2_1/c$	$P2_1/c$
a / Å	13.2776(3)	12.6361(6)	12.8813(4)	18.9083(3)
b / Å	13.2858(4)	13.4938(7)	14.1735(4)	48.0111(9)
c / Å	13.6211(3)	14.3473(7)	19.6258(5)	20.0833(3)
α / °	102.783(2)	80.455(4)	–	–
β / °	101.448(2)	89.884(4)	108.553(4)	93.963(2)
γ / °	117.943(3)	76.630(4)	–	–
V / Å^3	1938.57(10)	2345.4(2)	3396.93(18)	18188.2(5)
Z	2	2	4	16
μ{Cu-K_α} / mm^{-1}	3.935	3.492	6.630	3.335
D_c / gcm^{-3}	1.566	1.567	1.553	1.413
T / K	120	120	120	120
measured reflections	14940	16691	14343	71868
independent reflections	6681	8101	6680	35207
R_{int}	0.031	0.046	0.040	0.049
parameters	570	706	437	2412
restraints	0	79	0	107
R_1 [$F_0 > 4\sigma(F_0)$][a]	0.040	0.075	0.057	0.113
wR_2, all data[b]	0.110	0.212	0.164	0.306
goodness of fit	1.042	1.062	1.014	1.097
$\Delta\rho_{min/max}$ / eÅ^{-3}	−0.43/0.56	−0.53/0.76	−0.92/0.92	−0.67/0.95
Flack parameter	–	–	–	–
CCDC	2288878	2288879	2288880	2288881

[a] $R = \Sigma[\,|F_o| - |F_c|\,] / \Sigma|F_o|$ [b] $wR = [\Sigma w(F_o^2 - F_c^2) \;/\; \Sigma wF_o^4]^{1/2}$

Definitions of the structural parameters discussed in the paper

V_{Oh} is the volume (in Å^3) of the FeN_6 coordination octahedron in the complex,[8] which is typically <10 Å^3 in low-spin $[FeL_2]^{2+}$ derivatives related to the compounds in this work, and ≥11.5 Å^3 in their high-spin form.[9]

Σ and Θ are defined as follows:

$$\Sigma = \sum_{i=1}^{12} |90 - \beta_i| \qquad \Theta = \sum_{j=1}^{24} |60 - \gamma_j|$$

where β_i are the twelve *cis*-N–Fe–N angles about the iron atom and γ_i are the 24 unique N–Fe–N angles measured on the projection of two triangular faces of the octahedron along their common pseudo-threefold axis (Scheme S2). Σ is a general measure of the deviation of a metal ion from an ideal octahedral geometry, while Θ more specifically indicates its distortion towards a trigonal prismatic structure. A perfectly octahedral complex gives $\Sigma = \Theta = 0$.[8,10]

Because the high-spin state of a complex has a much more plastic structure than the low-spin, this is reflected in Σ and Θ which are usually much larger in the high-spin state. The absolute values of these parameters depend on the metal/ligand combination in the compound under investigation, however.

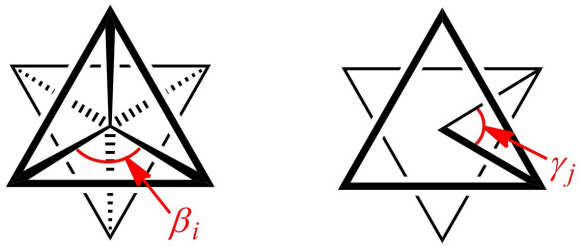

Scheme S2 Angles used in the definitions of the coordination distortion parameters Σ and Θ.

The parameters in Scheme S3 define an angular Jahn-Teller distortion, that is often observed in high-spin iron(II) complexes of meridional tridentate ligands ($\theta \leq 90°$, $\phi \leq 180°$).[11] They are also a useful indicator of the molecular geometry, in defining the disposition of the two ligands around the metal ion.

Significant changes in ϕ, especially, during SCO can lead to hysteretic spin-transitions in solid complexes of this type.[12] However, spin-crossover can also be inhibited if θ and ϕ deviate too strongly from their ideal values in the high-spin state, because the associated rearrangement to a more regular low-spin coordination geometry ($\theta \approx 90°$, $\phi \approx 180°$) cannot be accommodated by a rigid solid lattice.[11,13]

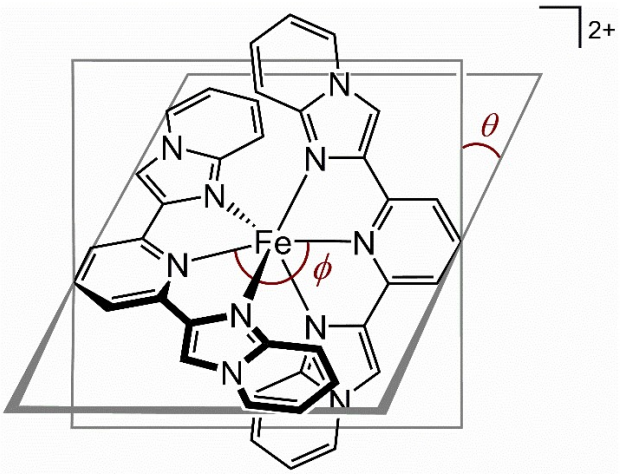

Scheme S3 Definition of the Jahn-Teller distortion parameters θ and ϕ in $[Fe(L^1)_2]^{2+}$.

Typical values of all these parameters in $[FeL_2]^{2+}$ complexes are listed in refs. 10 and 14-16.

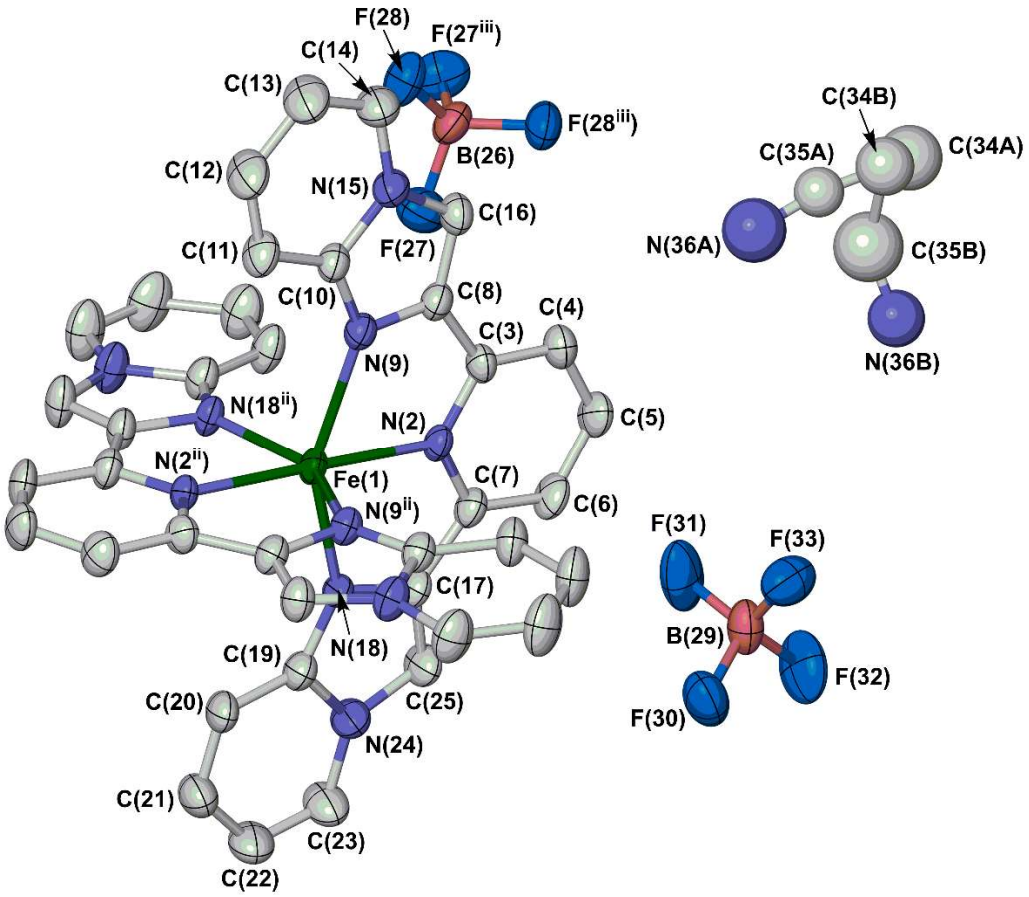

Figure S5 The asymmetric unit of **1[BF$_4$]$_2$**·MeCN, showing the full atom numbering scheme. All displacement ellipsoids are at the 50 % probability level, and H atoms are omitted for clarity. Both orientations of the disordered solvent half-molecule are shown.

Colour code: C, white; B, pink; F, cyan; Fe, green; N, blue.

Symmetry codes: (ii) $^1/_2-x$, $^3/_2-y$, z; (iii) $^3/_2-x$, $^3/_2-y$, z.

The asymmetric unit contains half a formula unit of the compound, with each residue in the Figure being half-occupied. Atoms Fe(1) and B(26) lie on crystallographic C_2 sites, while half-anion B(29)-F(33) and the two 0.25-occupied MeCN disorder orientations both lie close to other C_2 axes.

The refinement of **1[BF$_4$]$_2$**·*m*MeNO$_2$ is isomorphous with this one, and uses the same atom numbering scheme (Figure S6).

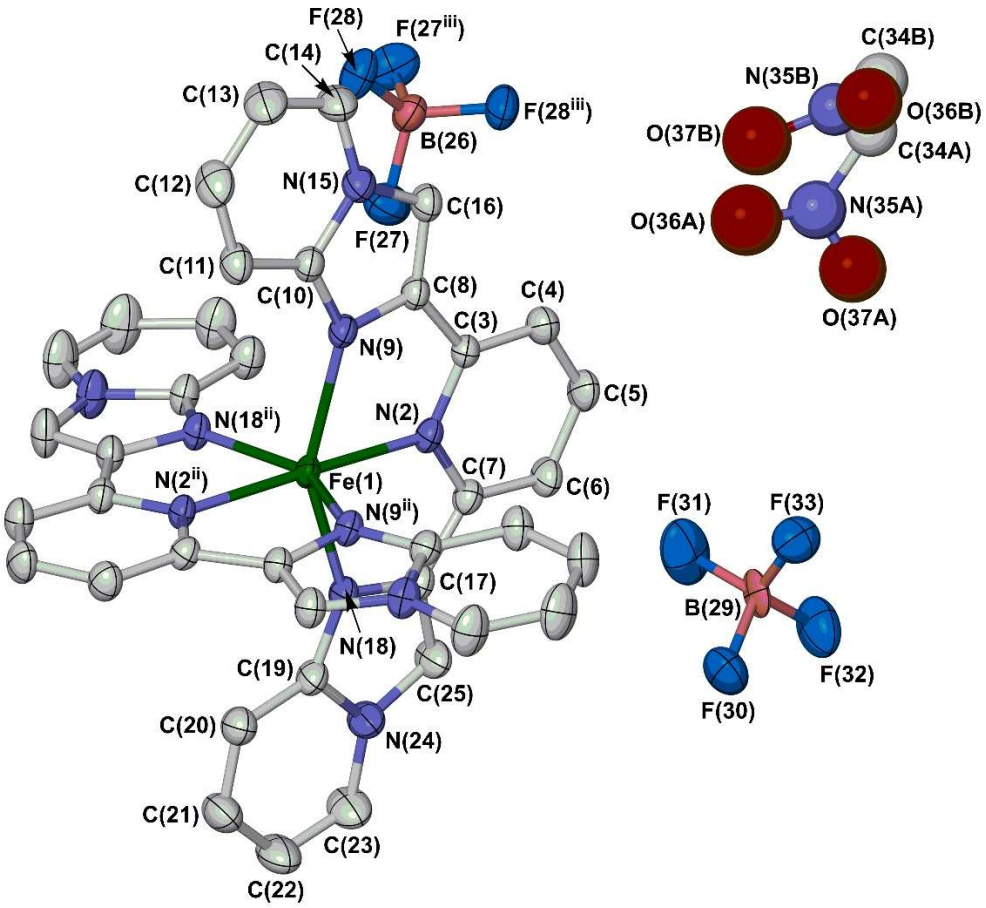

Figure S6 The asymmetric unit of **1[BF$_4$]$_2$**·*m*MeNO$_2$, showing the full atom numbering scheme. All displacement ellipsoids are at the 50 % probability level, and H atoms are omitted for clarity. Both orientations of the partial disordered solvent molecule are shown.

Colour code: C, white; B, pink; F, cyan; Fe, green; N, blue; O, red.

Symmetry codes: (ii) $^1/_2-x$, $^3/_2-y$, z; (iii) $^3/_2-x$, $^3/_2-y$, z.

This structure is isomorphous with **1[BF$_4$]$_2$**·MeCN (Figure S5), which is discussed on the previous page. The occupancy of the disordered nitromethane half-molecule site appears to be sub-stoichiometric, and was refined to a formula of m = 0.8.

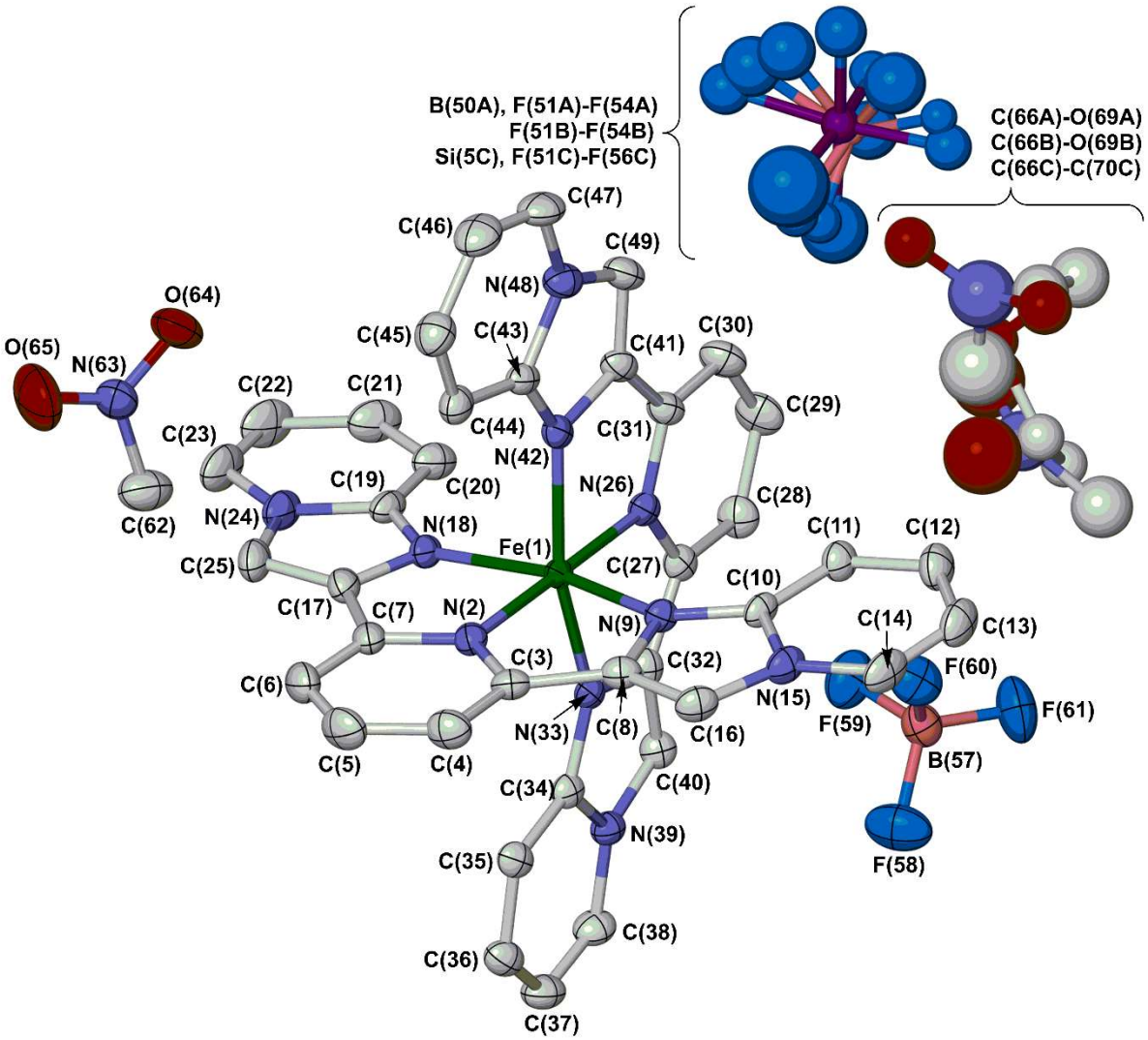

Figure S7 The asymmetric unit of $\mathbf{1[BF_4]_{1.6}[SiF_6]_{0.2}}\cdot 1.7MeNO_2\cdot 0.3MeNO_2$, showing the full atom numbering scheme. All displacement ellipsoids are at the 50 % probability level, and H atoms are omitted for clarity. All orientations of the disordered anion and solvent sites are shown.

Colour code: C, white; B, pink; F, cyan; Fe, green; N, blue; O, red.

The partial SiF_6^{2-} was included in the disordered anion site, to account for an anomalously low U_{iso} parameter when the central atom of that anion was refined as a wholly occupied B atom. It could arise from reaction of adventitious fluoride (produced by hydrolysis of BF_4^-) with the silica glass vial during the crystallisation process.[17] The model obeys charge balance, but there is no other evidence for the presence of SiF_6^{2-} in the material. The disordered solvent site is modelled as two nitromethane and one diethyl ether partial molecules.

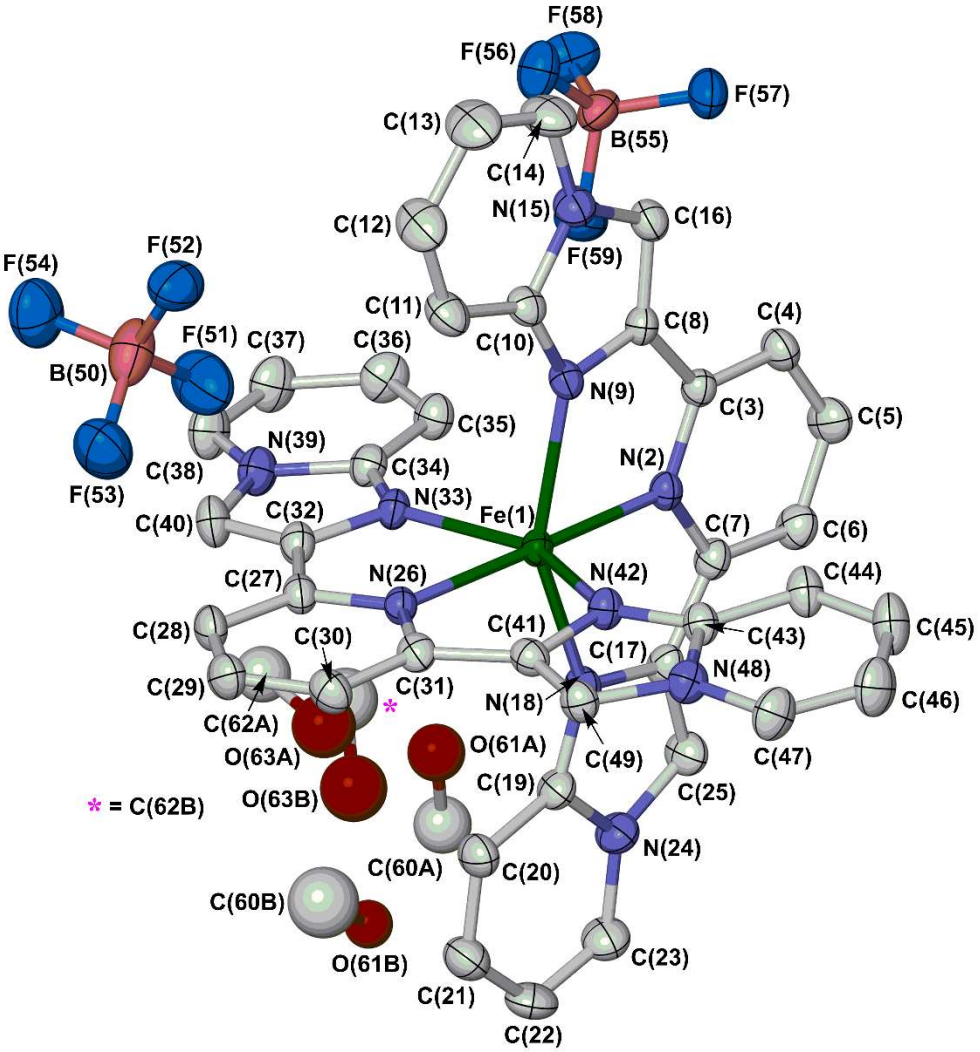

Figure S8 The asymmetric unit of **1[BF$_4$]$_2$**·1.5MeOH, showing the full atom numbering scheme. All displacement ellipsoids are at the 50 % probability level, and H atoms are omitted for clarity. All orientations of the disordered anion and solvent sites are shown.

Colour code: C, white; B, pink; F, cyan; Fe, green; N, blue; O, red.

This crystal has the same orthorhombic unit cell dimensions as **1[BF$_4$]$_2$**·MeCN and **1[BF$_4$]$_2$**·*m*MeNO$_2$, but lacks their crystallographic inversion symmetry.

Table S2 Selected bond lengths and angles in the solvate crystals of **1[BF$_4$]$_2$** (Å, º, Å^3). See Figures S5-S8 for the atom numbering scheme employed, and page S13 for definitions of the structural indices in the Table. Symmetry code: (ii) $^1/_2-x$, $^3/_2-y$, z.

	1[BF$_4$]$_2$·MeCN	**1[BF$_4$]$_2$**·*m*MeNO$_2$		**1[BF$_4$]$_{1.6}$[SiF$_6$]$_{0.2}$**·-1.7MeNO$_2$·0.3Et$_2$O	**1[BF$_4$]$_2$**·1.5MeOH
Fe(1)–N(2)	2.175(3)	2.168(3)	Fe(1)–N(2)	1.924(3)	2.171(4)
Fe(1)–N(9)	2.199(4)	2.199(3)	Fe(1)–N(9)	1.979(3)	2.193(4)
Fe(1)–N(18)	2.191(3)	2.195(3)	Fe(1)–N(18)	1.989(3)	2.199(4)
			Fe(1)–N(26)	1.920(3)	2.171(4)
			Fe(1)–N(33)	1.998(3)	2.194(4)
			Fe(1)–N(42)	2.002(3)	2.201(4)
N(2)–Fe(1)–N(9)	73.84(13)	73.96(10)	N(2)–Fe(1)–N(9)	80.37(11)	73.84(15)
N(2)–Fe(1)–N(18)	74.41(12)	74.15(10)	N(2)–Fe(1)–N(18)	80.71(12)	74.16(16)
N(2)–Fe(1)–N(2^{ii})	176.42(18)	175.81(14)	N(2)–Fe(1)–N(26)	178.78(11)	175.96(14)
N(2)–Fe(1)–N(9^{ii})	108.75(12)	109.08(10)	N(2)–Fe(1)–N(33)	98.99(11)	101.71(16)
N(2)–Fe(1)–N(18^{ii})	103.08(12)	102.90(10)	N(2)–Fe(1)–N(42)	99.76(11)	109.53(16)
N(9)–Fe(1)–N(18)	148.15(12)	148.01(10)	N(9)–Fe(1)–N(18)	161.06(12)	147.96(16)
			N(9)–Fe(1)–N(26)	100.73(11)	107.76(15)
N(9)–Fe(1)–N(9^{ii})	93.03(19)	92.54(14)	N(9)–Fe(1)–N(33)	92.03(10)	93.82(15)
N(9)–Fe(1)–N(18^{ii})	94.79(13)	95.47(10)	N(9)–Fe(1)–N(42)	91.06(11)	92.44(14)
			N(18)–Fe(1)–N(26)	98.20(11)	104.27(15)
N(18)–Fe(1)–N(18^{ii})	94.64(19)	93.93(15)	N(18)–Fe(1)–N(33)	91.78(10)	94.13(15)
			N(18)–Fe(1)–N(42)	91.28(11)	96.67(16)
			N(26)–Fe(1)–N(33)	80.46(11)	74.58(16)
			N(26)–Fe(1)–N(42)	80.79(11)	74.26(16)
			N(33)–Fe(1)–N(42)	161.24(11)	148.66(17)
V_{Oh}	12.901(15)	12.873(11)	V_{Oh}	9.896(8)	12.908(15)
Σ	144.4(5)	145.2(4)	Σ	81.5(4)	143.5(5)
Θ	473	476	Θ	268	470
ϕ	176.42(18)	175.81(14)	ϕ	178.78(11)	175.96(14)
θ	89.66(3)	89.87(2)	θ	88.89(2)	89.93(3)

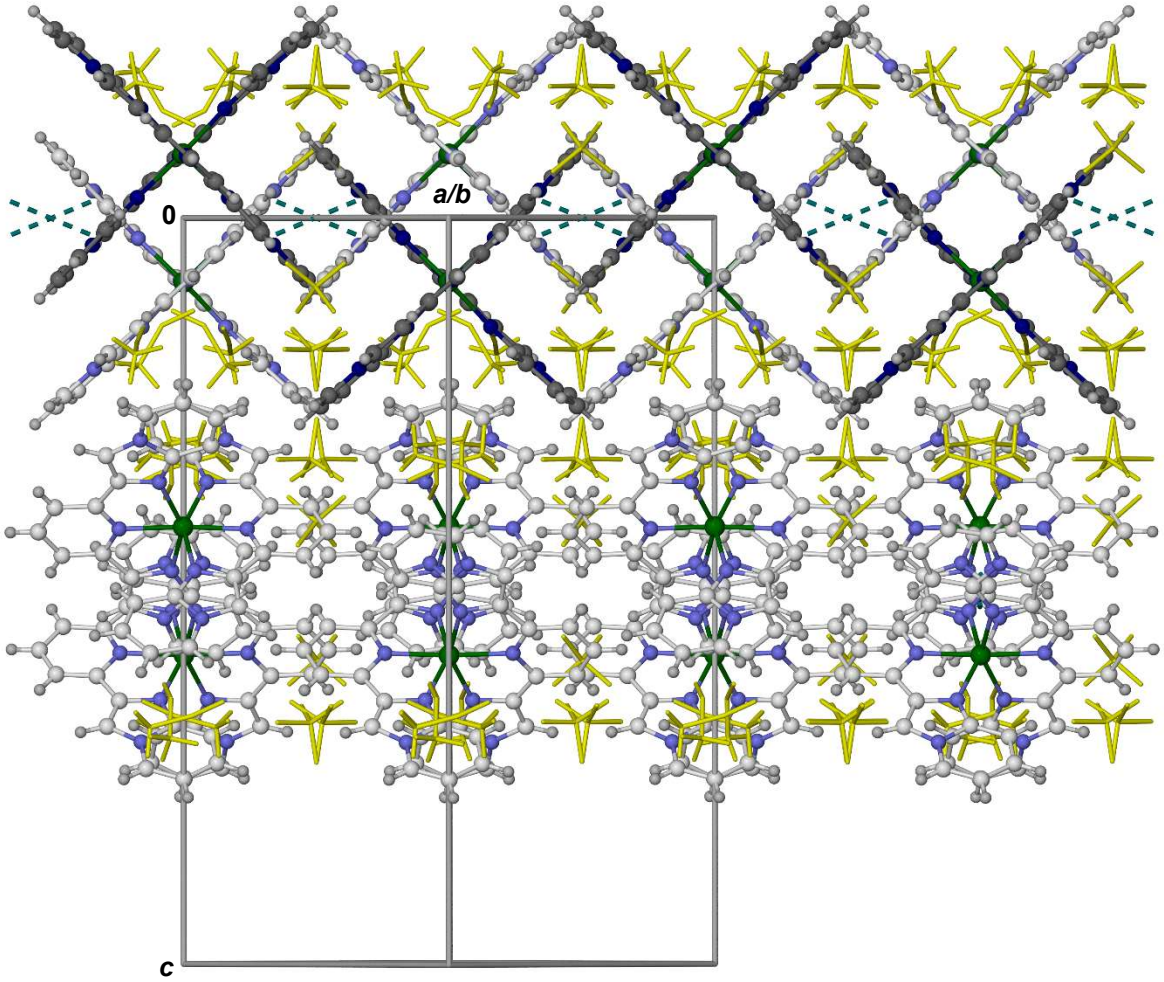

Figure S9 Packing diagram of **1[BF$_4$]$_2$**·MeCN, showing the association of the molecules into zig-zag chains through $\pi\cdots\pi$ interactions between their L^1 imidazopyridine residues (shown as dotted lines). One cation chain is highlighted with dark colouration, while the anions and disordered solvent molecules are de-emphasised for clarity.

Colour code: C, white or dark grey; H, pale grey; Fe, green; N, pale or dark blue; BF_4^- and MeCN, yellow.

The chains alternate along the [1$\bar{1}$0] and [$\bar{1}$10] crystal vectors, down the *c* axis. There is one unique $\pi\cdots\pi$ interaction in the lattice. The interacting imidazopyridine groups [C(17)-C(25)] and [C(17^{iv})-C(25^{iv})] are coplanar by symmetry and separated by 3.330(15) Å [symmetry code: (iv) –*x*, 1–*y*, –*z*]. Their centroids are horizontally offset by 1.27 Å.

The corresponding interaction in the isomorphous crystal **1[BF$_4$]$_2$**·*m*MeNO$_2$ has the overlapping imidazopyridine groups 3.351(11) Å apart, with a horizontal offset of 1.23 Å.

There are no short edge-to-face C–H$\cdots\pi$ contacts in the lattice.

The crystal packing in **1[BF$_4$]$_2$**·1.5MeOH is essentially the same as shown here, but with minor differences reflecting the different space group of the methanol solvate (Figure S13).

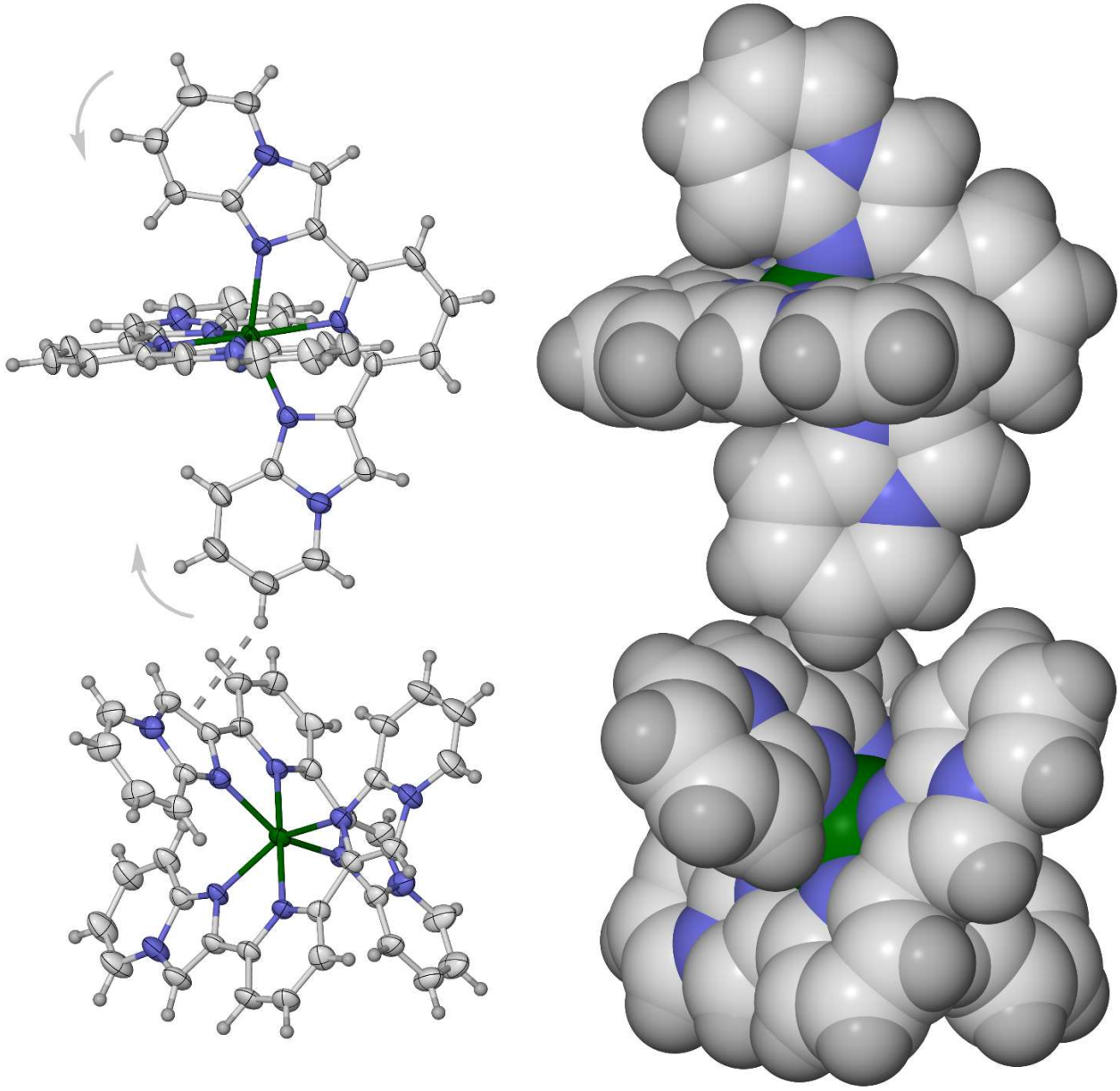

Figure S10 Two $[Fe(L^1)_2]^{2+}$ molecules in neighbouring cation chains in **1[BF$_4$]$_2$**·MeCN, related by 1−*x*, ½+*y*, ½−*z*, shown as thermal ellipsoid (left) and space-filling (right) plots. The intermolecular C–H···π contact that may inhibit thermal SCO in **1[BF$_4$]$_2$**·MeCN, **1[BF$_4$]$_2$**·*m*MeNO$_2$ and **1[BF$_4$]$_2$**·1.5MeOH is shown in grey. This is an alternative view of Figure 1 in the main article. Colour code: C, white; H, pale grey; Fe, green; N, blue.

The highlighted interaction is a 2.9 Å contact between an H atom and the centroid of a C−C bond, which is equal to the sum of the Van der Waals radii of an H atom and an aromatic ring.[17] Although the interaction is weak, it is positioned to inhibit displacement of those imidazopyridyl groups in the direction shown, which would accompany SCO.

Each C_2-symmetric cation donates two and accepts two of these C–H···π contacts, as shown in Figure 1.

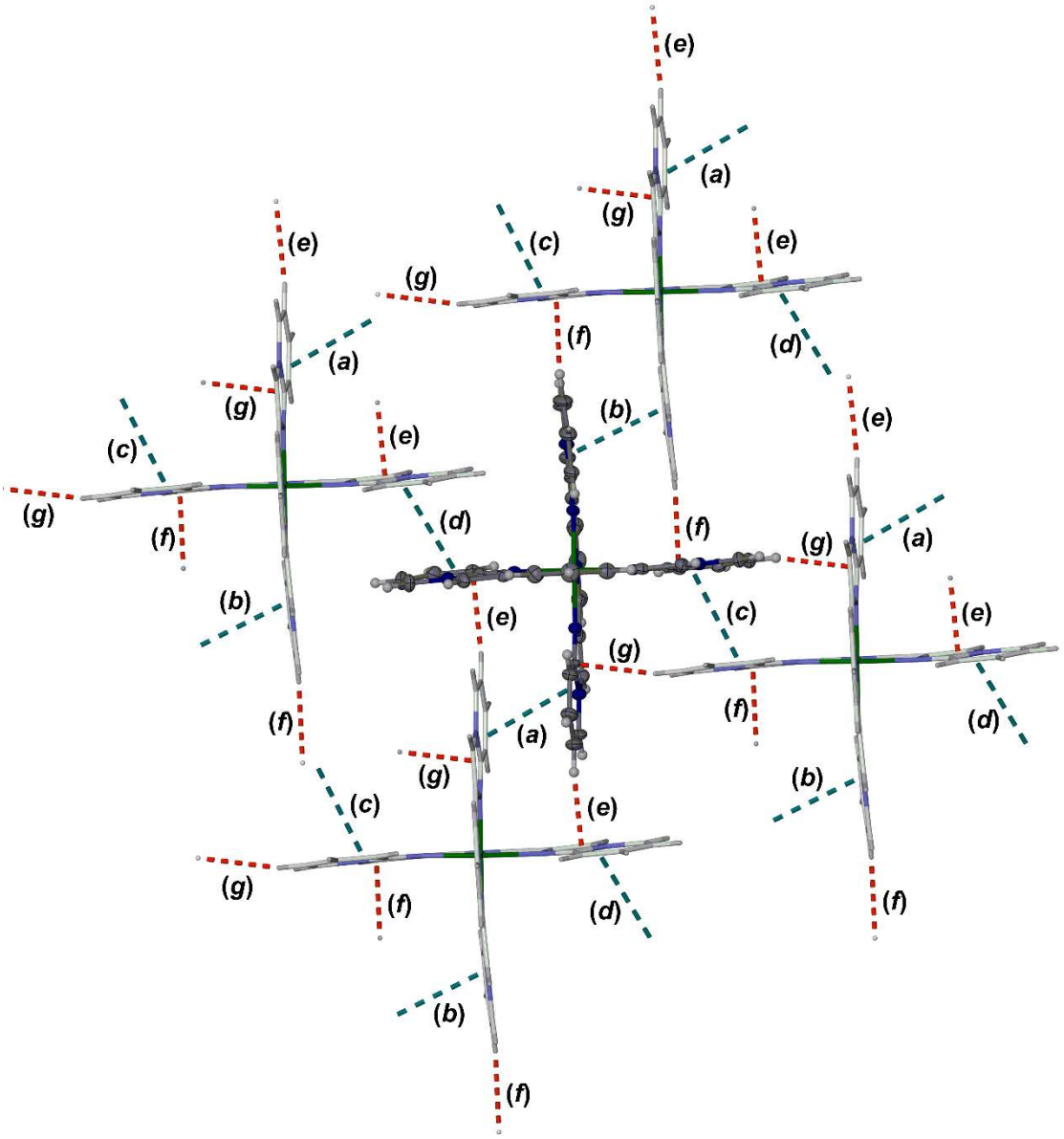

Figure S11 A terpyridine embrace layer of $\mathbf{1[BF_4]_{1.6}[SiF_6]_{0.2}}\cdot 1.7MeNO_2\cdot 0.3Et_2O$, showing the $\pi\cdots\pi$ (cyan) and C–H$\cdots\pi$ (red) intermolecular contacts. Each interaction is labelled with a code corresponding to that in Table S3. One cation is highlighted with dark colouration, while the anions and solvent molecules are not shown.

Colour code: C, white or dark grey; H, pale grey; Fe, green; N, pale or dark blue.

One imidazopyridyl group in each molecule, C(41)-C(49), does not form a close C–H$\cdots\pi$ contact with its nearest neighbour.

Table S3 Intermolecular interactions in the crystal structure of **1[BF_4]$_{1.6}$[SiF_6]$_{0.2}$**·1.7$MeNO_2$·0.3Et_2O (Å, °). See Figure S7 for the atom numbering scheme employed, while the codes for each interaction are those in Figure S11. Symmetry codes: (v) 1−*x*, 1−*y*, 1−*z*; (vi) 2−*x*, −*y*, −*z*; (vii) 2−*x*, −*y*, 1−*z*; (viii) 1−*x*, 1−*y*, −*z*.

$\pi\cdots\pi$	Dihedral angle	Interplanar spacing	Horizontal offset	
[C(8)-C(16)]···[C(8^{v})-C(16^{v})] (***a***)	0	3.311(15)	1.72	
[C(17)-C(25)]···[C(17^{vi})-C(25^{vi})] (***b***)	0	3.420(17)	1.27	
[C(32)-C(40)]···[C(32^{vii})-C(40^{vii})] (***c***)	0	3.46(2)	1.63	
[C(41)-C(49)]···[C(41^{viii})-C(49^{viii})] (***d***)	0	3.497(14)	1.74	
C–H···π[a]	C−H	H···C	C···C	C−H···C
C(13)–H(13)···C(44^{v}) (***e***)	0.95	2.76	3.681(5)	162.3
C(22)–H(22)···C(35^{vi}) (***f***)	0.95	2.73	3.656(5)	166.5
C(37)–H(37)···C(10^{vii}) (***g***)	0.95	2.74	3.608(5)	151.9
C(46)–H(46)···C(20^{viii})[b]	0.95	2.95	3.819(6)	152.8

[a]The sum of the Pauling van der Waals radii of an H atom and an aromatic ring is 2.9 Å.[18] [b]This is the closest edge-to-face C–H···π contact involving imidazopyridyl group C(41)-C(49). It is essentially equal to the sum of the van der Waals radii of those groups, and is not shown in Figure S11.

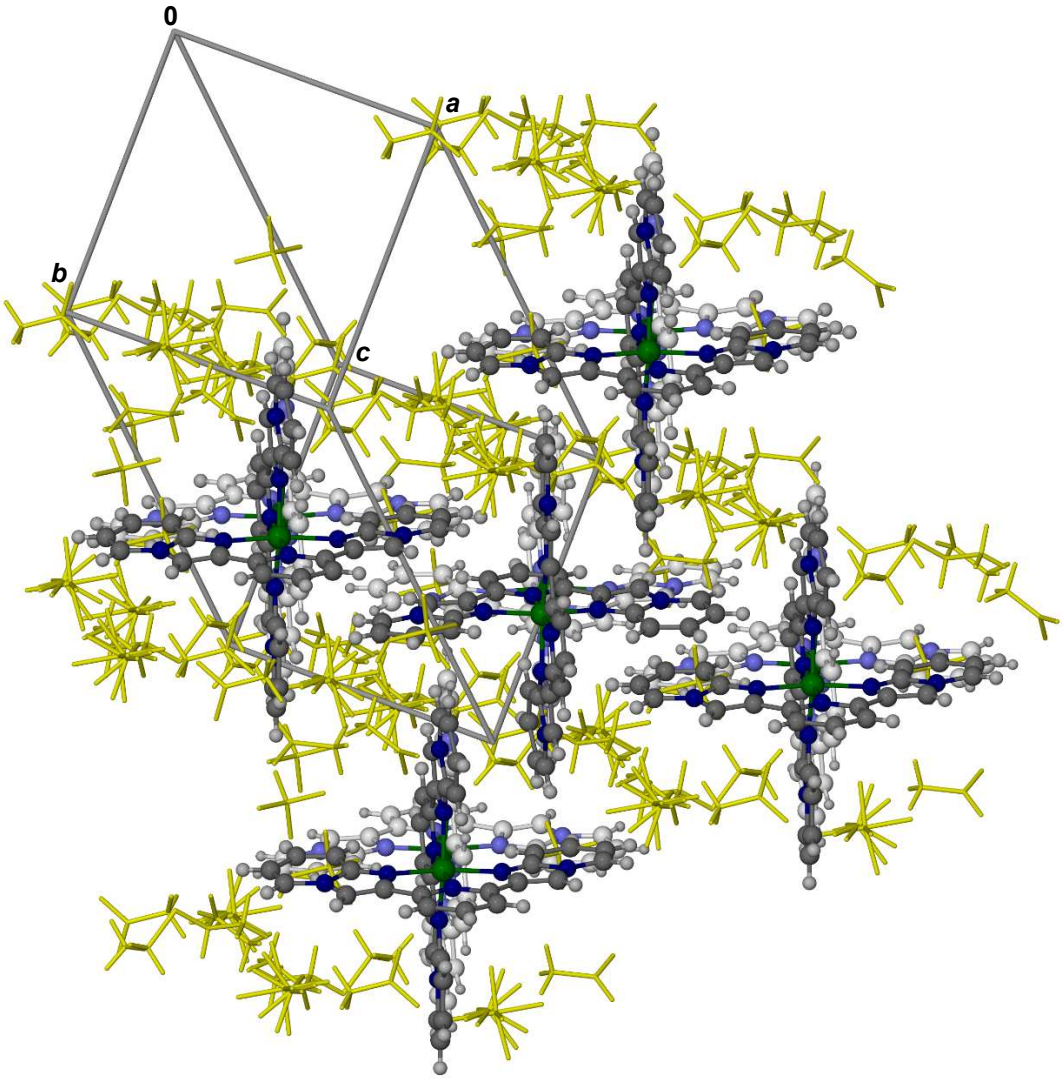

Figure S12 Full packing diagram of **1[BF_4]$_{1.6}$[SiF_6]$_{0.2}$**·1.7$MeNO_2$·0.3Et_2O, showing two terpyridine embrace cation layers which are distinguished with pale and dark colouration. The anions and disordered solvent molecules are de-emphasised for clarity.

Colour code: C, white or dark grey; H, pale grey; Fe, green; N, pale or dark blue; BF_4^-, SiF_6^{2-} and MeCN, yellow.

The complex molecules pack into layers parallel to the ($\bar{1}$10) crystal plane, through interdigitation of their imidazopyridine ligand arms (Figures S11 and S13).

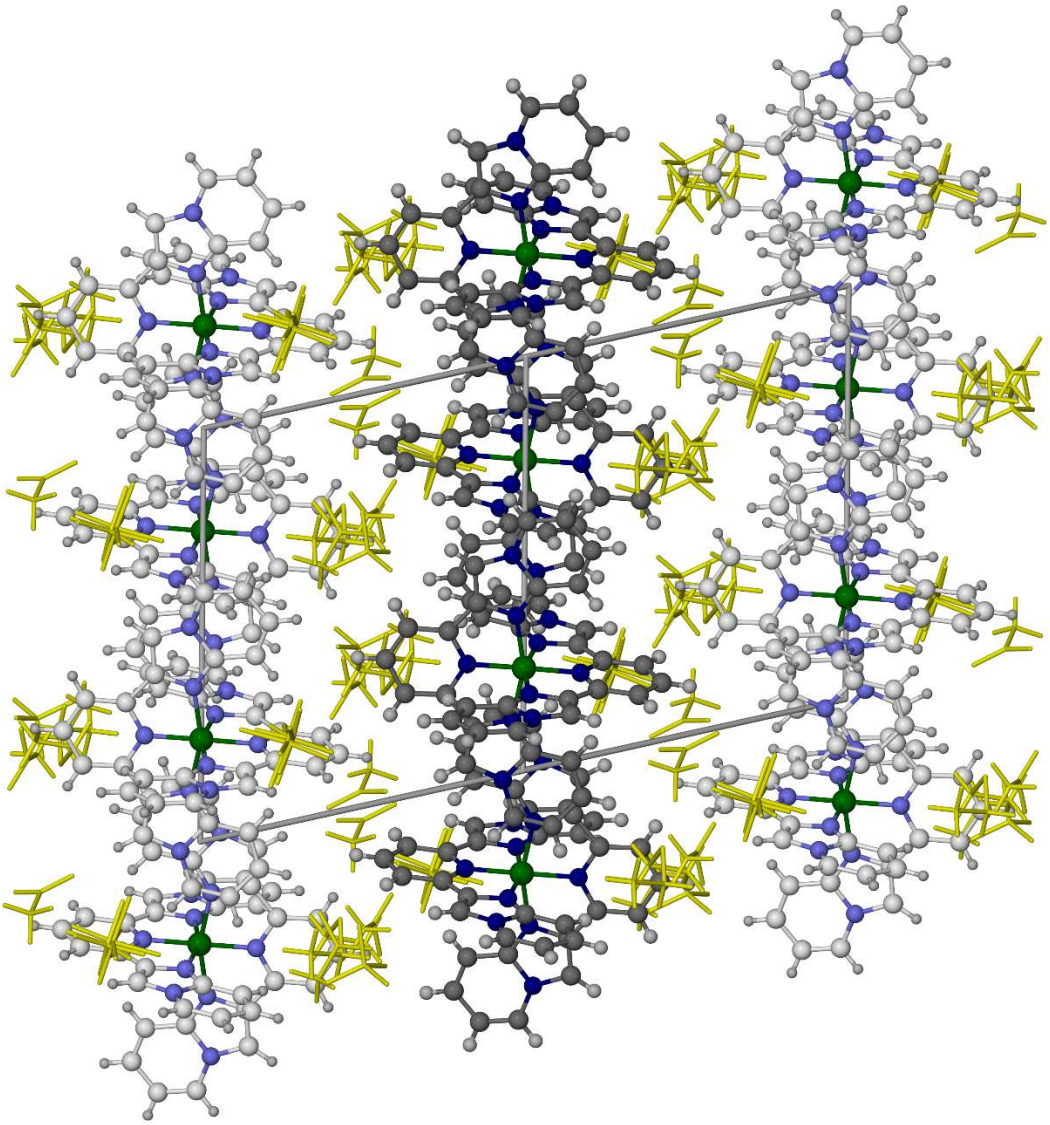

Figure S13 Alternative packing diagram of **1[BF_4]$_{1.6}$[SiF_6]$_{0.2}$**·1.7$MeNO_2$·0.3Et_2O, showing the terpyridine embrace cation layers. One layer is highlighted with dark colouration, and the anions and disordered solvent molecules are de-emphasised for clarity. The view is parallel to the [$\bar{1}$10] crystal vector, with the *c* axis vertical.

Colour code: C, white or dark grey; H, pale grey; Fe, green; N, pale or dark blue; BF_4^-, SiF_6^{2-} and MeCN, yellow.

The complex molecules pack into layers parallel to the ($\bar{1}$10) crystal plane, through interdigitation of their imidazopyridine ligand arms (Figure S11).

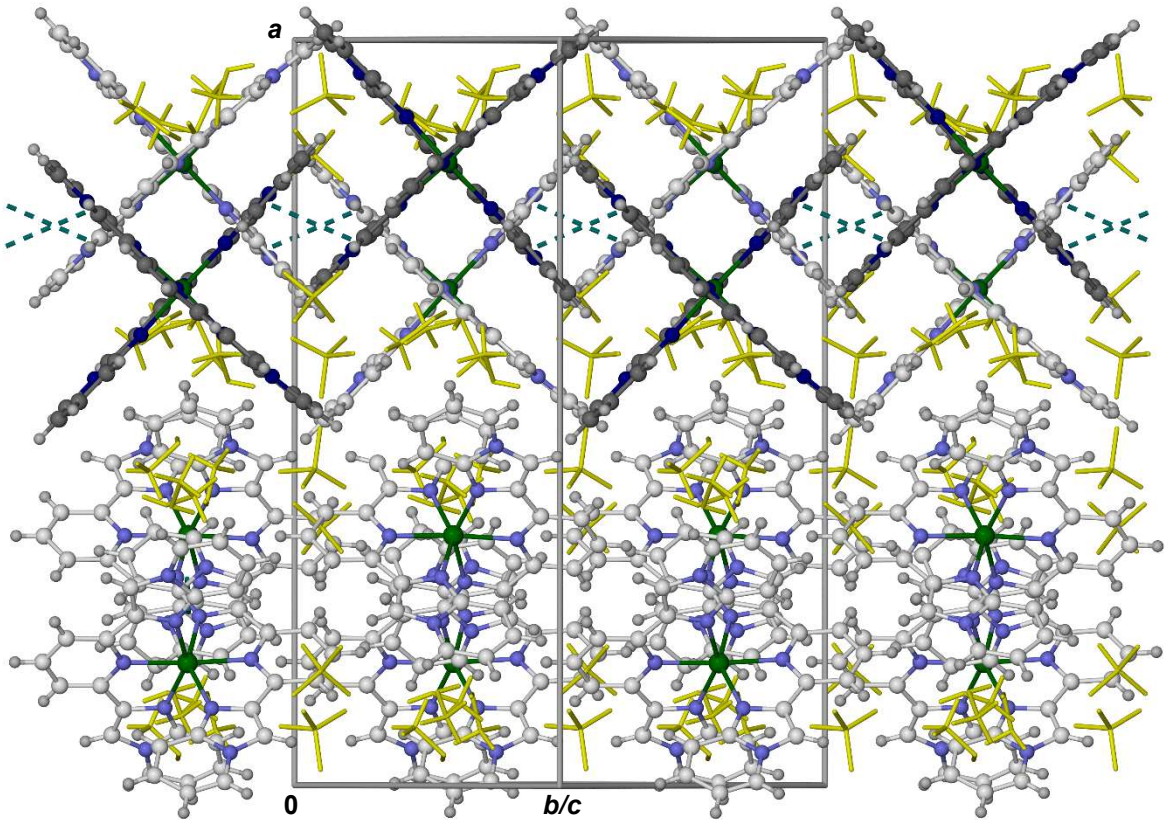

Figure S14 Packing diagram of **1[BF$_4$]$_2$**·1.5MeOH, showing the association of the molecules into zig-zag chains through $\pi\cdots\pi$ interactions between their L^1 imidazopyridine residues (shown as dotted lines). One cation chain is highlighted with dark colouration, while the anions and disordered solvent molecules are de-emphasised for clarity.

Colour code: C, white or dark grey; H, pale grey; Fe, green; N, pale or dark blue; BF_4^- and MeOH, yellow.

The chains alternate along the [01$\bar{1}$] and [0$\bar{1}$1] crystal vectors, down the *a* axis. There is one unique $\pi\cdots\pi$ interaction in the lattice. The dihedral angle between the least squares planes of the interacting imidazopyridine groups [C(17)-C(25)] and [C(3^{ix})-C(40^{ix})] is 4.5(2)°; the average distance between the overlapping rings is 3.275(17) Å; and their centroids are horizontally offset by 1.38 Å [symmetry code: (ix) $^3/_2$–*x*, $^1/_2$+*y*, $^1/_2$+*z*].

There are no short edge-to-face C–H$\cdots\pi$ contacts in the lattice.

Although they adopt different space groups, the packing in this crystal is the essentially same as **1[BF$_4$]$_2$**·MeCN and **1[BF$_4$]$_2$**·*m*MeNO$_2$ (Figure S9). The lattices differ in their $\pi\cdots\pi$-stacked molecules, which are related by the *n*-glide plane in **1[BF$_4$]$_2$**·2.5MeOH, and by an inversion centre in **1[BF$_4$]$_2$**·MeCN and **1[BF$_4$]$_2$**·*m*MeNO$_2$.

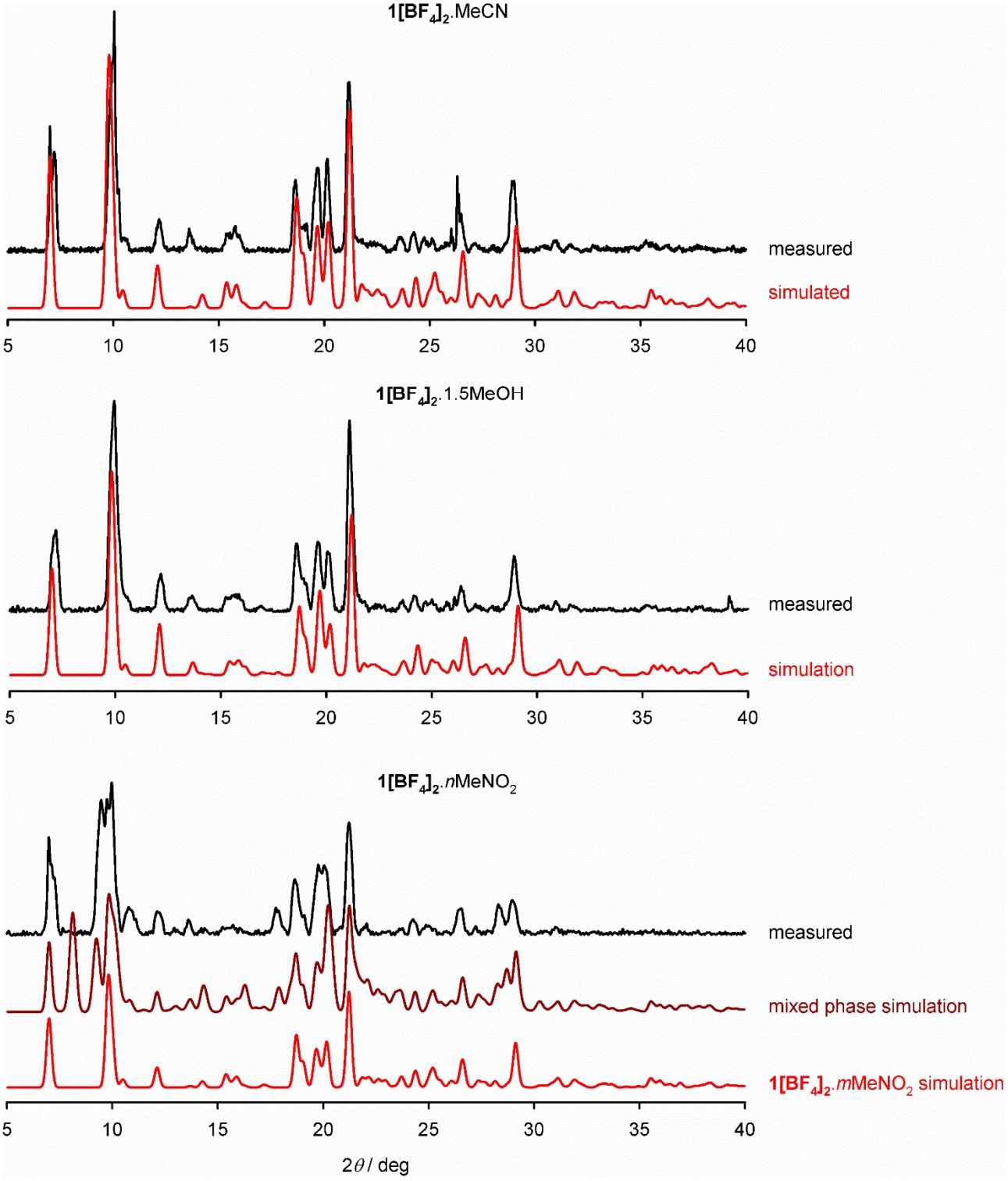

Figure S15 Room temperature X-ray powder diffraction data for the crystallographically characterised solvates of **1[BF$_4$]$_2$** (black), and simulations based on their low temperature crystal structures (red).

The samples retain crystallinity upon exposure to air and do not undergo gross structural changes upon loss or exchange of their lattice solvent.

The mixed-phase simulation of the nitromethane solvate is based on a 1:1 mixture of the **1[BF$_4$]$_2$**·*m*MeNO$_2$ and **1[BF$_4$]$_{1.6}$[SiF$_6$]$_{0.2}$**·1.7MeNO$_2$·0.3Et$_2$O crystal structures. While a peak at $2\theta = 8.1°$ in that simulation is not found experimentally, otherwise it is a reasonable match for the data. We conclude the sample is a mixture of high-spin **1[BF$_4$]$_2$**·*m*MeNO$_2$ and a second phase related to **1[BF$_4$]$_{1.6}$[SiF$_6$]$_{0.2}$**·1.7MeNO$_2$·0.3Et$_2$O, which is SCO-active (Figure S16).

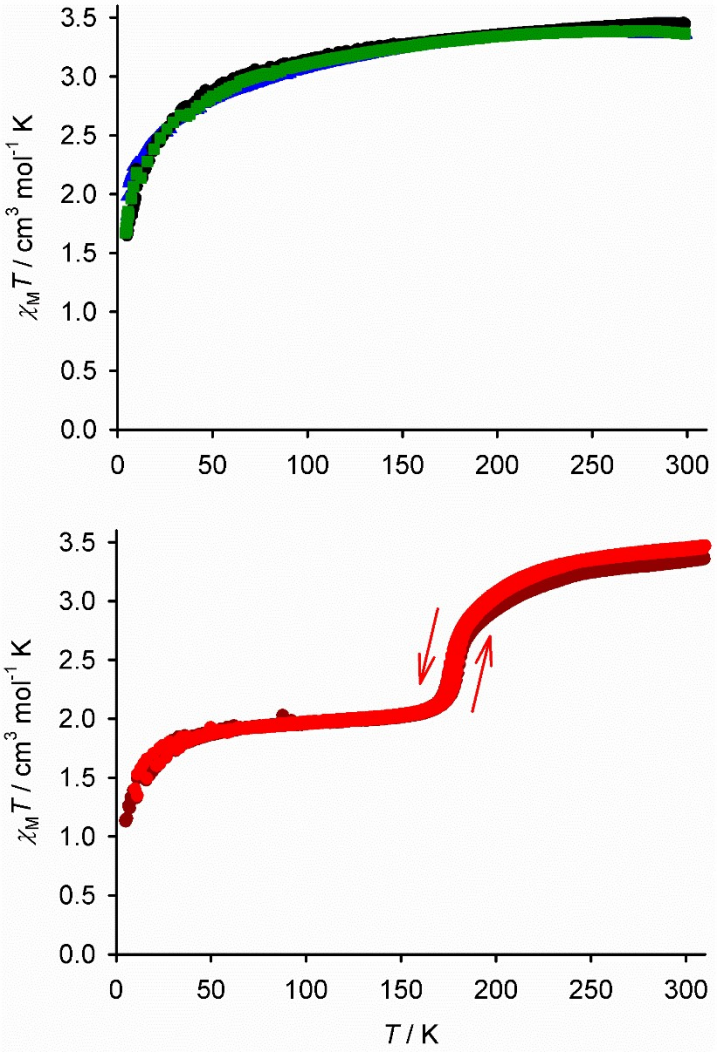

Figure S16 Top: Variable temperature magnetic susceptibility data from freshly crystallised **1[BF$_4$]$_2$**·MeCN (black), **1[BF$_4$]$_2$**·1.5MeOH (green) and **1[BF$_4$]$_2$**·*n*Me$_2$CO (blue). Bottom: Magnetic susceptibility data from a mixed-phase sample **1[BF$_4$]$_2$**·*n*MeNO$_2$ (Figure S15). Two cooling and warming scans of that material are shown, in pale and dark red colouration respectively. The samples were protected against solvent loss during the measurement.

The samples in the top graph are all high-spin, which is consistent with the crystal structures of **1[BF$_4$]$_2$**·MeCN and **1[BF$_4$]$_2$**·1.5MeOH. It is unclear if **1[BF$_4$]$_2$**·*n*Me$_2$CO is isomorphous with those solvates however, since its powder pattern was not measured (that sample was only available in mg quantities, because of the poor solubility of the complex in acetone).

The nitromethane solvate sample contains (at least) two different phases by powder diffraction (Figure S15). These data imply it is a mixture of high-spin and SCO-active material, which is consistent with a combination of the two crystallographically characterised phases. Iron(II) complexes related to **1[BF$_4$]$_{1.6}$[SiF$_6$]$_{0.2}$**·1.7MeNO$_2$·0.3Et$_2$O, that crystallise in a terpyridine embrace lattice, often show abrupt thermal spin-transitions.[19,20]

Since the two scans in the lower graph are identical the partial SCO in the sample is not influenced by *in situ* solvent loss, which presumably happened before the measurement took place.

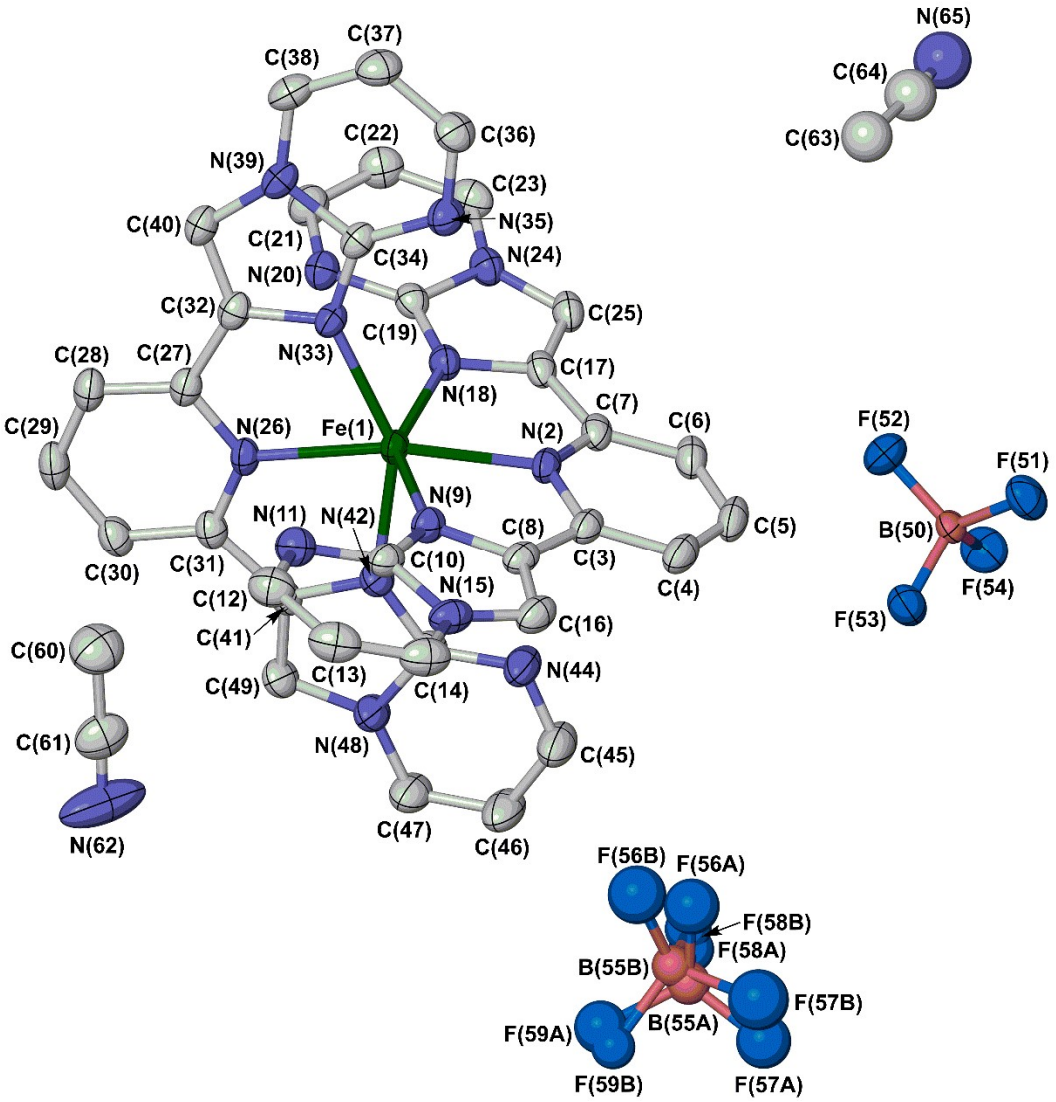

Figure S17 The asymmetric unit of **2[BF_4]$_2$**·1.5MeCN, showing the full atom numbering scheme. All displacement ellipsoids are at the 50 % probability level, and H atoms are omitted for clarity. Both orientations of the disordered BF_4^- ion are shown. Atom C(43) is obscured behind C(14).

Colour code: C, white; B, pink; F, cyan; Fe, green; N, blue.

Atoms C(63)-N(65) comprise a half-molecule of acetonitrile, which spans a crystallographic inversion centre.

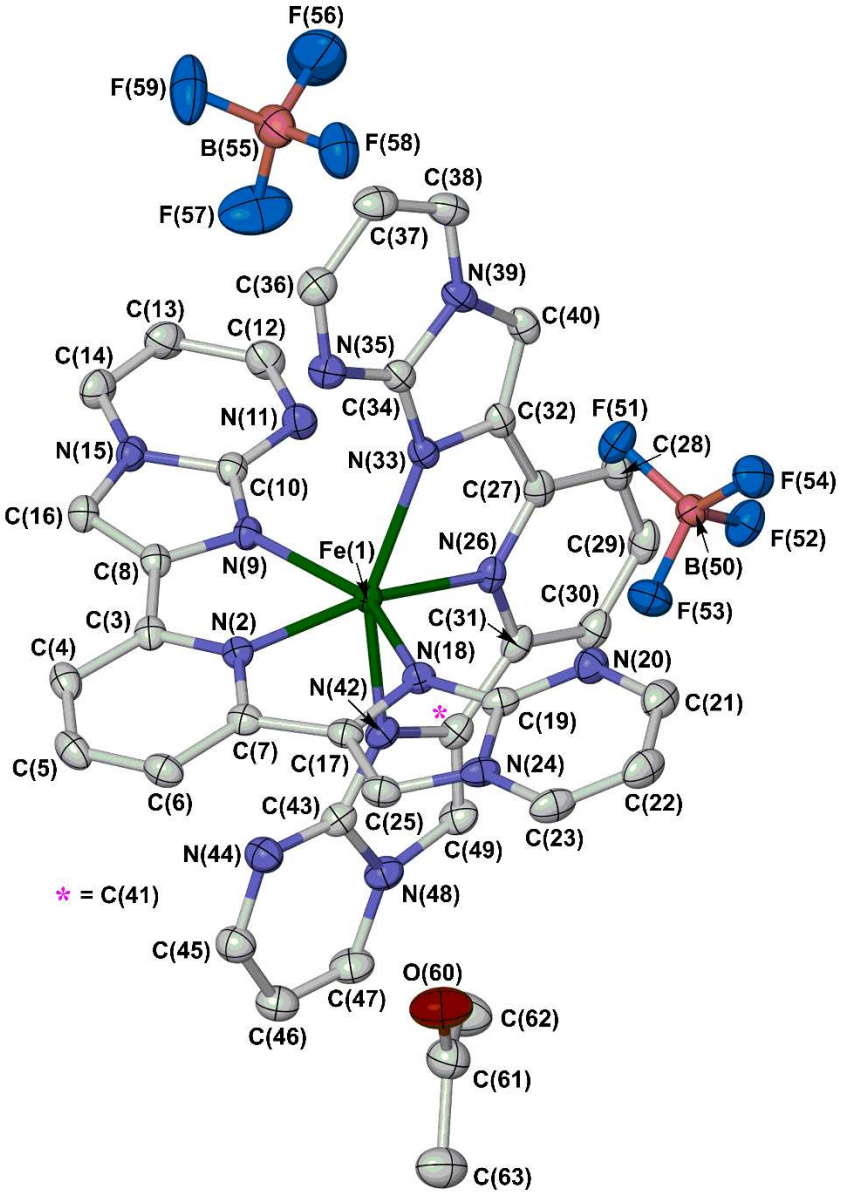

Figure S18 The asymmetric unit of **2[BF$_4$]$_2$**·Me$_2$CO, showing the full atom numbering scheme. All displacement ellipsoids are at the 50 % probability level, and H atoms are omitted for clarity.

Colour code: C, white; B, pink; F, cyan; Fe, green; N, blue; O, red.

This structure is isomorphous with **2[BF$_4$]$_2$**·1.5MeCN (Figure S17), but lacks the additional solvent half-molecule disordered about the crystallographic inversion centre in that crystal.

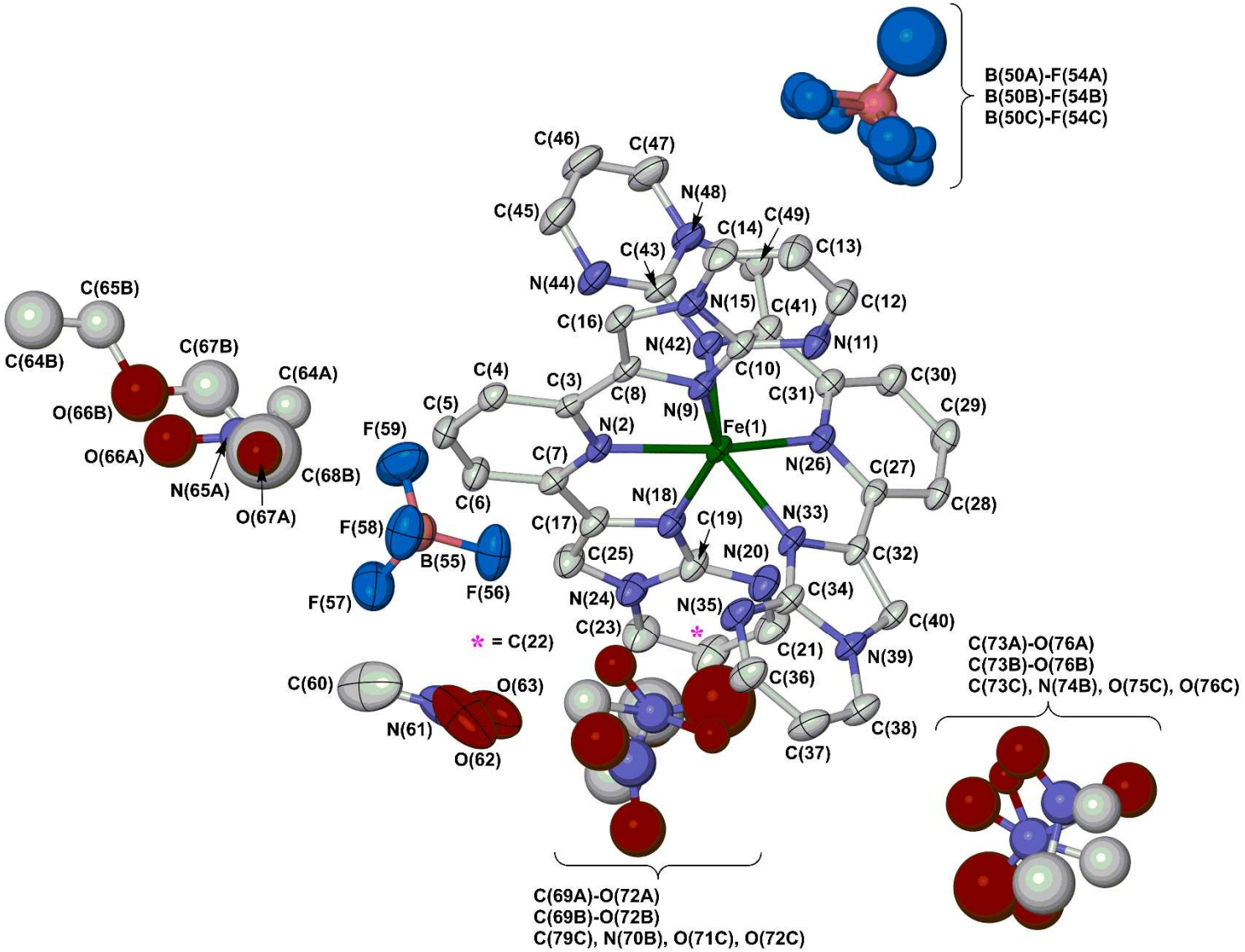

Figure S19 The asymmetric unit of **2[BF$_4$]$_2$**·3.5MeNO$_2$·0.5Et$_2$O, showing the full atom numbering scheme. All displacement ellipsoids are at the 50 % probability level, and H atoms are omitted for clarity.

Colour code: C, white; B, pink; F, cyan; Fe, green; N, blue; O, red.

Table S4 Selected bond lengths and angles in the solvate crystals of **2[BF$_4$]$_2$** (Å, º, Å^3). See Figures S17-S19 for the atom numbering scheme employed, and page S13 for definitions of the structural indices in the Table.

	2[BF$_4$]$_2$·1.5MeCN	**2[BF$_4$]$_2$**·Me$_2$CO	**2[BF$_4$]$_2$**·3.5MeNO$_2$·0.5Et$_2$O
Fe(1)–N(2)	2.148(2)	2.1499(16)	2.160(3)
Fe(1)–N(9)	2.193(2)	2.2076(17)	2.209(3)
Fe(1)–N(18)	2.183(2)	2.1859(17)	2.203(3)
Fe(1)–N(26)	2.154(2)	2.1538(16)	2.162(3)
Fe(1)–N(33)	2.197(2)	2.1849(18)	2.196(3)
Fe(1)–N(42)	2.201(2)	2.1994(18)	2.212(3)
N(2)–Fe(1)–N(9)	74.78(9)	74.45(6)	74.54(12)
N(2)–Fe(1)–N(18)	74.57(9)	75.13(6)	74.36(12)
N(2)–Fe(1)–N(26)	163.52(9)	164.72(7)	156.26(12)
N(2)–Fe(1)–N(33)	120.61(9)	119.88(6)	122.64(13)
N(2)–Fe(1)–N(42)	90.12(9)	91.00(7)	89.15(12)
N(9)–Fe(1)–N(18)	148.43(9)	148.92(6)	148.29(13)
N(9)–Fe(1)–N(26)	110.48(9)	108.55(6)	121.03(13)
N(9)–Fe(1)–N(33)	98.12(9)	98.68(6)	100.68(12)
N(9)–Fe(1)–N(42)	91.67(9)	89.59(6)	91.12(12)
N(18)–Fe(1)–N(26)	101.07(9)	102.48(6)	90.43(13)
N(18)–Fe(1)–N(33)	90.99(9)	90.93(6)	90.88(12)
N(18)–Fe(1)–N(42)	95.79(9)	97.19(6)	94.47(13)
N(26)–Fe(1)–N(33)	74.86(9)	74.95(7)	74.69(12)
N(26)–Fe(1)–N(42)	74.35(9)	74.20(7)	73.69(12)
N(33)–Fe(1)–N(42)	149.19(9)	149.11(6)	147.95(13)
V_{Oh}	12.536(10)	12.586(6)	12.430(12)
Σ	140.3(3)	140.4(2)	144.8(4)
Θ	467	463	482
ϕ	163.52(9)	164.72(7)	156.26(12)
θ	87.59(3)	84.65(1)	88.37(2)

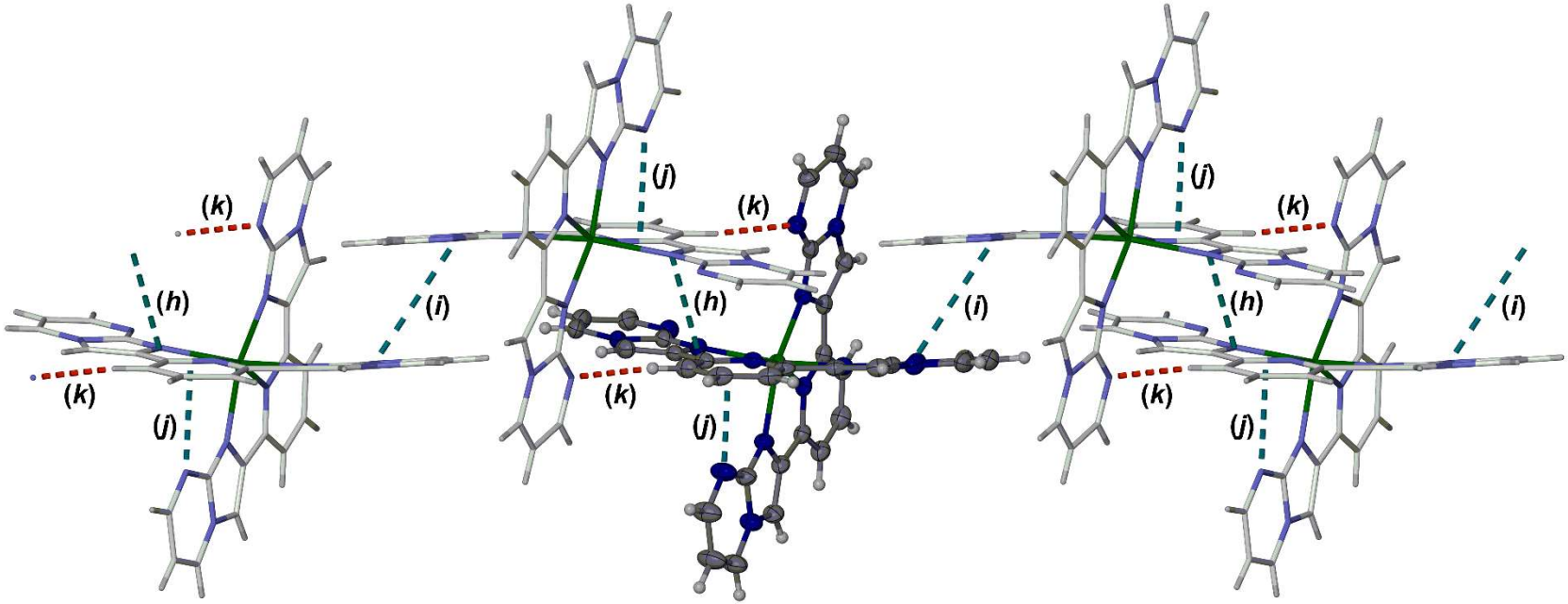

Figure S20 Partial packing diagram of **2[BF$_4$]$_2$**·1.5MeCN, showing the $\pi\cdots\pi$ (cyan) and C–H···N (red) intermolecular contacts between the cations. Each interaction is labelled with a code corresponding to that in Table S5. One cation is highlighted with dark colouration, while the anions and solvent molecules are not shown. Intramolecular N$\cdots\pi$ interactions in these molecules are also omitted (Figure 2, main article).

Colour code: C, white or dark grey; H, pale grey; Fe, green; N, pale or dark blue.

The solvate **2[BF$_4$]$_2$**·Me$_2$CO is isomorphous with this structure, and shows the same pattern of intermolecular contacts.

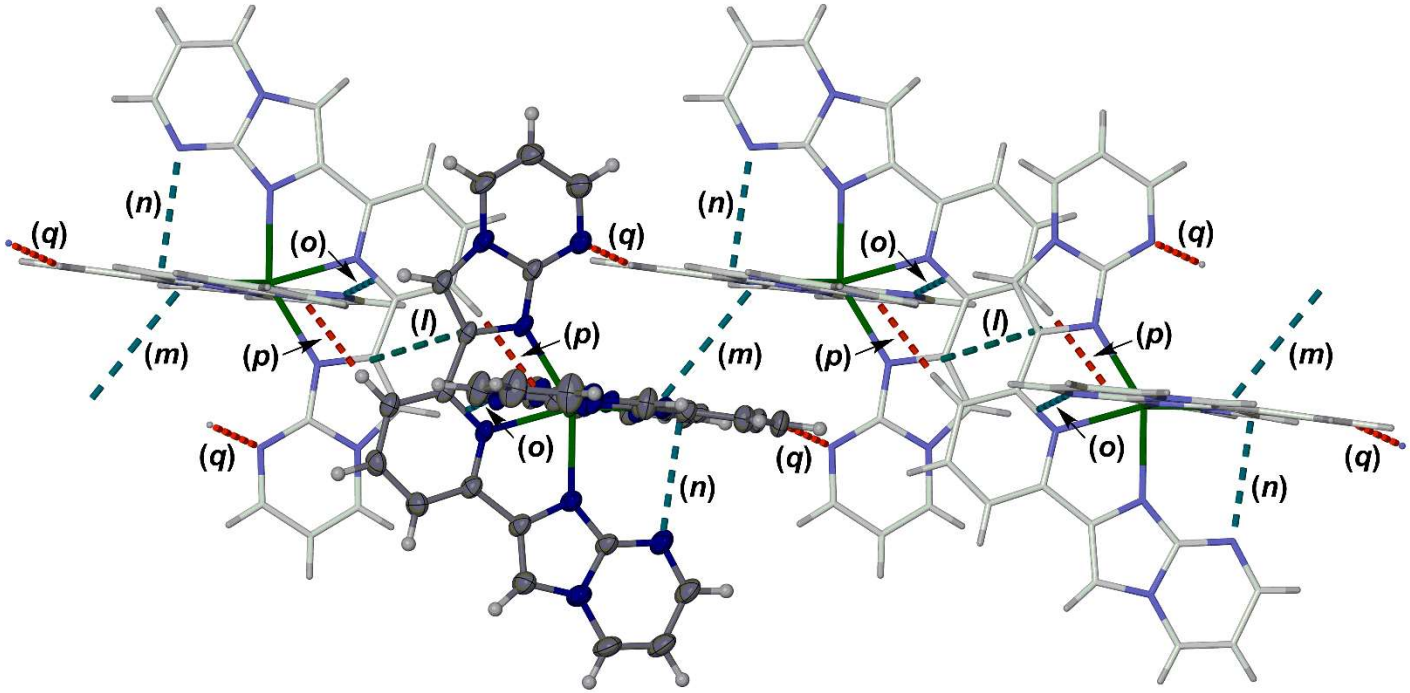

Figure S21 Partial packing diagram of **2[BF$_4$]$_2$**·3.5MeNO$_2$·0.5Et$_2$O, showing the $\pi\cdots\pi$ (cyan) and C–H···N (red) intermolecular contacts between the cations. Each interaction is labelled with a code corresponding to that in Table S5. Other details as for Figure S21.

Colour code: C, white or dark grey; H, pale grey; Fe, green; N, pale or dark blue.

Table S5 Secondary intra- and intermolecular interactions in the solvate crystals of **2[BF$_4$]$_2$** (Å, °). See Figures S17-S19 for the atom numbering scheme employed, while the codes for each interaction are those in Figures S20-S21. Symmetry codes: (v) 1−*x*, 1−*y*, 1−*z*; (x) 2−*x*, 2−*y*, 2−*z*; (xi) 1−*x*, 1−*y*, 2−*z*; (xii) 1−*x*, 2−*y*, 2−*z*.

Intermolecular $\pi\cdots\pi$	Dihedral angle	Interplanar spacing	Horizontal offset	
2[BF$_4$]$_2$·1.5MeCN:				
[N(2)-C(10),N(15),C(16)]⋯ [N(2^{v})-C(10^{v}),N(15^{v}),C(16^{v})] (***h***)	0	3.255(9)	1.24	
[C(17)-C(25)]⋯[C(17^{x})-C(25^{x})] (***i***)	0	3.369(15)	2.46	
2[BF$_4$]$_2$·Me$_2$CO:				
[N(2)-C(10),N(15),C(16)]⋯ [N(2^{v})-C(10^{v}),N(15^{v}),C(16^{v})] (***h***)	0	3.239(6)	1.20	
[C(17)-C(25)]⋯[C(17^{x})-C(25^{x})] (***i***)	0	3.449(11)	2.37	
2[BF$_4$]$_2$·3.5MeNO$_2$·0.5Et$_2$O:				
[N(2)-C(16)]⋯[N(2^{xi})-C(16^{xi})] (***l***)	0	3.388(16)	2.08	
[N(26)-C(40)]⋯[N(26^{xii})-C(40^{xii})] (***m***)	0	3.32(3)	2.07	
Intramolecular N⋯π[a]	N⋯X			
2[BF$_4$]$_2$·1.5MeCN:				
N(44)⋯[N(2)-C(3)] (***j***)	3.059			
2[BF$_4$]$_2$·Me$_2$CO:				
N(44)⋯[N(2)-C(3)] (***j***)	3.067			
2[BF$_4$]$_2$·3.5MeNO$_2$·0.5Et$_2$O:				
N(20)⋯[N(26)-C(27)] (***n***)	3.145			
N(44)⋯[N(2)-C(3)] (***o***)	3.066			
Intermolecular C–H⋯N[b]	C−H	H⋯N	C⋯N	C−H⋯N
2[BF$_4$]$_2$·1.5MeCN:				
C(4)–H(4)⋯N(35^{v}) (***k***)	0.95	2.40	3.335(4)	167.3
2[BF$_4$]$_2$·Me$_2$CO:				
C(4)–H(4)⋯N(35^{v}) (***k***)	0.95	2.45	3.386(3)	170.0
2[BF$_4$]$_2$·3.5MeNO$_2$·0.5Et$_2$O:				
C(4)–H(4)⋯N(35^{xi}) (***p***)	0.95	2.47	3.408(5)	168.5
C(28)–H(28)⋯N(11^{xii}) (***q***)	0.95	2.44	3.379(5)	169.4

[a]This is an intramolecular dipolar contact, between the lone pair of a peripheral N atom of one ligand and the centroid of a pyridyl C−N bond on the other. The sum of the Pauling van der Waals radii of an N atom and an aromatic ring is 3.1 Å.[17] [b]The sum of the Pauling van der Waals radii of an H atom and an N atom is 2.6 Å.[18]

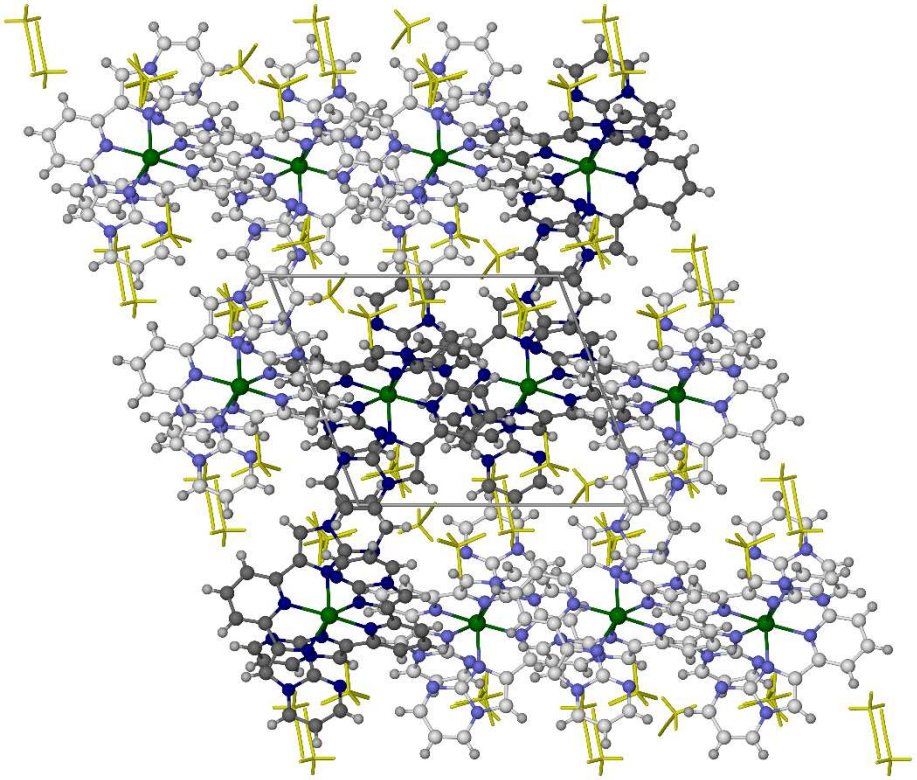

Figure S22 Full packing diagram of **2[BF$_4$]$_2$**·1.5MeCN. The view is parallel to the [010] crystal vector, with the unit cell *c* axis horizontal. One cation chain (Figure S20) is highlighted with dark colouration, while the anions and solvent molecules are de-emphasised for clarity. Both orientations are shown for the MeCN half-molecule disordered about the crystallographic inversion centre.

Colour code: C, white or dark grey; H, pale grey; Fe, green; N, pale or dark blue; BF_4^- and MeCN, yellow.

The complex cations associate into zig-zag chains along the [111] direction, through intermolecular $\pi\cdots\pi$ interactions and C–H···N contacts (Figure S20, Table S5).

2[BF$_4$]$_2$·Me_2CO is isomorphous with this structure and exhibits the same crystal packing motif. However, the pair of solvent half-molecules spanning inversion centres in this Figure, is missing in the acetone solvate.

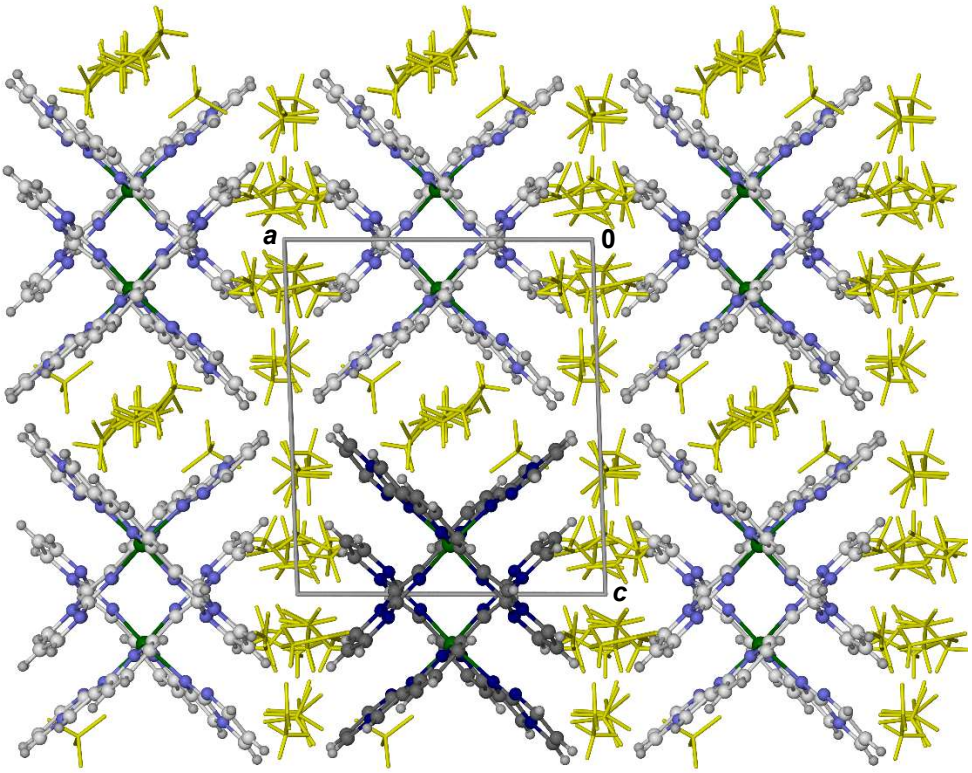

Figure S23 Full packing diagram of **2[BF_4]$_2$**·3.5$MeNO_2$·0.5Et_2O, viewed parallel to the [010] crystal vector. One π-stacked cation chain (Figure S21) is highlighted with dark colouration, while the anions and solvent molecules are de-emphasised for clarity.

Colour code: C, white or dark grey; H, pale grey; Fe, green; N, pale or dark blue; BF_4^- and MeCN, yellow.

The complex cations associate into zig-zag chains along the unit cell *b* axis, through intermolecular $\pi\cdots\pi$ interactions and C–H···N contacts (Figure S21, Table S5).

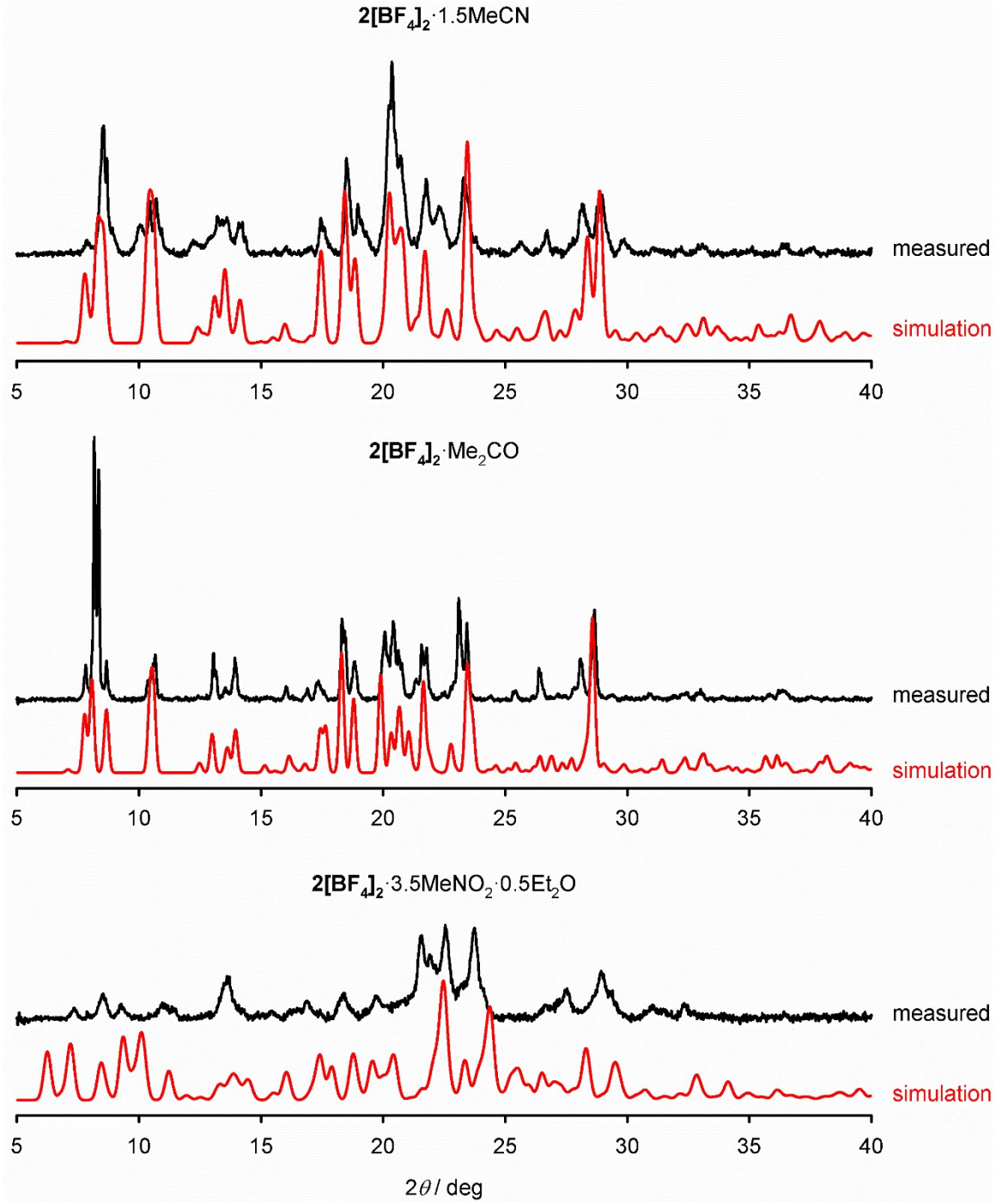

Figure S24 Experimental X-ray powder diffraction data for the crystallographically characterised solvates of **2[BF$_4$]$_2$** (black), and simulations based on their low temperature crystal structures (red).

The acetonitrile and acetone solvates retain good crystallinity upon exposure to air, with just small structural changes compared to the single crystal phases. However, **2[BF$_4$]$_2$**·3.5MeNO$_2$·0.5Et$_2$O collapses to a poorly crystalline powder showing significant structural differences from the parent solvate material.

.

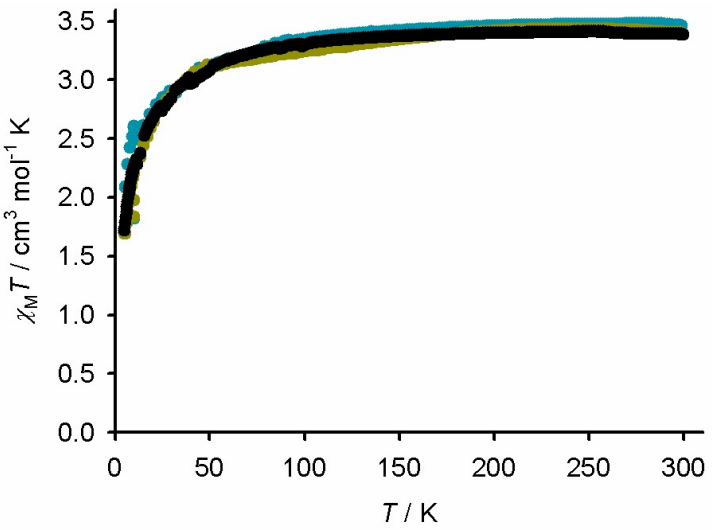

Figure S25 Variable temperature magnetic susceptibility data from freshly crystallised $[Fe(L^2)_2][BF_4]_2 \cdot Me_2CO$ (black), **2[BF$_4$]$_2$**·1.5MeCN (yellow) and **2[BF$_4$]$_2$**·3.5$MeNO_2$·0.5Et_2O (cyan). The samples were protected against solvent loss during the measurement.

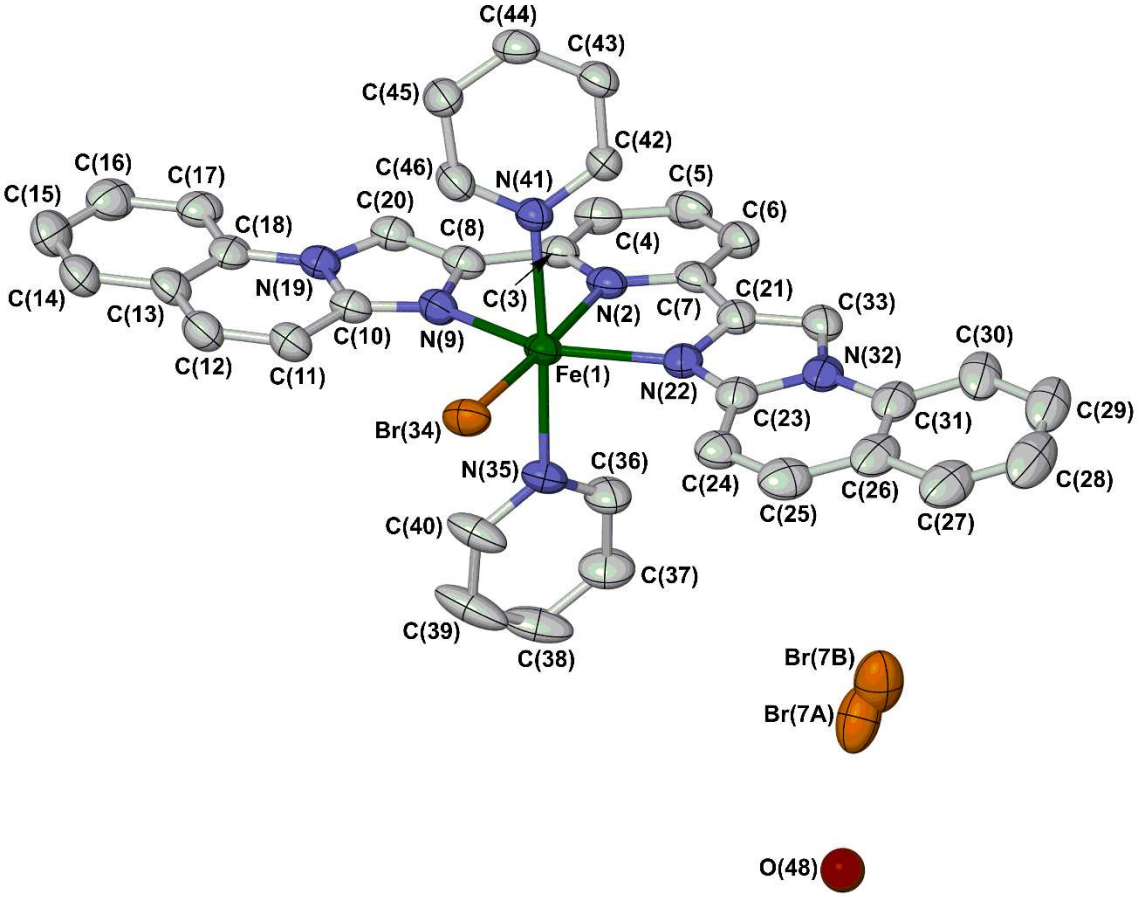

Figure S26 The asymmetric unit of $[FeBr(py)_2(L^3)]Br{\cdot}0.5H_2O$, showing the full atom numbering scheme. All displacement ellipsoids are at the 50 % probability level, and H atoms are omitted for clarity. Both orientations of the disordered bromide ion are shown, while the partial water molecule O(48) is half-occupied.

Colour code: C, white; Br, orange; Fe, green; N, blue; O, red.

The disordered bromide ion and water half-molecule occupy the same cavity surrounding a crystallographic inversion centre. Although its H atoms were not located, the partial water site is positioned to hydrogen bond to Br(7B) and Br(7A^{i}) [symmetry code: (i) $-x$, $1-y$, $1-z$; O(48)···Br(7B) = 3.357(7) Å; O(48)···Br(7A^{i}) = 3.286(7) Å; Br(7B)···O(48)···Br(7A^{i}) =101.50(19)°].

Table S6 Selected bond lengths, angles and other metric parameters for $[FeBr(py)_2(L^3)]Br{\cdot}0.5H_2O$ (Å, °, Å^3). See Figure S25 for the atom numbering scheme, while definitions of V_{Oh}, Σ and Θ are on page S13.

Fe(1)–N(2)	2.176(4)	Fe(1)–Br(34)	2.5079(8)
Fe(1)–N(9)	2.175(4)	Fe(1)–N(35)	2.252(4)
Fe(1)–N(22)	2.165(4)	Fe(1)–N(41)	2.260(3)
N(2)–Fe(1)–N(9)	73.99(14)	N(9)–Fe(1)–N(41)	87.00(13)
N(2)–Fe(1)–N(22)	74.73(15)	N(22)–Fe(1)–Br(34)	106.49(11)
N(2)–Fe(1)–Br(34)	176.85(9)	N(22)–Fe(1)–N(35)	90.52(14)
N(2)–Fe(1)–N(35)	90.54(14)	N(22)–Fe(1)–N(41)	93.39(13)
N(2)–Fe(1)–N(41)	86.18(13)	Br(34)–Fe(1)–N(35)	92.35(11)
N(9)–Fe(1)–N(22)	148.61(15)	Br(34)–Fe(1)–N(41)	90.83(10)
N(9)–Fe(1)–Br(34)	104.88(10)	N(35)–Fe(1)–N(41)	174.07(14)
N(9)–Fe(1)–N(35)	87.34(14)		
V_{Oh}	14.692(15)	Σ	79.8(4)
		Θ	202

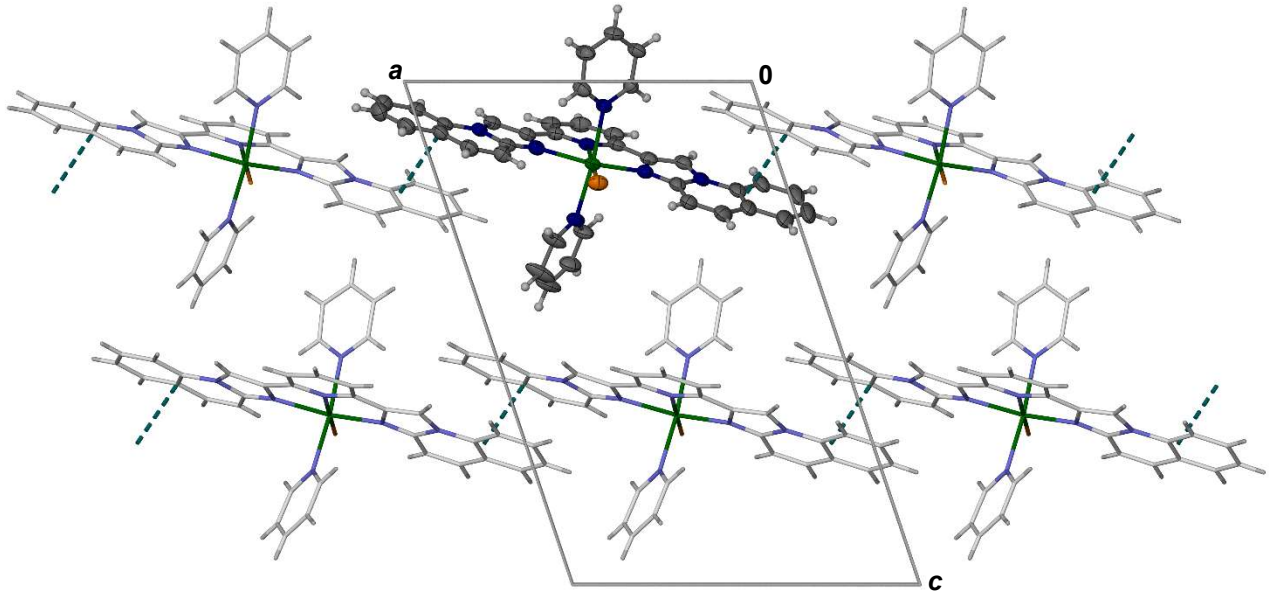

Figure S27 Packing diagram of $[FeBr(py)_2(L^3)]Br{\cdot}0.5H_2O$, showing the association of the molecules into chains parallel to [100] through $\pi\cdots\pi$ interactions between their L^3 quinolyl residues (shown as dotted lines). One molecule is highlighted with dark colouration, while the other molecules are de-emphasised for clarity. The bromide anions and water half-molecules are not shown.

Colour code: C, white or dark grey; H, pale grey; Br, orange; Fe, green; N, pale or dark blue; O, red.

The dihedral angle between the least squares planes of the interacting quinolyl groups [C(10)-N(19)] and [C(23^{xiii})-N(32^{xiii})] is 8.45(16)°; the average distance between the overlapping rings is 3.520(18) Å; and their centroids are horizontally offset by 1.13 Å [symmetry code: (xiii) 1+x, y, z].

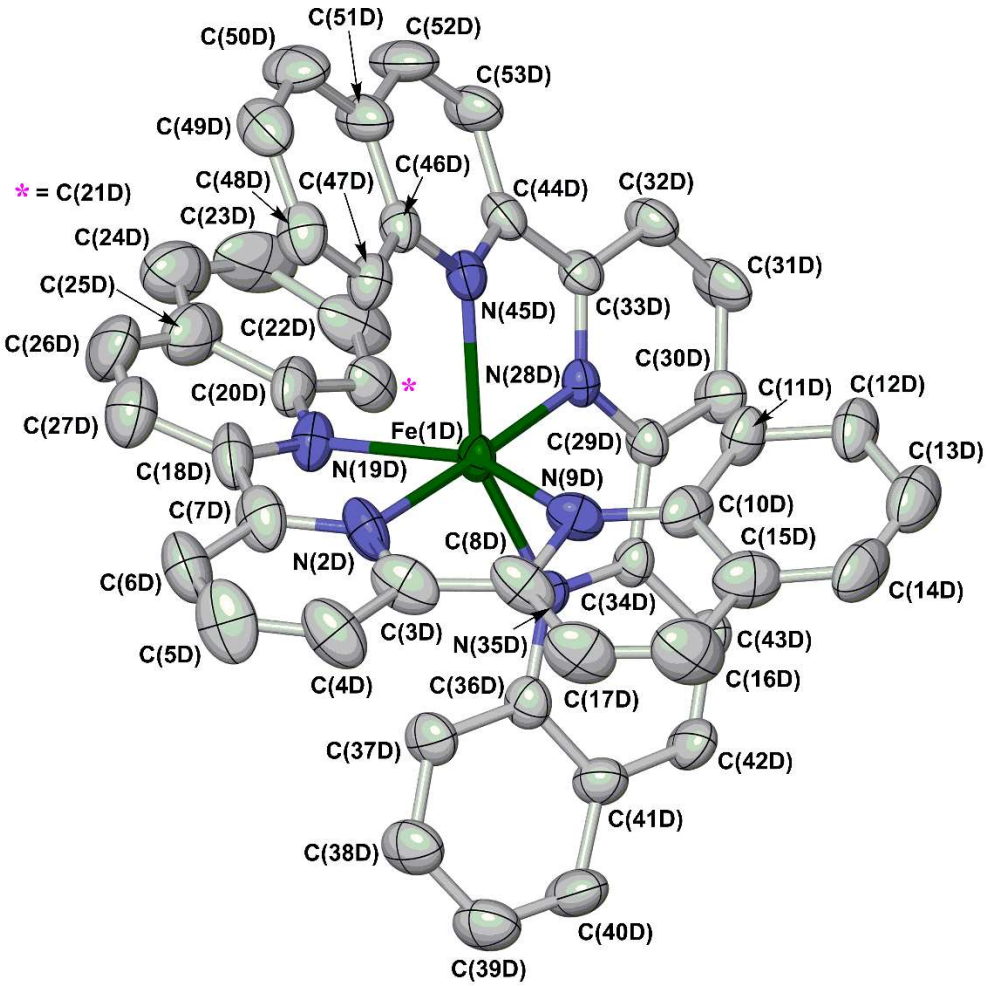

Figure S28 Molecule D in the refinement of **4[BF_4]$_2$**·1.39MeCN·0.125Et_2O·0.25H_2O, showing the full atom numbering scheme. All displacement ellipsoids are at the 50 % probability level, and H atoms are omitted for clarity.

Colour code: C, white; Fe, green; N, blue.

Molecule D is shown here as the least distorted cation in the asymmetric unit, which gives the clearest view. Molecules A-C in the model follow the same atom numbering scheme as shown here, with 'A', 'B' or 'C' suffixes on the atom labels as appropriate (Figure S28).

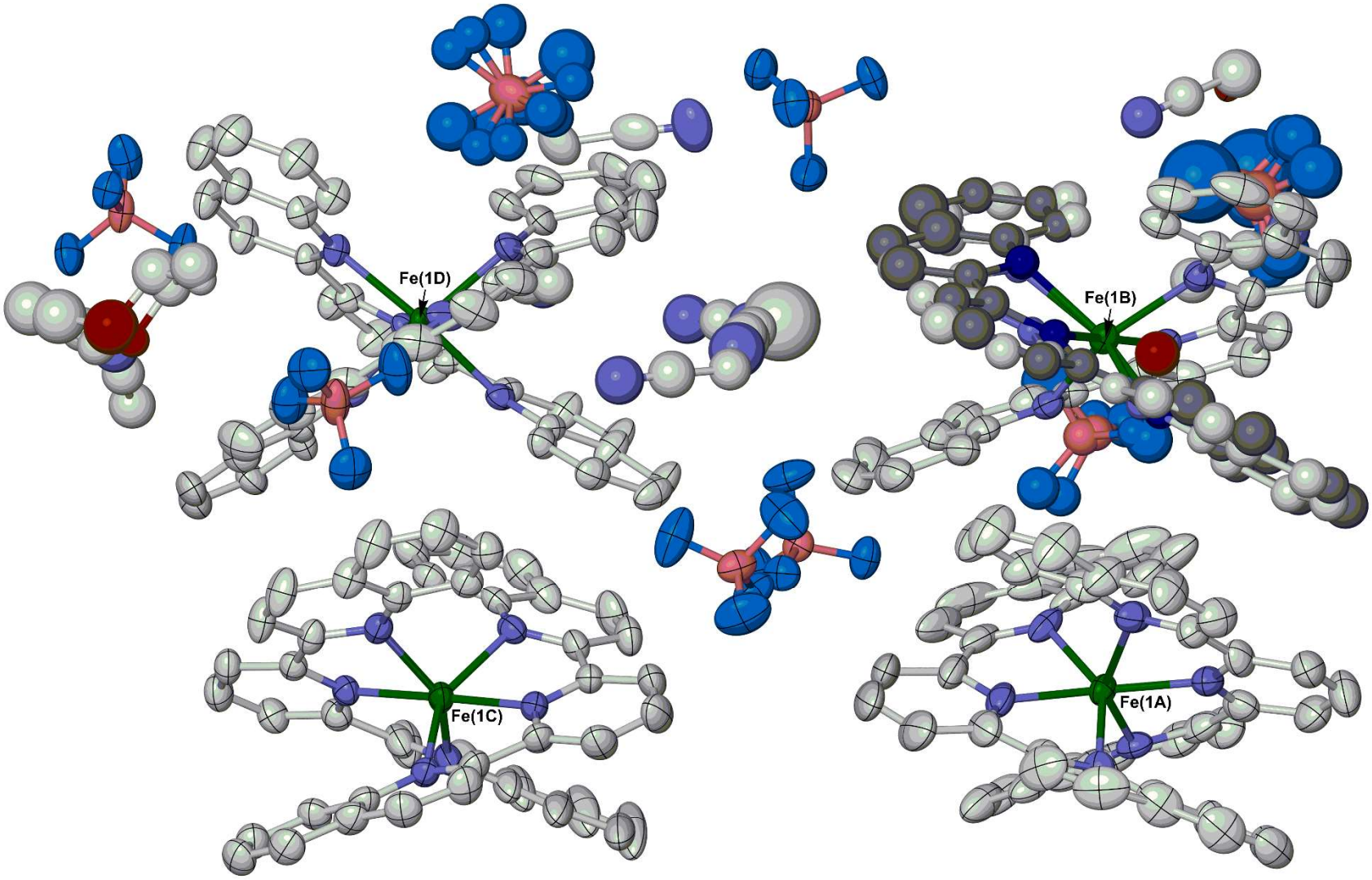

Figure S29 The asymmetric unit of **4[BF_4]$_2$**·1.39MeCN·0.125Et_2O·0.25H_2O. The iron atoms in molecules A, B, C and D are labelled in the Figure; the other atoms labels in the complex molecules follow the scheme in Figure S27. The two ligand disorder orientations bound to Fe(1B) are distinguished by pale and dark colouration. All displacement ellipsoids are at the 50 % probability level, and H atoms are omitted for clarity.

Colour code: C, white or dark gray; B, pink; F, cyan; Fe, green; N, pale or dark blue; O, red.

Table S7 Selected bond lengths and angles in **4[BF$_4$]$_2$**·1.39MeCN·0.125Et$_2$O·0.25H$_2$O (Å, º, Å^3). See Figures S28-S29 for the atom numbering scheme employed, and page S13 for definitions of the structural indices in the Table.

	molecule A	molecule B[a]	molecule C	molecule D
Fe(1)–N(2)	2.073(6)	2.100(5)	2.088(5)	2.114(5)
Fe(1)–N(9)	2.234(5)	2.271(5)	2.252(5)	2.249(5)
Fe(1)–N(19)	2.319(6)	2.299(5)	2.280(5)	2.252(5)
Fe(1)–N(28)	2.102(6)	2.148(9)/2.049(15)	2.088(5)	2.099(4)
Fe(1)–N(35)	2.315(5)	2.287(9)/2.235(10)	2.298(6)	2.252(5)
Fe(1)–N(45)	2.221(5)	2.252(9)/2.335(8)	2.265(5)	2.286(5)
N(2)–Fe(1)–N(9)	76.2(2)	73.44(19)	74.58(19)	73.4(2)
N(2)–Fe(1)–N(19)	72.5(2)	73.08(19)	73.71(19)	74.6(2)
N(2)–Fe(1)–N(28)	164.9(2)	173.6(3)/173.1(5)	177.8(2)	177.6(2)
N(2)–Fe(1)–N(35)	95.2(2)	103.3(3)/109.5(3)	106.8(2)	106.9(2)
N(2)–Fe(1)–N(45)	117.6(2)	112.9(3)/101.2(3)	105.0(2)	104.8(2)
N(9)–Fe(1)–N(19)	148.0(2)	146.53(19)	148.29(18)	147.99(19)
N(9)–Fe(1)–N(28)	115.8(2)	111.5(3)/101.8(5)	107.60(19)	108.75(18)
N(9)–Fe(1)–N(35)	107.15(18)	109.8(3)/105.1(3)	81.06(19)	88.89(18)
N(9)–Fe(1)–N(45)	83.46(19)	84.2(3)/80.4(3)	106.42(18)	101.61(18)
N(19)–Fe(1)–N(28)	96.2(2)	101.9(3)/111.5(5)	104.11(18)	103.25(18)
N(19)–Fe(1)–N(35)	82.62(19)	78.3(3)/86.2(3)	107.5(2)	100.14(18)
N(19)–Fe(1)–N(45)	104.96(19)	108.7(3)/106.0(3)	82.60(18)	86.72(18)
N(28)–Fe(1)–N(35)	73.1(2)	71.3(4)/76.3(5)	74.03(19)	74.34(17)
N(28)–Fe(1)–N(45)	74.4(2)	72.3(4)/72.8(5)	74.19(19)	73.94(17)
N(35)–Fe(1)–N(45)	147.2(2)	143.6(4)/149.1(3)	148.13(19)	148.28(16)
V_{Oh}	12.73(2)	12.85(3)/12.99(4)	12.94(2)	13.149(18)
Σ	174.6(7)	195.5(11)/172.9(13)	177.3(7)	153.6(7)
Θ	486	529/482	476	476
ϕ	164.9(2)	173.6(3)/173.1(5)	177.8(2)	177.6(2)
θ	57.75(5)	60.15(7)/61.04(9)	62.64(5)	73.38(4)

[a]Ligand N(28B)-C(53B) is disordered over two orientations, with a refined occupancy ratio of 0.61:0.39.

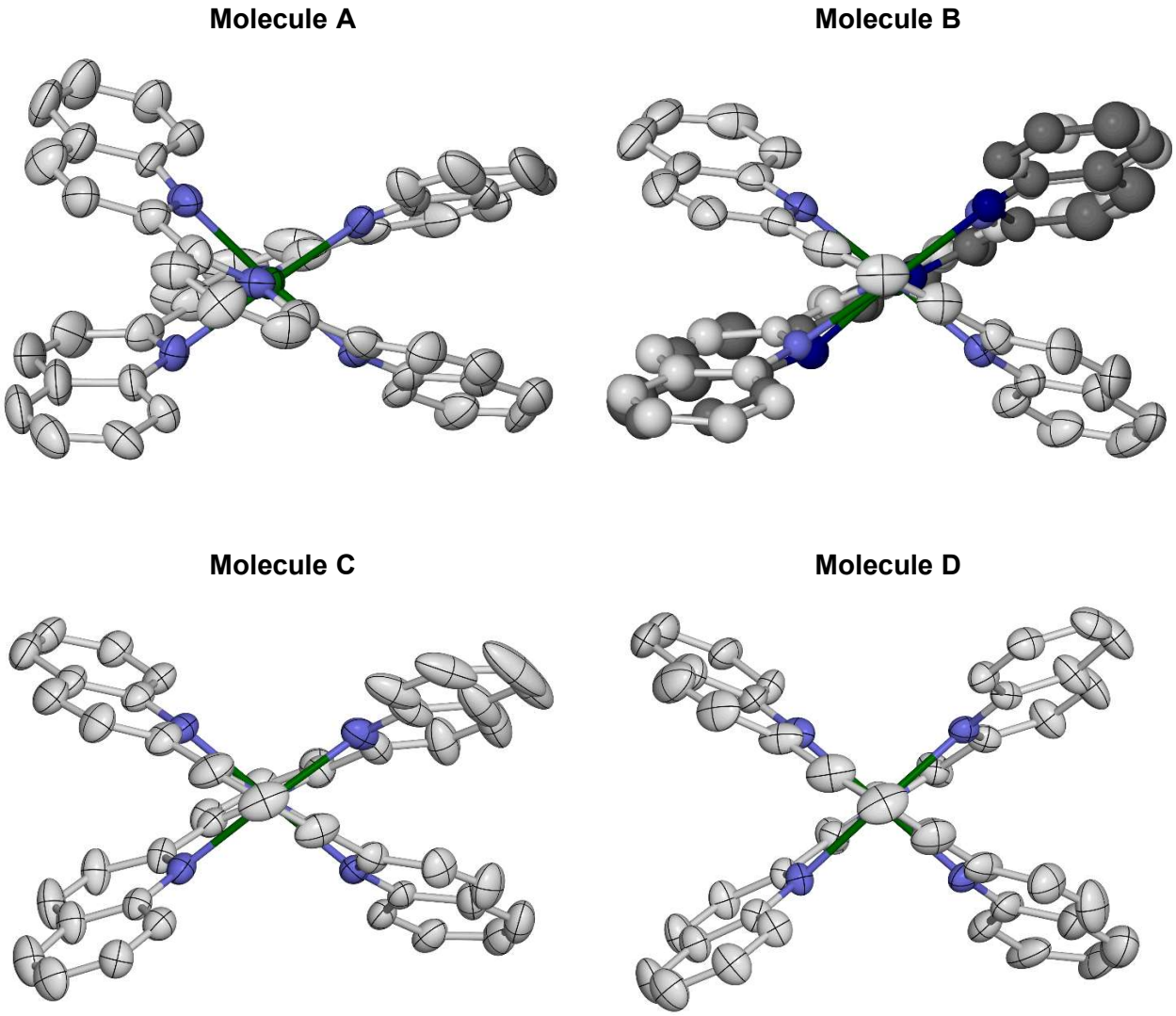

Figure S30 The four unique complex molecules in **4[BF$_4$]$_2$**·1.39MeCN·0.125Et$_2$O·0.25H$_2$O. The views are parallel to the N(2)···N(28) vector in each molecule (Figure S28), which is chosen to highlight their helical ligand conformations. Other details as for Figure S29.

Molecules C and D are inverted in the Figure, so their handedness is the same as molecules A and B (the crystal adopts a centrosymmetric space group, $P2_1/c$).

Colour code: C, white or dark gray; Fe, green; N, pale or dark blue.

The degree of helicity in the molecules runs as A > B ≈ C > D, based on two criteria: the canting of the two L^4 ligands away from the perpendicular (θ, Table S6); and, the dihedral angle between overlapping pairs of quinolyl residues in each molecule (Table S7).

There are short interatomic contacts between overlapping quinolyl groups on the two ligands in each molecule, implying a degree of $\pi\cdots\pi$ contact between them. Only in molecule A are these groups close enough, and coplanar enough, to be considered a traditional weak $\pi\cdots\pi$ interaction however (Table S7).

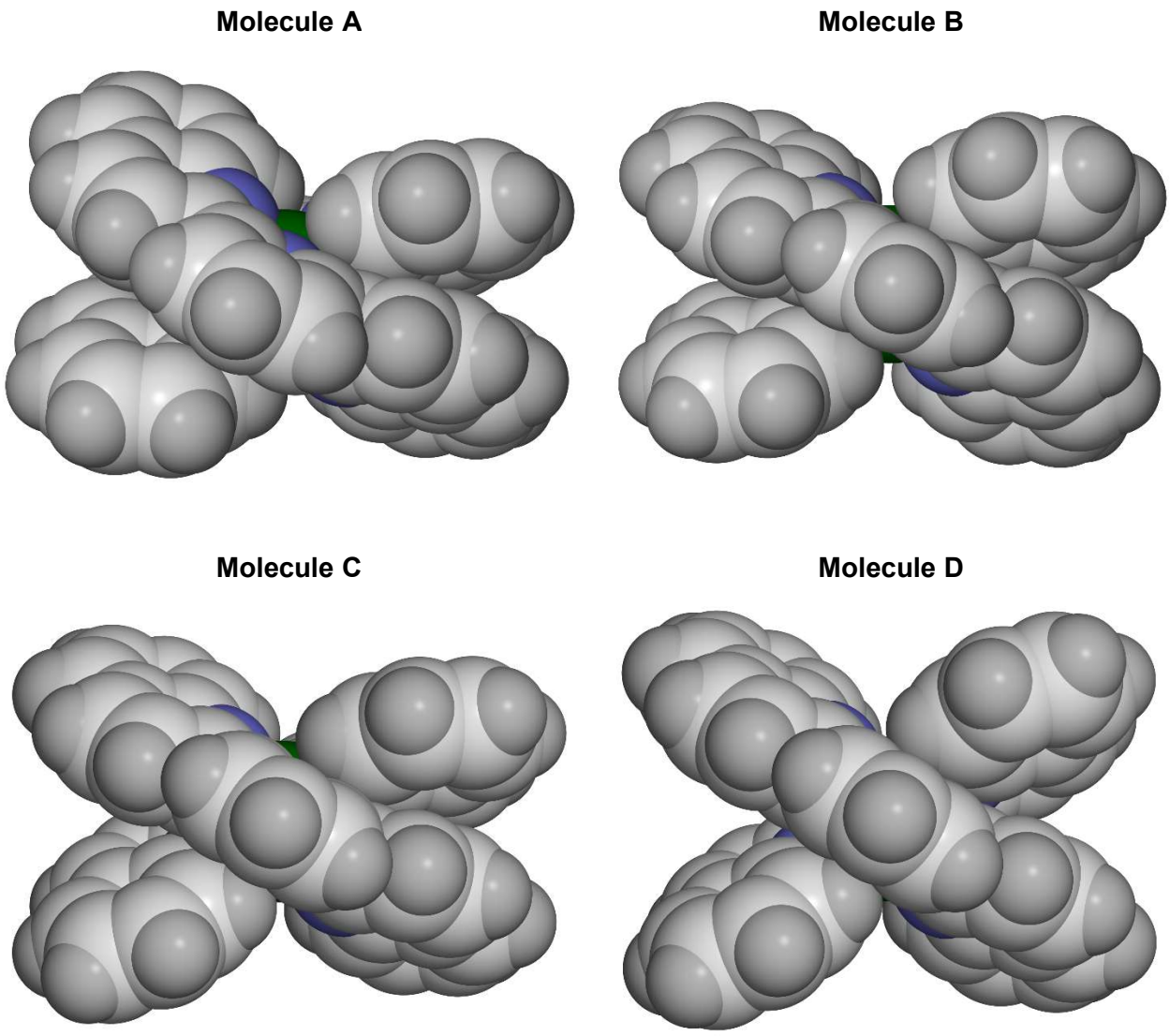

Figure S31 Space-filling views of the four unique complex molecules in **4[BF$_4$]$_2$**·1.39MeCN·0.125Et$_2$O·-0.25H$_2$O. The views are the same as in Figure S30, parallel to the N(2)···N(28) vector in each molecule. Only the major ligand disorder orientation for mol B is shown. Other details as for Figure S30.

Colour code: C, white; H, pale grey; Fe, green; N, blue.

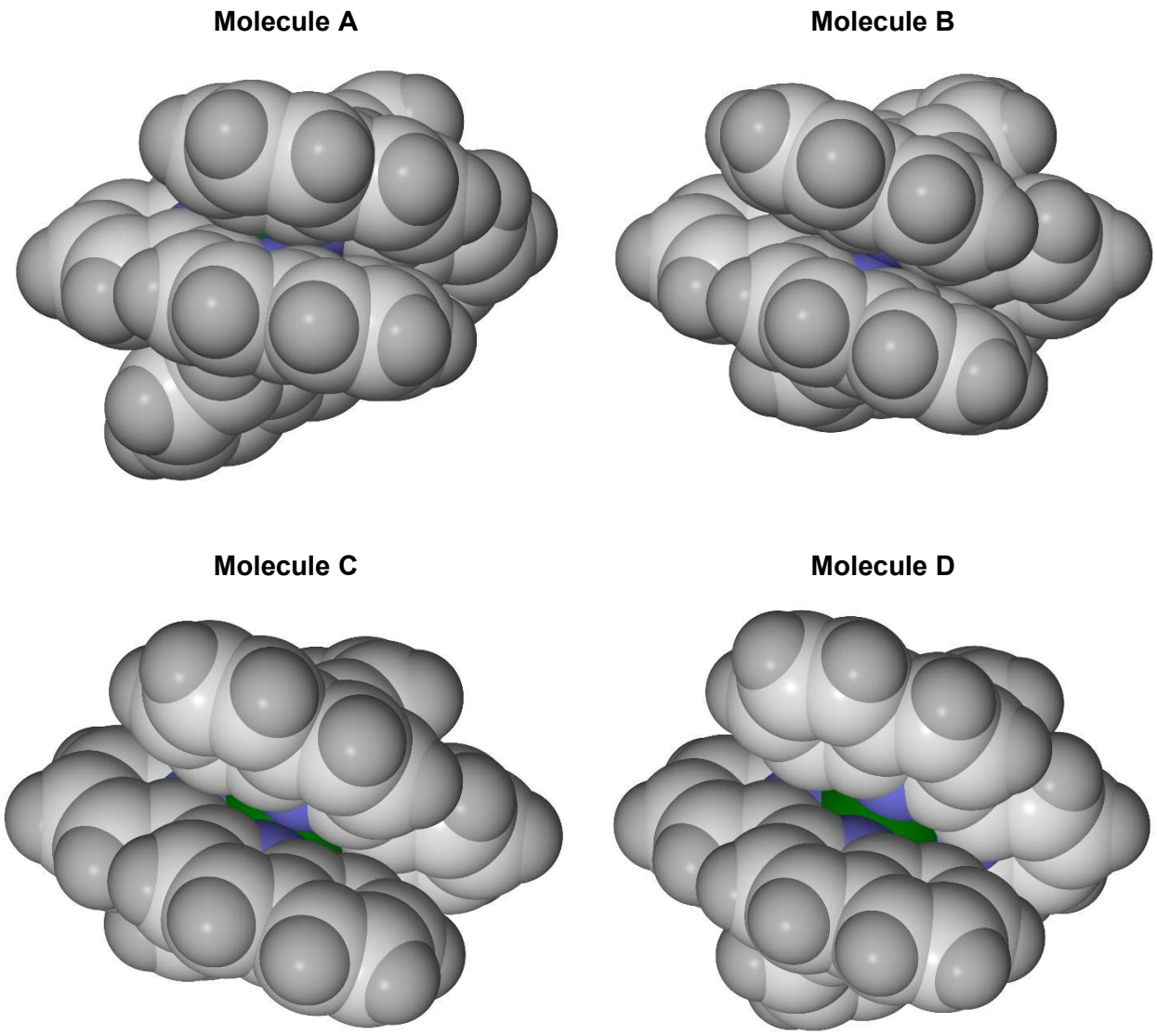

Figure S32 Alternative space-filling views of the four unique complex molecules in **4[BF$_4$]$_2$**·1.39MeCN·-0.125Et$_2$O·0.25H$_2$O. The views are perpendicular to those in Figures S30 and S31, and emphasise the helical conformations of the molecules. Other details as for Figure S30.

Colour code: C, white; H, pale grey; Fe, green; N, blue.

Table S8 Intramolecular contacts between overlapping quinolyl groups in the helical ligand conformation of **4[BF_4]$_2$**·1.39MeCN·0.125Et_2O·0.25H_2O (Å, °; Figures S31-S32). The Table lists the standard metric parameters for face-to-face $\pi\cdots\pi$ interactions between overlapping quinolyl groups, with the most significant closest interatomic contacts between each pair of quinolyl rings.

$\pi\cdots\pi$	Dihedral angle	Average inter-planar spacing	Horizontal offset	Shortest interatomic contacts	
[C(8A)-C(17A)]···[C(44A)-C(53A)]	19.7(2)	3.43(3)	0.72	C(8A)···C(47A) N(9A)···C(46A)	3.174(10) 3.239(8)
[N(2A)-C(7A), C(18A)-C(27A)]··· [N(28A)-C(33A), C(34A)-C(43A)][a]	28.85(18)	3.15(4)	1.07	N(2A)···C(37A) C(18A)···C(36A) N(19A)···N(35A) C(21A)···N(28A)	3.084(8) 3.362(10) 3.059(8) 3.103(8)
[C(8B)-C(17B)]···[C(44B)-C(53B)][b]	27.0(3)/24.5(5)	3.78(3)/3.61(5)	1.32/1.91	C(8B)···C(47B) N(9B)···N(45B) C(11B)···C(33B) C(11B)···C(44B)	3.410(13)/3.376(13) 3.034(10)/2.973(12) 3.458(13)/3.26(2) 3.408(13)/3.374(14)
[C(18B)-C(27B)]···[C(34B)-C(43B)][b]	15.9(3)/21.7(5)	3.56(3)/3.75(5)	1.61/1.17	C(18B)···C(36B) C(18B)···C(37B) N(19B)···N(35B)	3.296(14)/3.474(10) 3.441(15)/3.327(14) 2.896(11)/3.098(13)
[C(8C)-C(17C)]···[C(34C)-C(43C)]	18.6(2)	3.52(3)	1.30	C(8C)···C(37C) N(9C)···N(35C) C(10C)···N(35C)	3.310(10) 2.957(7) 3.294(8)
[C(18C)-C(27C)]···[C(44C)-C(53C)]	38.4(2)	3.82(3)	2.29	N(19C)···N(45C) C(21C)···C(33C)	2.999(7) 3.229(8)
[C(8D)-C(17D)]···[C(34D)-C(43D)]	54.05(14)	4.18(3)	2.43	N(9D)···N(35D)	3.152(7)
[C(18D)-C(27D)]···[C(44D)-C(53D)]	37.48(15)	3.94(3)	2.29	N(19D)···N(45D) C(21D)···C(33D)	3.116(7) 3.382(8)

[a]These residues are oriented so there is significant overlap between the {pyridyl}quinolyl residues on each ligand, rather than simply the quinolyl groups. More reasonable metric parameters are obtained when the pyridyl group on each ligand is included in the interaction. [b]Values are given for both disorder sites of ligand N(28B)-C(53B) (Figure S30).

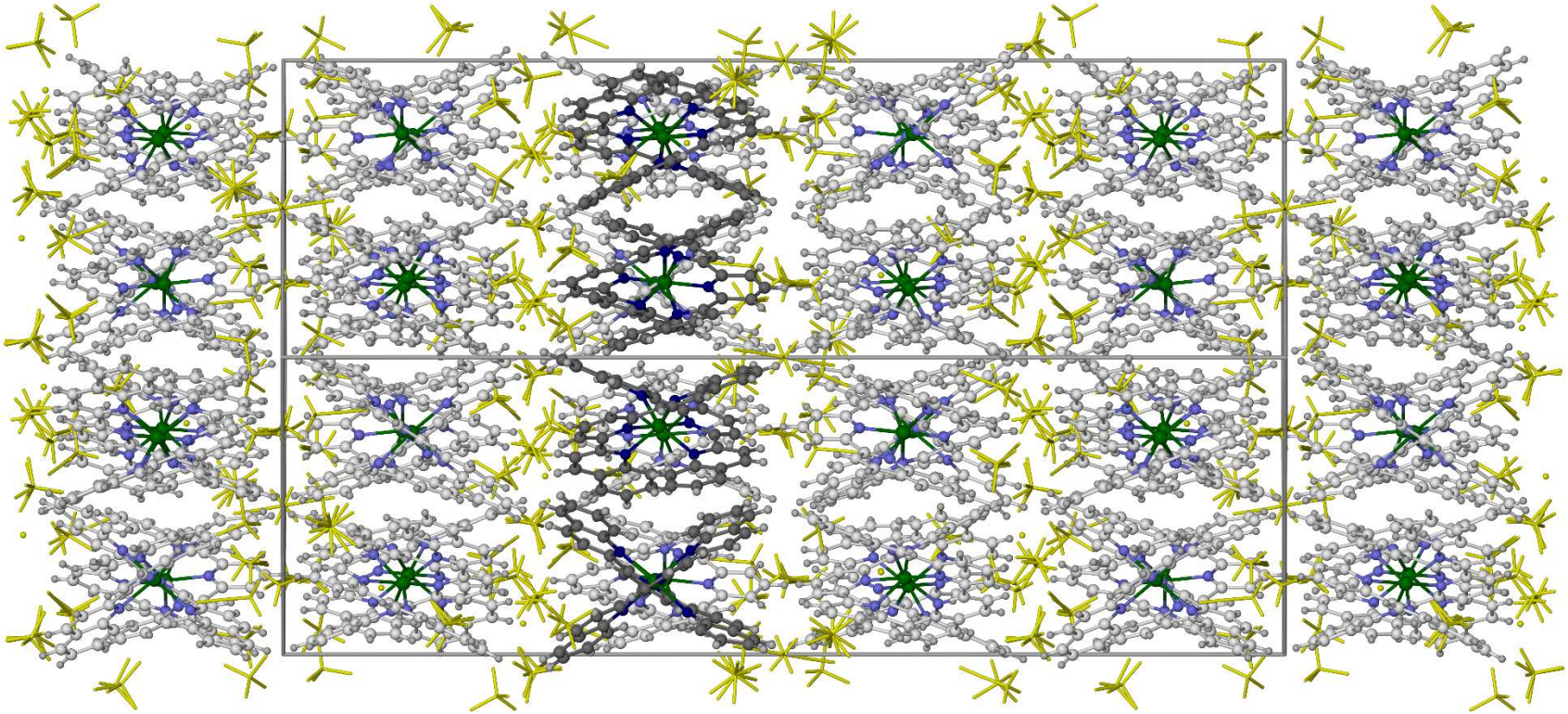

Figure S33 Full packing diagram of **4[BF_4]$_2$**·1.39MeCN·0.125Et_2O·0.25H_2O, viewed parallel to the [101] crystal vector with the *b* horizontal. One helical cation stack is highlighted with dark colouration, while the anions and solvent molecules are de-emphasised for clarity.

Colour code: C, white or dark gray; H, pale gray; B, pink; F, cyan; Fe, green; N, pale or dark blue; BF_4^-, MeCN, Et_2O and H_2O, yellow.

The A, B, D and C cation sites alternate (in that order) down the [$10\bar{1}$] vector, forming helical stacks through intermolecular $\pi\cdots\pi$ interactions (Figures S34 and S35, Table S9).

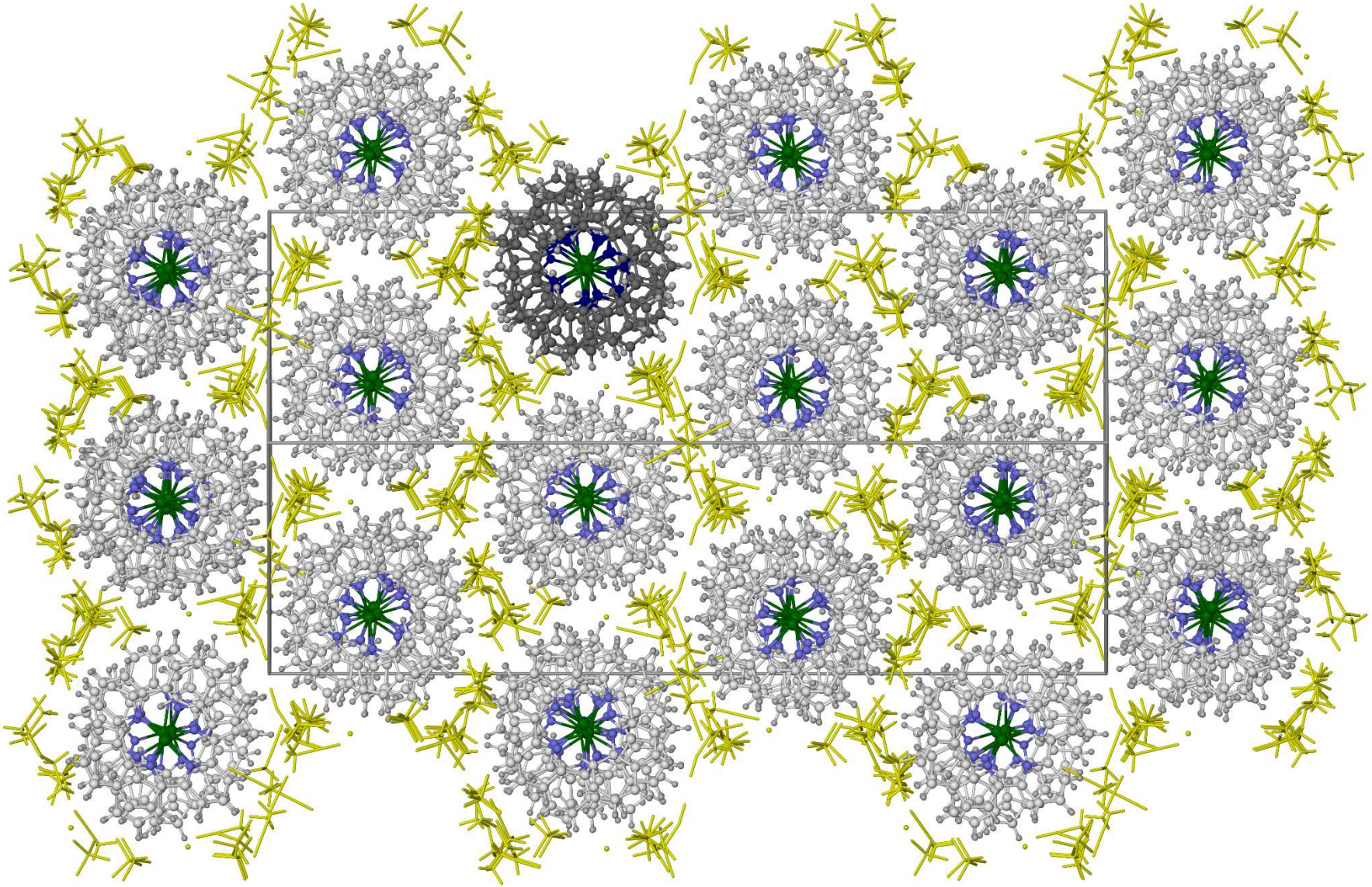

Figure S34 Alternative packing diagram of **4[BF$_4$]$_2$**·1.39MeCN·0.125Et$_2$O·0.25H$_2$O, viewed parallel to the [10$\bar{1}$] crystal vector with *b* horizontal. Details as for Figure S33.

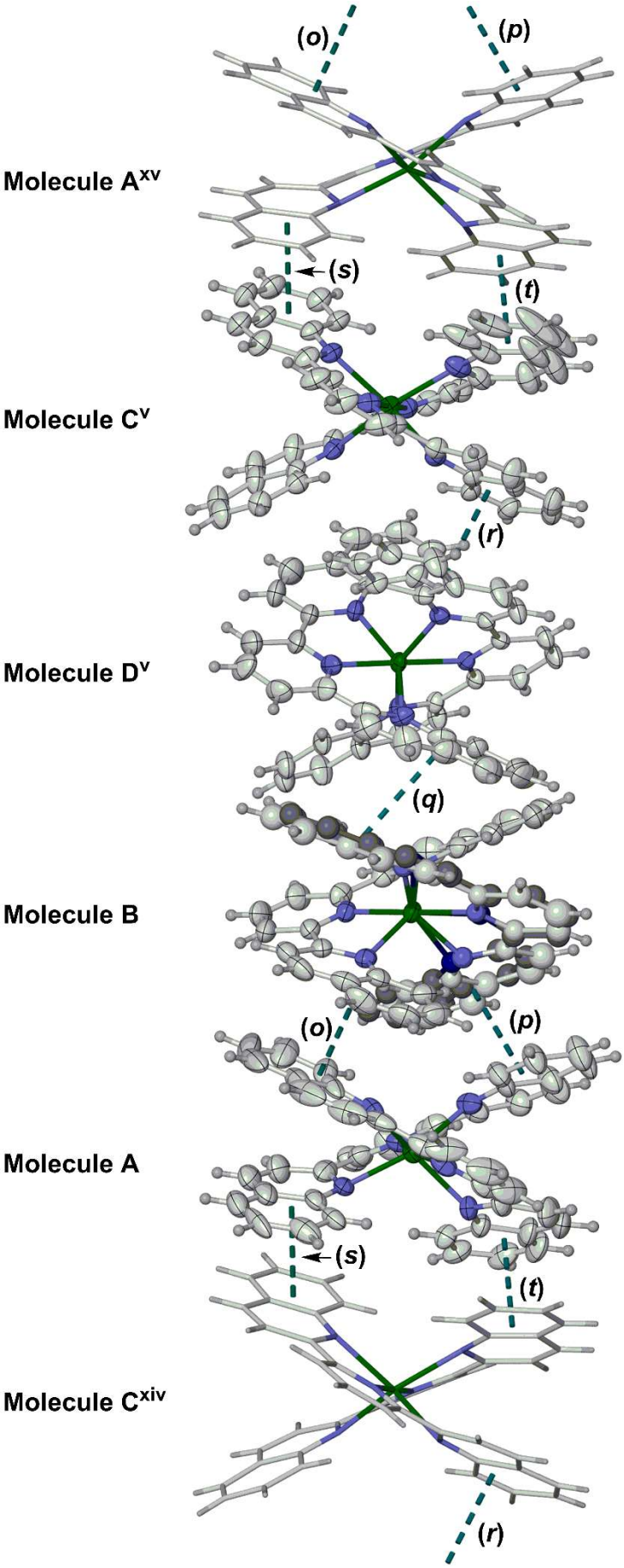

Figure S35 A helical cation stack in the lattice of **4[BF$_4$]$_2$**·1.39MeCN·0.125Et$_2$O·0.25H$_2$O (Figure S33), highlighting the intermolecular $\pi\cdots\pi$ interactions. The code letters for each interaction correspond to those in Table S8. Symmetry codes: (v) 1−*x*, 1−*y*, 1−*z*; (xiv) −*x*, 1−*y*, 2−*z*; (xv) 1+*x*, *y*, −1+*z*.

Table S9 Intermolecular $\pi\cdots\pi$ contacts in **4[BF$_4$]$_2$**·1.39MeCN·0.125Et$_2$O·0.25H$_2$O (Å, °). See Figures S28-S29 for the atom numbering scheme employed, while the codes for each interaction are those in Figure S35. Symmetry codes: (v) 1−*x*, 1−*y*, 1−*z*; (xiv) −*x*, 1−*y*, 2−*z*.

$\pi\cdots\pi$	Dihedral angle	Average inter-planar spacing	Horizontal offset
[C(44A)-C(53A)]···[C(18B)-C(27B)] (***o***)	10.4(3)	3.63(3)	0.91
[C(18A)-C(27A)]···[C(44B)-C(53B)] (***p***)[a]	7.9(5)/5.4(7)	3.70(4)/3.89(6)	1.39/2.01
[C(34B)-C(43B)]···[C(18D^{v})-C(27D^{v})] (***q***)[a]	8.35(3)/14.5(5)	3.60(4)/3.40(9)	1.50/1.19
[C(8C)-C(17C)]···[C(44D)-C(53D)] (***r***)	13.2(2)	3.66(2)	0.75
[C(8A)-C(17A)]···[C(18C^{xiv})-C(27C^{xiv})] (***s***)	11.7(3)	3.52(3)	1.28
[C(34A)-C(43A)]···[C(34C^{xiv})-C(43C^{xiv})] (***t***)	3.5(3)	3.58(3)	1.09

[a]Values are given for both disorder sites of ligand N(28B)-C(53B) (Figure S30).

Strong $\pi\cdots\pi$ interactions between identical arene residues typically involve overlapping arenes that are coplanar (*ie* dihedral angle ≈ 0°), and separated by < 3.4 Å (the sum of the van der Waals radii of two arene rings[18]). The interacting rings should be horizontally offset from each other to minimise electrostatic repulsion between their π-systems, although the ideal offset distance depends on their relative orientation.[21]

On that basis, the interactions in the Table are weak dipolar or van der Waals contacts. However, as in Table S7, some interactions that are weak by this measure lead to short intermolecular contacts between individual atoms. These include:
C(42B)/C(42E)···C(26D^{v}) = 3.445(13)/3.280(15) and C(43B)/C(43E)···C(24D^{v}) = 3.445(13)/3.205(15) Å;
C(14C)···C(53D) = 3.433(8), C(15C)···C(52D) = 3.426(9) and C(17C)···C(50D) = 3.315(9) Å;
C(52C)···C(16D) = 3.382(10) Å.

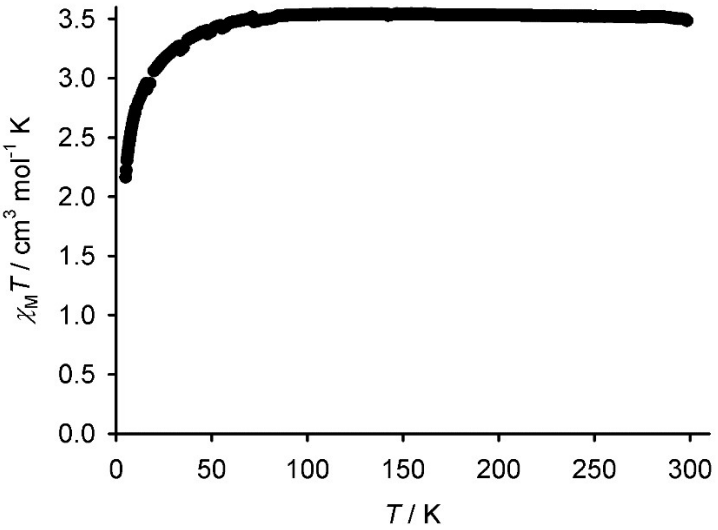

Figure S36 Variable temperature magnetic susceptibility data for a powder sample of **4[BF$_4$]$_2$**.

These data are consistent with an earlier report of the perchlorate salt of this complex, which was high spin above 80 K.[22]

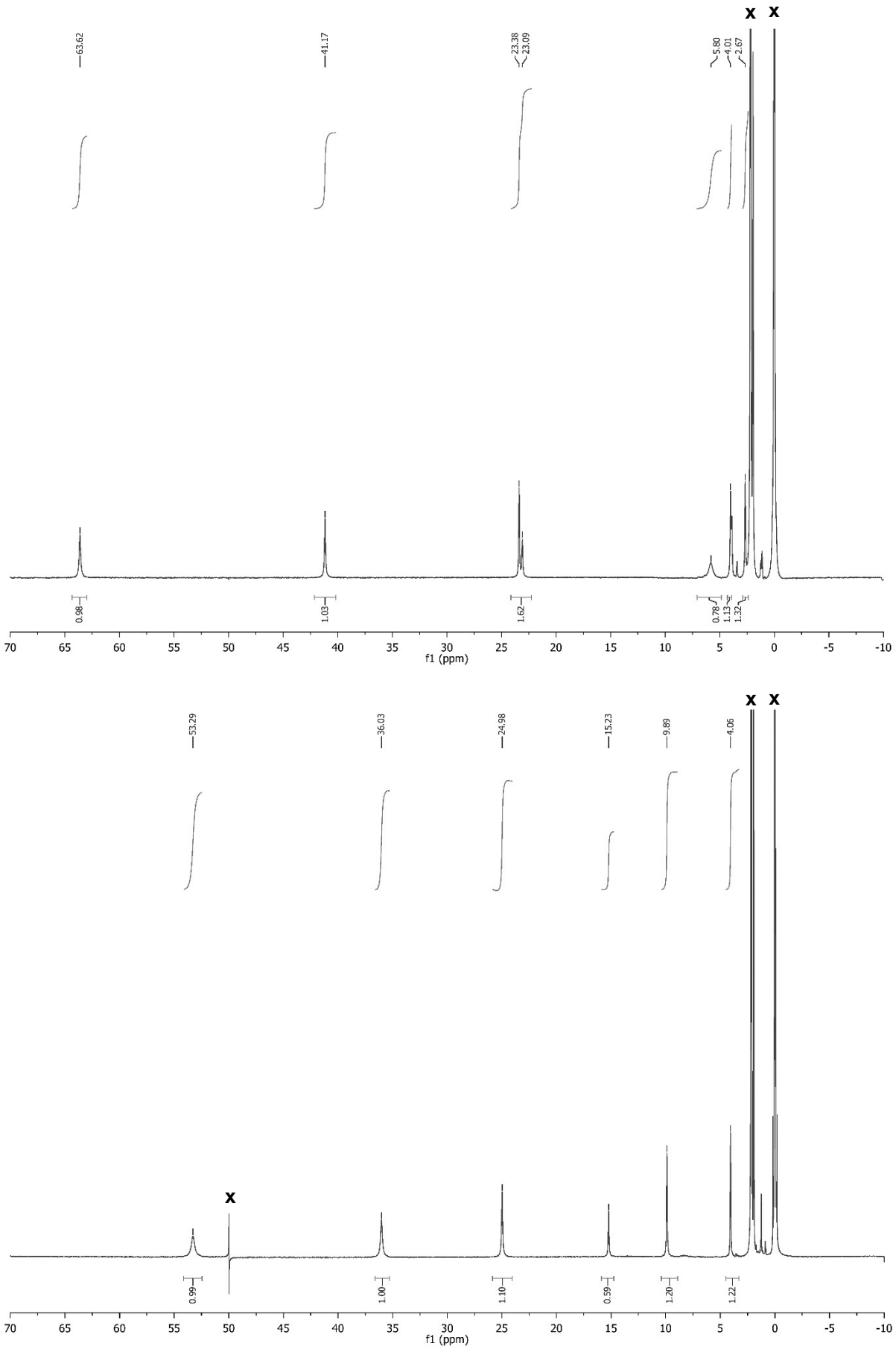

Figure S37 ^{1}H NMR spectra of **1[BF$_4$]$_2$** (top) and **2[BF$_4$]$_2$** (bottom) in CD_3CN. The feature near 50 ppm in the bottom spectrum is a spectrometer artefact.

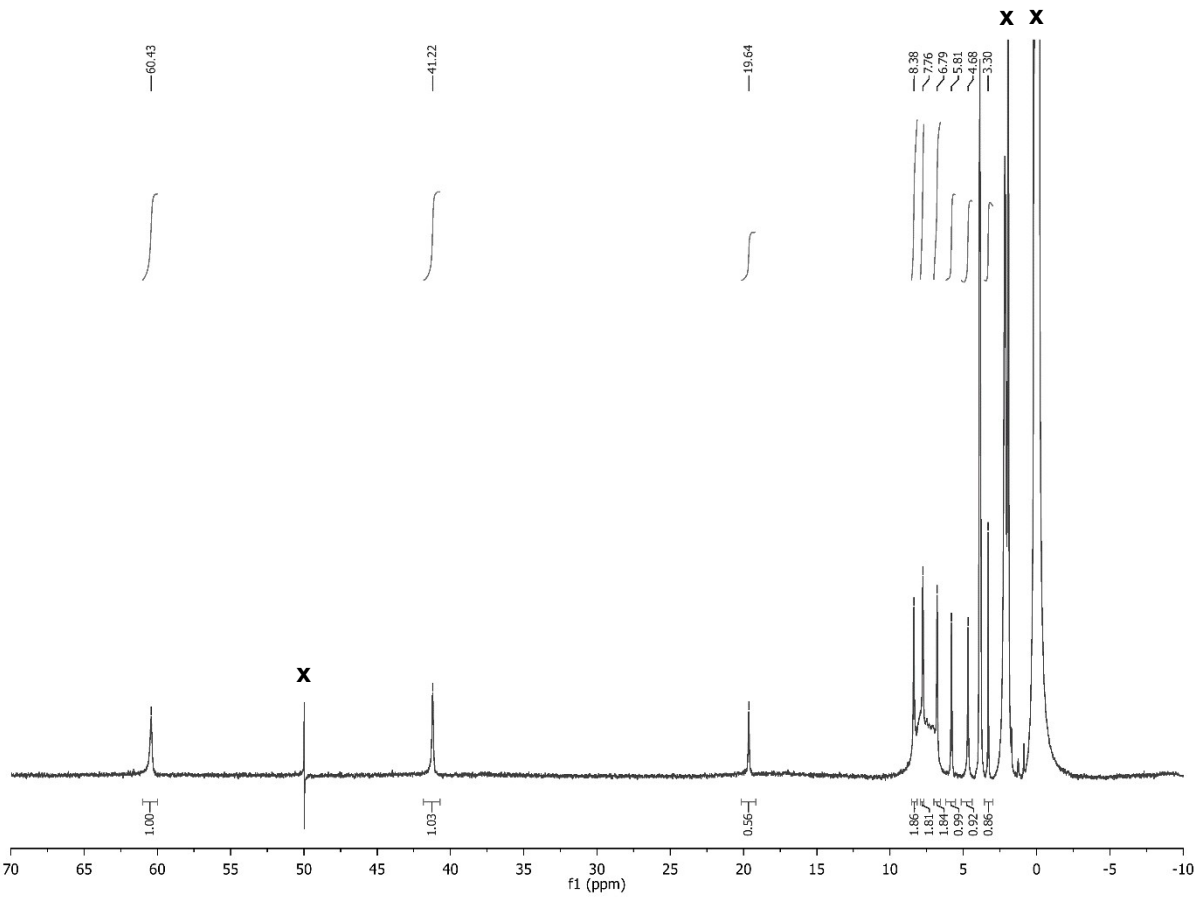

Figure S38 ^{1}H NMR spectrum of a mixture of $Fe[BF_4]_2 \cdot 6H_2O$ and 2 equiv L^3 in CD_3CN at room temperature, which was stirred until all the solid had dissolved. The feature near 50 ppm is a spectrometer artefact.

The nine unique ^{1}H resonances expected for a paramagnetic L^3 species with C_2 or *m* symmetry are clearly resolved as sharp peaks in the spectrum. Between 7-9 ppm, these are superimposed on a broader envelope of peaks which we attribute to uncoordinated L^3 (Figure S3).

The existence of a significant quantity of free L^3 in such solutions is consistent with our inability to isolate $[Fe(L^3)_2][BF_4]_2$ as a pure material. This contrasts with solutions of $[Fe(L^1)_2][BF_4]_2$ and $[Fe(L^2)_2][BF_4]_2$, which contain no free ligand by NMR (Figure S37).

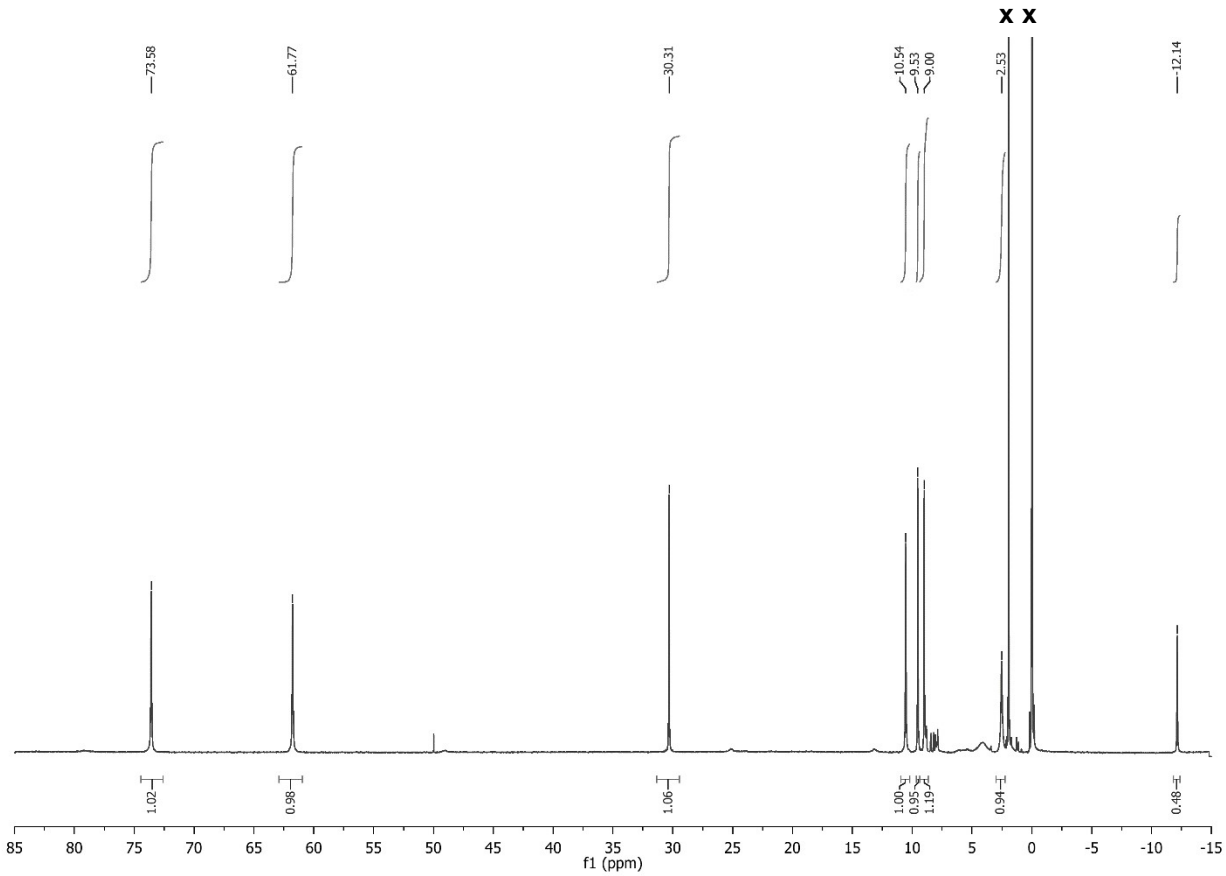

Figure S39 ^{1}H NMR spectrum of **4[BF$_4$]$_2$** in CD_3CN at room temperature.

Eight unique resonances are expected from this complex, which are clearly resolved. A small amount of uncoordinated L^4 is also present in the diamagnetic region (Figure S4), in a *ca* 1:10 ratio compared to the paramagnetic complex.

Table S10 UV-vis absorption and emission spectrum data for the compounds in this work, from acetonitrile solution at room temperature. The spectra are shown in Figure 7 (main article).

	Absorption	Emission	
	λ_{max} / nm [ε_{max} / 10^3 dm^3 mol^{-1} cm^{-1}]	λ^{em}_{max} / nm	λ_{ex} / nm
L^{1} [a]	278 (sh), 308 (sh), 325 (sh), 331 [21], 342 (sh)	423	330
1[BF$_4$]$_2$	340 [39.3]	446	345
L^{2} [a]	338 [20], 364 (sh)	457	335
2[BF$_4$]$_2$	328 (sh), 343 [34.1], 355 (sh)	445	340
L^{3} [a]	274 (sh), 315 (sh), 328 [22], 347 [19]	434	330
3'[BF$_4$]$_2$·H_2O	327 [24.2], 344 [24.4], 367 (sh)	453	345
L^{4} [b]	310 [30.7], 321 [30.4], 336 [15.5]	435	310
4[BF$_4$]$_2$	282 (sh), 312 (sh), 327 [17.1], 364 [23.1]	499	320

[a]Errors on the extinction coefficients in the absorption spectra of L^1-L^3 are estimated at ±2 x10^3 dm^3 mol^{-1} cm^{-1}, because of the low solubility of those compounds. [b]These data are consistent with literature values.[23]

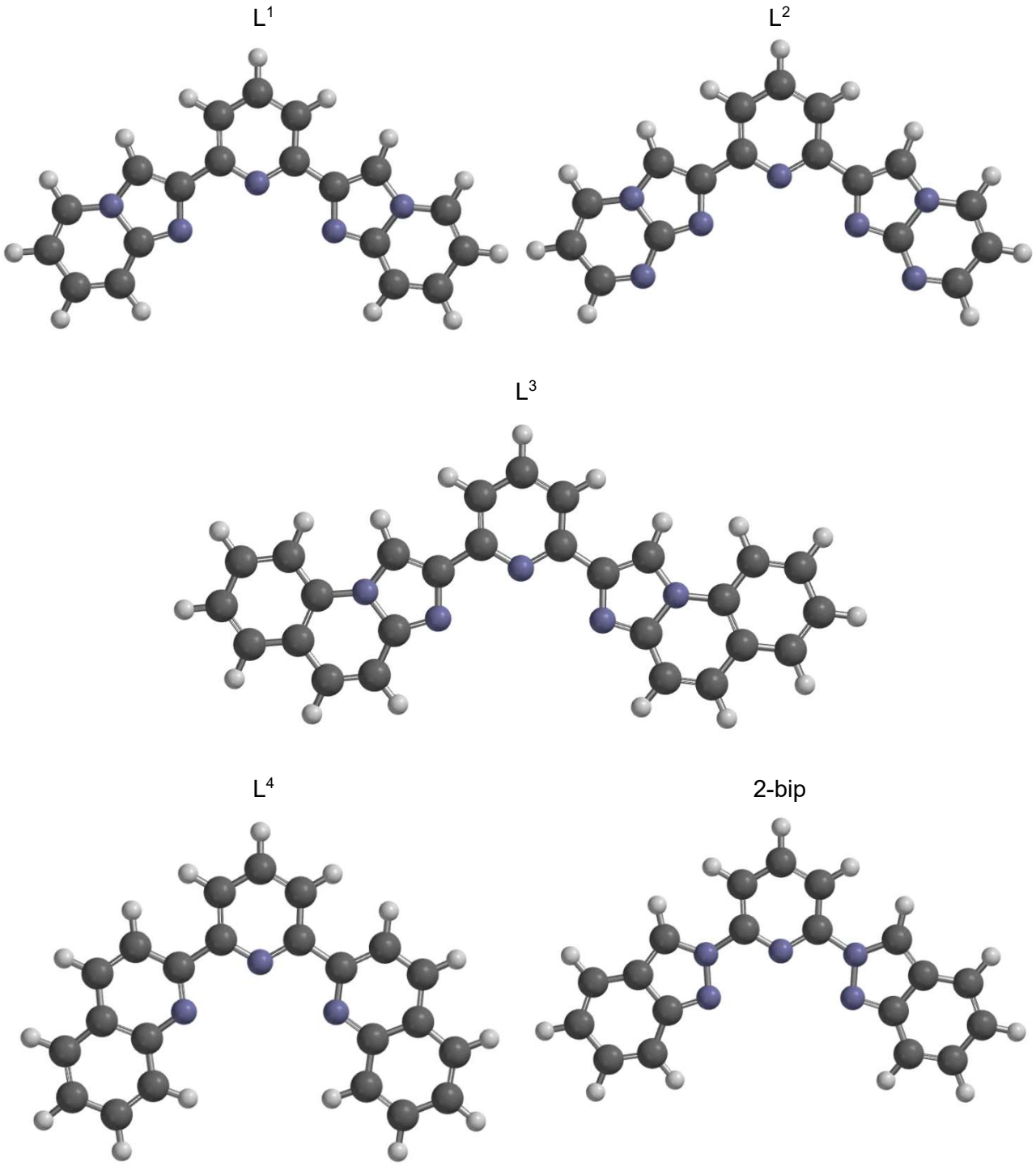

Figure S40 Computed molecular structures for the organic ligands, minimised in the *cisoid* conformation appropriate for metal binding. Colour code: C, dark grey; H, white; N, blue.

A minimisation of L^4 in this conformation was only achieved by fixing the torsions between the pyridyl and quinolyl rings to ± 1.5°. The other ligands in the Figure minimised to a *cisoid* conformation without constraints.

The calculation of metal-free bimpy in Table S11 and Figure S42 is taken from ref. 24.

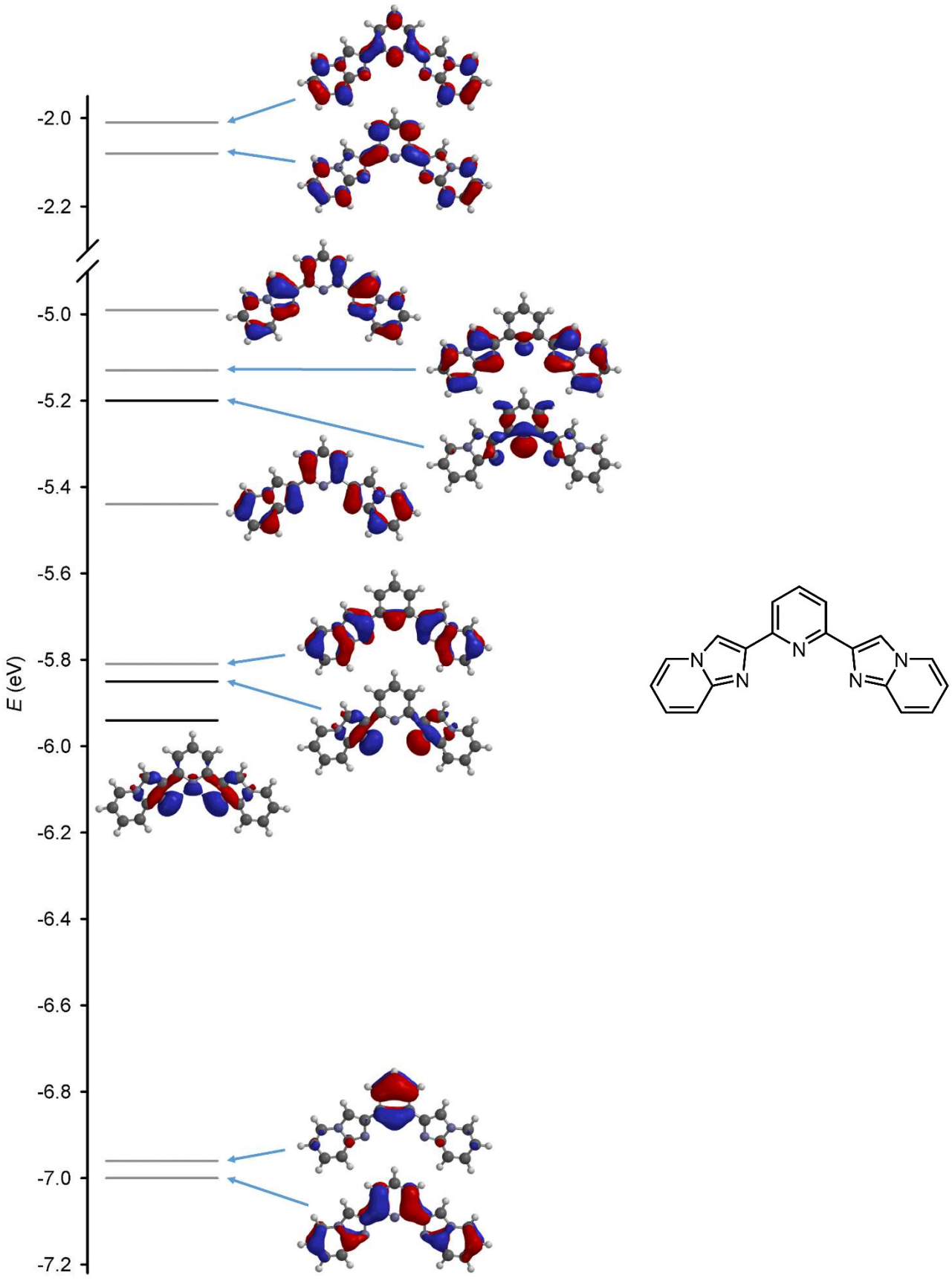

Figure S41 Frontier orbital plots for L^1. The energy levels are colour-coded as: N atom lone pair combination MOs (black); and π or π^* MOs (grey).

The frontier orbitals of all the ligands in Figure S42 have the same form as the ones in this Figure, with minor differences reflecting the disposition of N atoms around each ligand framework.

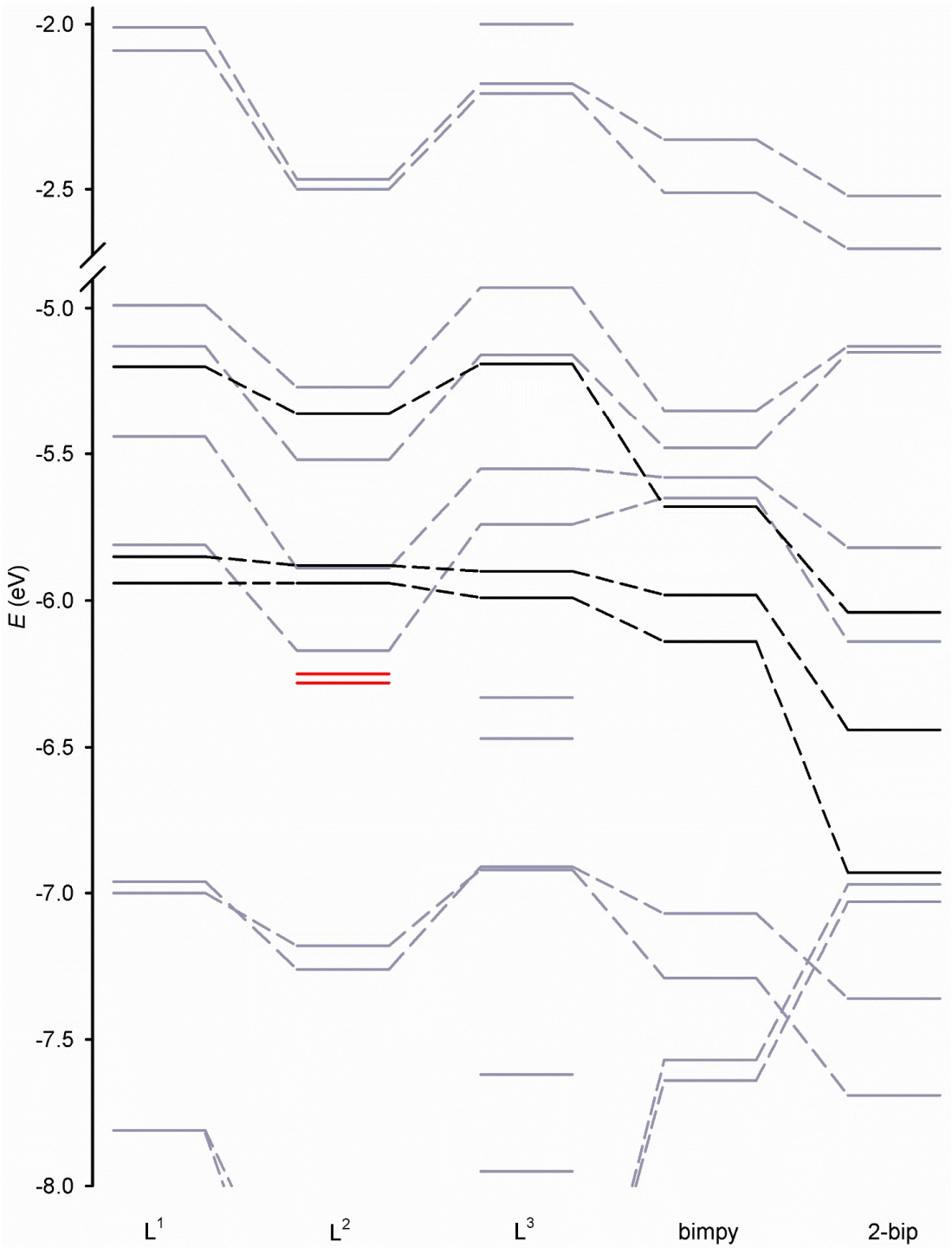

Figure S42 Frontier orbital energies for the *bis*(azolyl)pyridine ligands computed in this work (Figure S40). The energy levels are colour coded as N-donor lone pair combinations (black); other N atom lone pair MOs (red, L^2 only); and π or π^* MOs (grey). The data for bimpy are taken from ref. 24.

The metal-binding N lone pair MO energies run as $L^1 \approx L^2 \approx L^3 >$ bimpy > 2-bip (Table S11).

The HOMO and HOMO–1 of L^1, L^3, bimpy and 2-bip are azole-centred π orbitals with smaller pyridyl contributions, which should contribute to ligand⟶metal π-bonding (Figure S41). The equivalent orbitals in L^2 are the HOMO and HOMO–2.

The LUMO and LUMO+1 are π^*-orbitals which are mostly centered on the pyridyl ring (Figure S41). The LUMO has a node at the pyridyl N atom, but the LUMO+1 should contribute to metal⟶ligand π-bonding.

See the next page for more discussion.

Table S11 Computed energies of the minimised organic ligands, and the energies of their N-donor lone pair (LP) combination MOs (Figure S41-S42). The $E_{av}\{LP\}$ values are also listed in Table 4 (main article).

	E / Ha	$E\{LP\ 1\}$ / eV	$E\{LP\ 2\}$ / eV	$E\{LP\ 3\}$ / eV	$E_{av}\{LP\}$ / eV
L^1	–1005.255057	–5.20	–5.85	–5.94	–5.66
L^2 [a]	–1037.308291	–5.36	–5.88	–5.94	–5.73
L^3	–1312.455142	–5.19	–5.90	–5.99	–5.69
L^4	–1049.388607	–5.15	–5.42	–5.71	–5.43
bimpy[b]	–1005.289103	–5.68	–5.98	–6.14	–5.93
2-bip	–1005.216032	–6.04	–6.44	–6.93	–6.47

[a]This ligand has two additional lone pair combinations at lower energy, with larger contributions from their peripheral imidazopyrimidinyl *N*8 atoms (coloured red in Figure S42). [b]Data from ref 24.

Discussion of these data, and the other frontier orbitals in the ligands (Figures S41 and S42)

$E_{av}\{LP\}$ is a measure of the Brønsted basicity of the ligands in the gas phase. These give the following trend, where the most basic ligand has the highest $E_{av}\{LP\}$ energy:

$$\text{2-bip} < \text{bimpy} < L^2 \approx L^3 \approx L^1 < L^4$$

That is, 2-bip is the least σ-donating ligand in the series and L^4 is the strongest. The basicity of L^4 resembles its non-annelated analogue 2,2':6',2''-terpyridine (terpy) computed by this method ($E_{av}\{LP\} = –5.40$), while 2-bip is similar to non-annelated 2,6-di(pyrazol-1-yl)pyridine (1-bpp; $E_{av}\{LP\} = –6.39$).[24]

It is impossible to deconvolute the individual basicities of the different heterocyclic N-donors from these data, because there is extensive mixing of the N lone pair MOs. However, excepting L^4, the order reflects the basic pK_as of the distal heterocyclic donors on each ligand:[26]

2-methylindazole ($pK_a = 2.0$) < 1*H*-benzimidazole (5.6) < imidazo[1,2-a]pyridine (6.9)

Both π-donor (from the distal heterocyclic donor groups) and π-acceptor (to the central pyridyl ring) properties must be considered when ranking the π-acidity of the ligands.

- The HOMO−1 and HOMO of each ligand are π-orbitals with significant contributions from the azolyl N-donor atoms, which should both have π-donor character to a coordinated metal ion (Figure S41).
- While the LUMO and LUMO+1 are pyridyl-centred π*-MOs, only the LUMO+1 has π-acceptor capability since the LUMO has a node at the pyridyl N-donor atom (Figure S41).

With that in mind, the following observations can be made from Figure S42.

(i) The frontier orbitals of L^2 imply it is both a worse π-donor, and a better π-acceptor, than L^1 or L^3. The greater π-acidity of L^2 should explain why **2[BF$_4$]$_2$** has a higher SCO $T_{½}$ value than **1[BF$_4$]$_2$** in solution.

(ii) 2-bip has similar HOMO−1 and HOMO energies to L^1, but a lower LUMO+1. Hence, while 2-bip is the weakest σ-donor ligand in this study, that is partly offset by its stronger π-acceptor properties. As a result, the computed $\Delta E_{rel}\{HS–LS\}$ and experimental $T_{½}$ for $[Fe(bip)_2][BF_4]_2$ are only slightly lower than for **1[BF$_4$]$_2$**.

(iii) The bimpy ligand is computed to be less basic than L^1-L^3, but with comparable M−L π-bonding properties to L^2 (L^2 and bimpy have similar energies for their HOMO−1 and HOMO, but the LUMO+1 of bimpy is slightly higher energy). Hence, unlike the other complexes, the properties of the free ligands do not simply relate to the stabilisation of the low-spin state in $[Fe(bimpy)_2][BF_4]_2$. This is discussed in the main article.

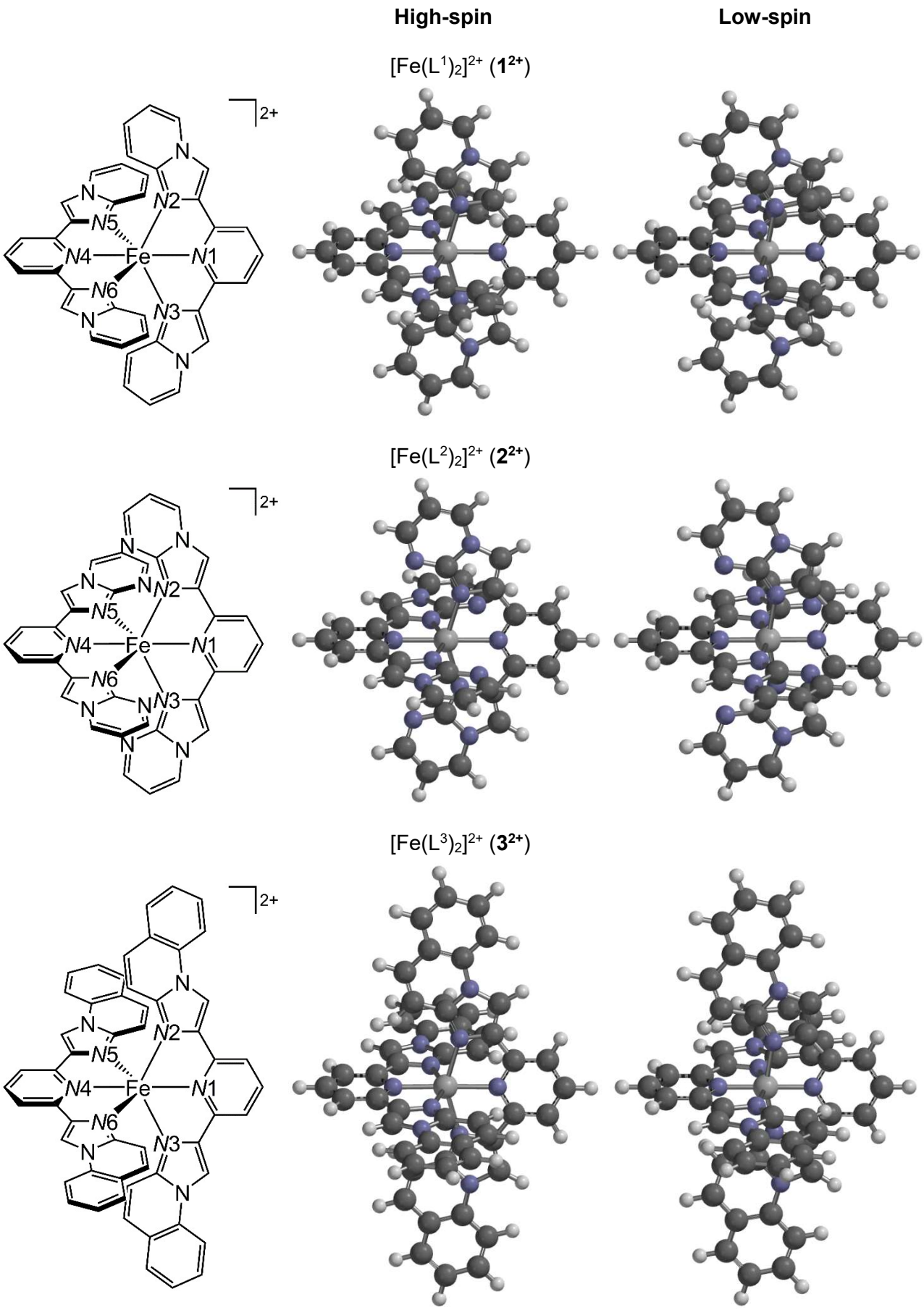

Figure S43 Energy-minimised structures of the complexes in the gas phase. The atom numbering used in Table S12 is also shown (which is different from the atom numbering in the crystal structures). Colour code: C, dark grey; H, white; N, blue; Fe, pale grey.

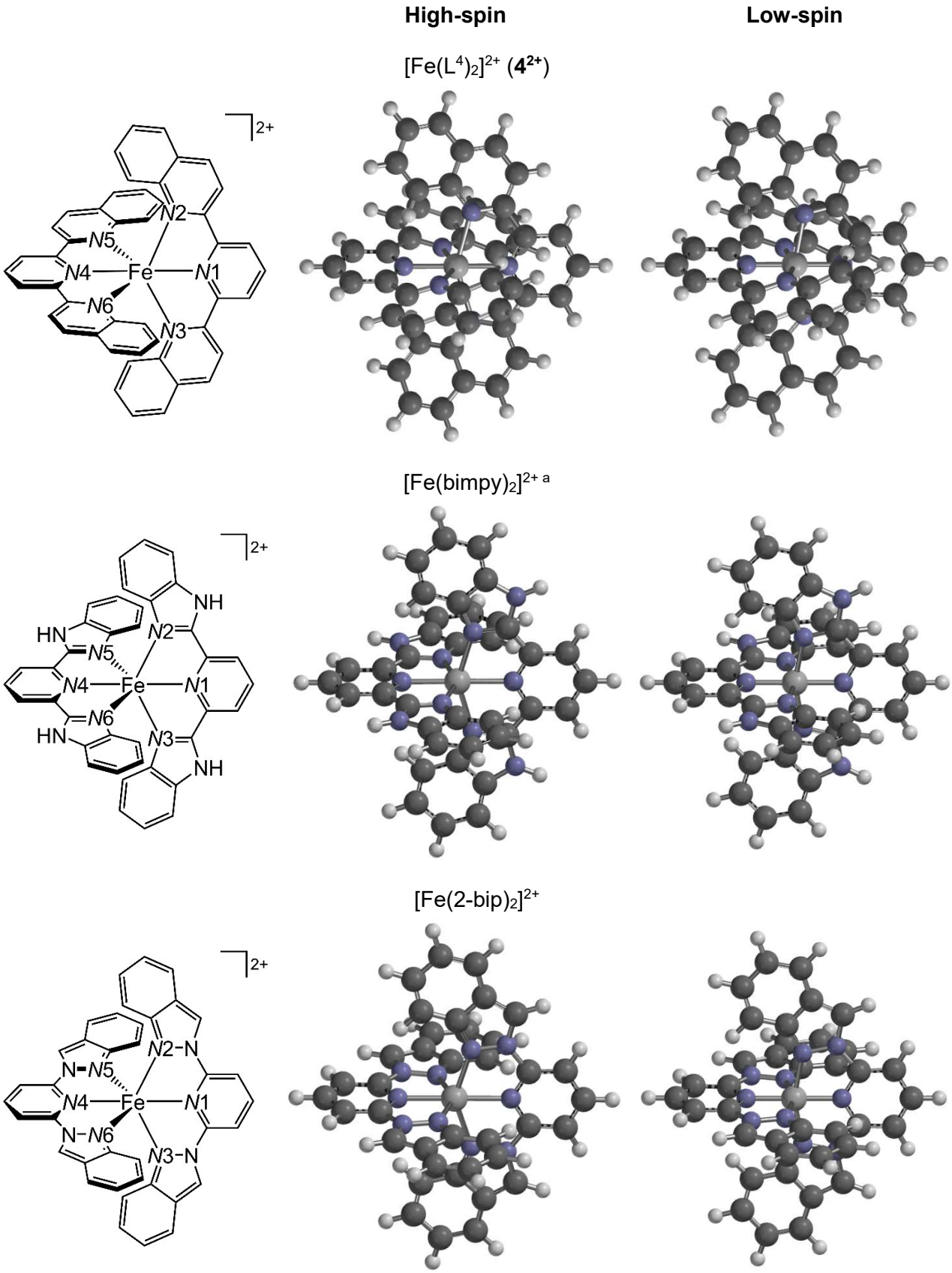

Figure S43 continued.

[a]From ref. 24.

Table S12 Computed metric parameters for the complexes in this work (Å, deg). See Figure S43 for the atom numbering scheme in the Table. Where available, crystallographic values are also given in square brackets for comparison. HS = high-spin, LS = low-spin. α is the average ligand bite angle in the molecule; see page S13 for definitions of ϕ and θ.

	$[Fe(L^1)_2]^{2+}$ (**1**$^{2+}$)		$[Fe(L^2)_2]^{2+}$ (**2**$^{2+}$)		$[Fe(L^3)_2]^{2+}$ (**3**$^{2+}$)	
	HS[a]	LS[b]	HS[c]	LS	HS	LS
Fe–*N*1	2.167 [2.175(3)]	1.923 [1.923(3)]	2.164 [2.148(2)]	1.924	2.169	1.926
Fe–*N*2	2.228 [2.199(4)]	2.011 [1.979(3)]	2.204 [2.193(2)]	1.984	2.225	2.012
Fe–*N*3	2.228 [2.191(3)]	2.011 [1.988(3)]	2.204 [2.183(2)]	1.984	2.226	2.012
Fe–*N*4	2.167 [2.175(3)]	1.923 [1.921(3)]	2.164 [2.154(2)]	1.924	2.169	1.926
Fe–*N*5	2.228 [2.199(3)]	2.011 [1.997(3)]	2.204 [2.197(2)]	1.984	2.231	2.012
Fe–*N*6	2.228 [2.191(4)]	2.011 [2.002(3)]	2.204 [2.201(2)]	1.984	2.222	2.012
Fe–N{pyridyl}$_{av}$	2.167 [2.175(3)]	1.923 [1.922(4)]	2.164 [2.151(3)]	1.924	2.169	1.926
Fe–N{distal}$_{av}$	2.228 [2.195(5)]	2.011 [1.992(6)]	2.204 [2.182(4)]	1.984	2.226	2.012
*N*1–Fe–*N*2	74.6 [73.84(13)]	80.6 [80.33(12)]	74.6 [74.78(9)]	80.6	74.6	80.7
*N*1–Fe–*N*3	74.6 [74.41(12)]	80.6 [80.71(12)]	74.6 [74.57(9)]	80.6	74.6	80.7
*N*1–Fe–*N*4	180.0 [176.42(18)]	180.0 [178.82(11)]	180.0 [163.52(9)]	180.0	178.5	180.0
*N*1–Fe–*N*5	105.4 [108.75(12)]	99.4 [99.07(11)]	105.4 [120.61(9)]	99.4	104.0	99.3
*N*1–Fe–*N*6	105.4 [103.08(12)]	99.4 [99.79(12)]	105.4 [90.12(9)]	99.4	106.8	99.3
*N*2–Fe–*N*3	149.2 [148.15(12)]	161.3 [161.01(13)]	149.1 [148.43(9)]	161.1	149.2	161.4
*N*2–Fe–*N*4	105.4 [108.75(12)]	99.4 [100.75(11)]	105.4 [110.48(9)]	99.4	105.8	99.3
*N*2–Fe–*N*5	95.9 [93.03(19)]	91.5 [92.01(11)]	96.2 [98.12(9)]	91.5	97.0	91.5
*N*2–Fe–*N*6	92.2 [94.79(13)]	91.5 [91.12(11)]	91.9 [91.67(9)]	91.5	91.1	91.5
*N*3–Fe–*N*4	105.4 [103.08(12)]	99.4 [98.23(12)]	105.4 [101.07(9)]	99.4	105.0	99.3
*N*3–Fe–*N*5	92.2 [94.79(13)]	91.5 [91.82(11)]	91.9 [90.99(9)]	91.5	91.3	91.5
*N*3–Fe–*N*6	95.9 [94.64(19)]	91.5 [91.24(11)]	96.2 [95.79(9)]	91.5	96.8	91.5
*N*4–Fe–*N*5	74.6 [73.84(13)]	80.6 [80.43(12)]	74.6 [74.86(9)]	80.6	74.6	80.7
*N*4–Fe–*N*6	74.6 [74.41(12)]	80.6 [80.70(12)]	74.6 [74.35(9)]	80.6	74.7	80.7
*N*5–Fe–*N*6	149.2 [148.15(12)]	161.3 [161.14(12)]	149.1 [149.19(9)]	161.1	149.3	161.4
α	74.6 [74.13(18)]	80.6 [80.5(2)]	74.6 [74.64(18)]	80.6	74.6	80.7
ϕ	180.0 [176.42(18)]	180.0 [178.82(11)]	180.0 [163.52(9)]	180.0	178.5	180.0
θ	89.2 [89.66(3)]	90.0 [88.90(3)]	89.2 [87.59(3)]	90.0	87.7	90.0

[a]Crystallographic data from **1[BF$_4$]$_2$**·MeCN (Table S2). [c]Crystallographic data from **1[BF$_4$]$_2$**·1.7MeNO$_2$·0.3MeNO$_2$ (Table S2). [c]Crystallographic data from **2[BF$_4$]$_2$**·1.5MeCN (Table S4). [d]Crystallographic data from molecule D of **4[BF$_4$]$_2$**·1.39MeCN·0.125Et$_2$O·0.25H$_2$O (Figure S36, Table S7). [e]From ref. 25. [f]Crystallographic data from ref. 23. [g]Crystallographic data from ref. 19.

Table S12 continued.

	$[Fe(L^4)_2]^{2+}$ (**4**$^{2+}$)		$[Fe(bimpy)_2]^{2+}$ [e]		$[Fe(2\text{-}bip)_2]^{2+}$	
	HS[d]	LS	HS	LS[f]	HS	LS[g]
Fe–*N*1	2.103 [2.114(5)]	1.897	2.161	1.920 [1.8759(14)]	2.163	1.901 [1.886(2)]
Fe–*N*2	2.304 [2.249(5)]	2.090	2.223	2.004 [1.9880(17)]	2.188	1.997 [1.962(2)]
Fe–*N*3	2.304 [2.252(5)]	2.090	2.226	2.004 [1.9892(19)]	2.199	1.998 [1.974(2)]
Fe–*N*4	2.103 [2.099(4)]	1.897	2.161	1.920 [1.8734(14)]	2.168	1.899 [1.884(2)]
Fe–*N*5	2.304 [2.286(5)]	2.090	2.227	2.004 [1.9832(18)]	2.191	1.998 [1.968(2)]
Fe–*N*6	2.304 [2.252(5)]	2.090	2.223	2.004 [1.9922(19)]	2.194	2.000 [1.966(2)]
Fe–N{pyridyl}$_{av}$	2.103 [2.107(6)]	1.897	2.161	1.920 [1.875(2)]	2.166	1.900 [1.885(3)]
Fe–N{distal}$_{av}$	2.304 [2.260(10)]	2.090	2.225	2.004 [1.988(4)]	2.193	1.998 [1.968(4)]
*N*1–Fe–*N*2	74.4 [73.4(2)]	79.8	74.6	80.4 [79.21(5)]	73.1	80.1 [80.32(9)]
*N*1–Fe–*N*3	74.4 [74.6(2)]	79.8	74.5	80.4 [79.57(4)]	72.9	80.0 [80.68(9)]
*N*1–Fe–*N*4 (ϕ)	180.0 [177.6(2)]	180.0	178.9	180.0 [177.7(2)]	179.3	179.9 [177.08(10)]
*N*1–Fe–*N*5	105.6 [104.8(2)]	100.2	104.7	99.6 [97.21(6)]	107.8	99.9 [99.33(9)]
*N*1–Fe–*N*6	105.6 [106.9(2)]	100.2	106.2	99.6 [101.47(8)]	106.4	100.0 [99.39(9)]
*N*2–Fe–*N*3	148.8 [147.99(19)]	159.5	149.1	160.8 [158.7(3)]	146.0	160.1 [160.98(10)]
*N*2–Fe–*N*4	105.6 [108.75(18)]	100.2	106.2	99.6 [100.99(5)]	106.8	99.8 [102.60(10)]
*N*2–Fe–*N*5	103.1 [101.61(18)]	98.2	96.5	91.6 [91.80(6)]	97.8	91.8 [91.41(9)]
*N*2–Fe–*N*6	85.3 [88.89(18)]	85.3	91.6	91.6 [90.88(6)]	92.7	91.8 [91.40(9)]
*N*3–Fe–*N*4	105.6 [103.25(18)]	100.2	104.7	99.6 [100.26(8)]	107.3	100.2 [96.40(9)]
*N*3–Fe–*N*5	85.3 [86.72(18)]	85.4	91.7	91.6 [92.05 (7)]	91.3	91.7 [90.94(9)]
*N*3–Fe–*N*6	103.1 [100.14(18)]	98.2	96.5	91.6 [92.12(7)]	98.1	91.6 [92.41(9)]
*N*4–Fe–*N*5	74.4 [73.94(17)]	79.8	74.5	80.4 [80.46(5)]	72.9	80.1 [80.51(9)]
*N*4–Fe–*N*6	74.4 [74.34(17)]	79.8	74.6	80.4 [80.87(5)]	72.9	80.0 [80.81(9)]
*N*5–Fe–*N*6	148.8 [148.28(16)]	159.5	149.1	160.8 [161.3(4)]	145.8	160.1 [161.28(9)]
α	74.4 [74.1(4)]	79.8	74.6	80.4 [80.03(10)]	73.0	80.1 [80.58(18)]
ϕ	180.0 [177.6(2)]	180.0	178.9	180.0 [177.7(2)]	179.3	179.9 [177.08(10)]
θ	76.0 [73.38(4)]	80.4	88.5	90.0 [87.27]	87.6	90.0 [89.21(1)]

[a]Crystallographic data from **1[BF$_4$]$_2$**·MeCN (Table S2). [c]Crystallographic data from **1[BF$_4$]$_2$**·1.7MeNO$_2$·0.3MeNO$_2$ (Table S2). [c]Crystallographic data from **2[BF$_4$]$_2$**·1.5MeCN (Table S4). [d]Crystallographic data from molecule D of **4[BF$_4$]$_2$**·1.39MeCN·0.125Et$_2$O·0.25H$_2$O (Figure S36, Table S7). [e]From ref. 25. [f]Crystallographic data from ref. 23. [g]Crystallographic data from ref. 19.

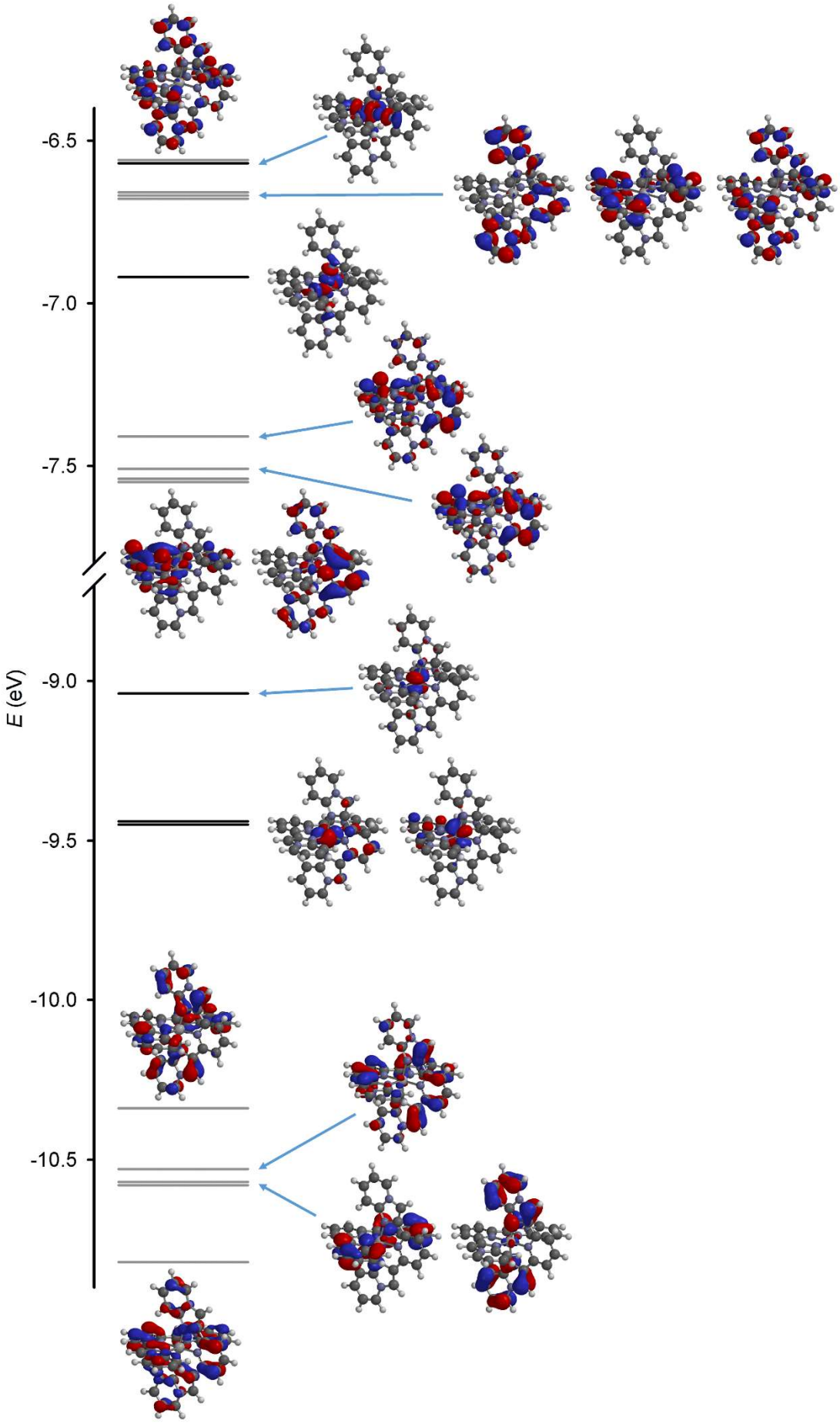

Figure S44 Frontier orbital plots for $\mathbf{1}^{2+}$, colour-coded as: metal-centred *d*-orbitals (black); and ligand-based π or π^* MOs (grey). The d_{z2} orbital is accidentally degenerate with a ligand-based π^* orbital in the diagram.

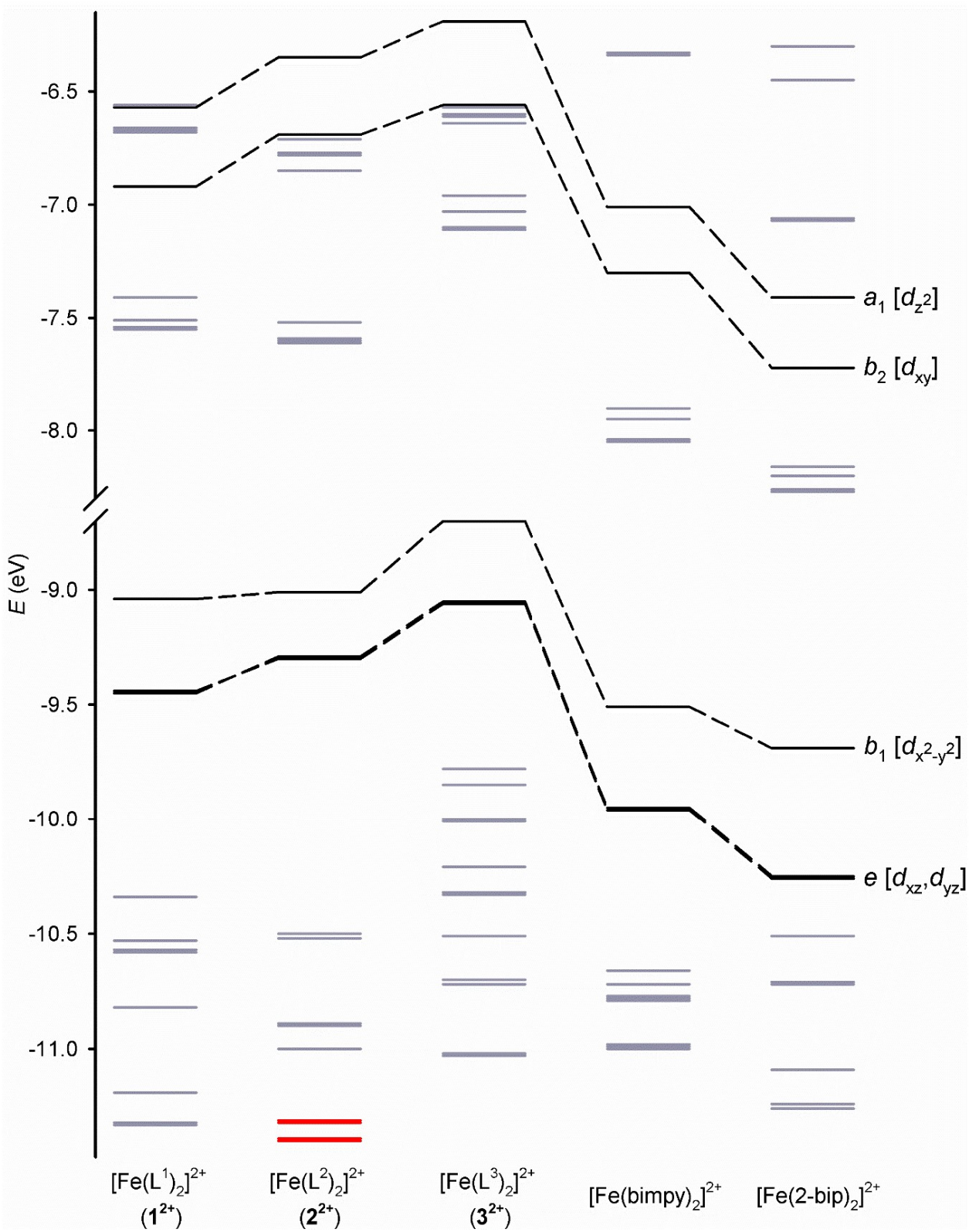

Figure S45 Frontier molecular orbital energies of low-spin complexes in this work. Metal *d*-orbitals are in black, and ligand-centred orbitals are in grey; the red energy levels for $\mathbf{2}^{2+}$ are lone pairs from their peripheral N atoms. The *d*-orbitals have D_{2d} symmetry labels, which is the idealised point group of these molecules. Data for $[Fe(bimpy)_2]^{2+}$ are from ref. 24.

- d_{zz} and d_{yz} report on out-of-plane π-bonding to the ligand pyridyl groups.
- $d_{y2\text{-}y2}$ reports on out-of-plane π-bonding to the distal ligand azolyl donors.
- d_{z2} and d_{xy} are σ* antibonding with respect to the Fe−N bonds.

The interpretation of these data is discussed on page S66.

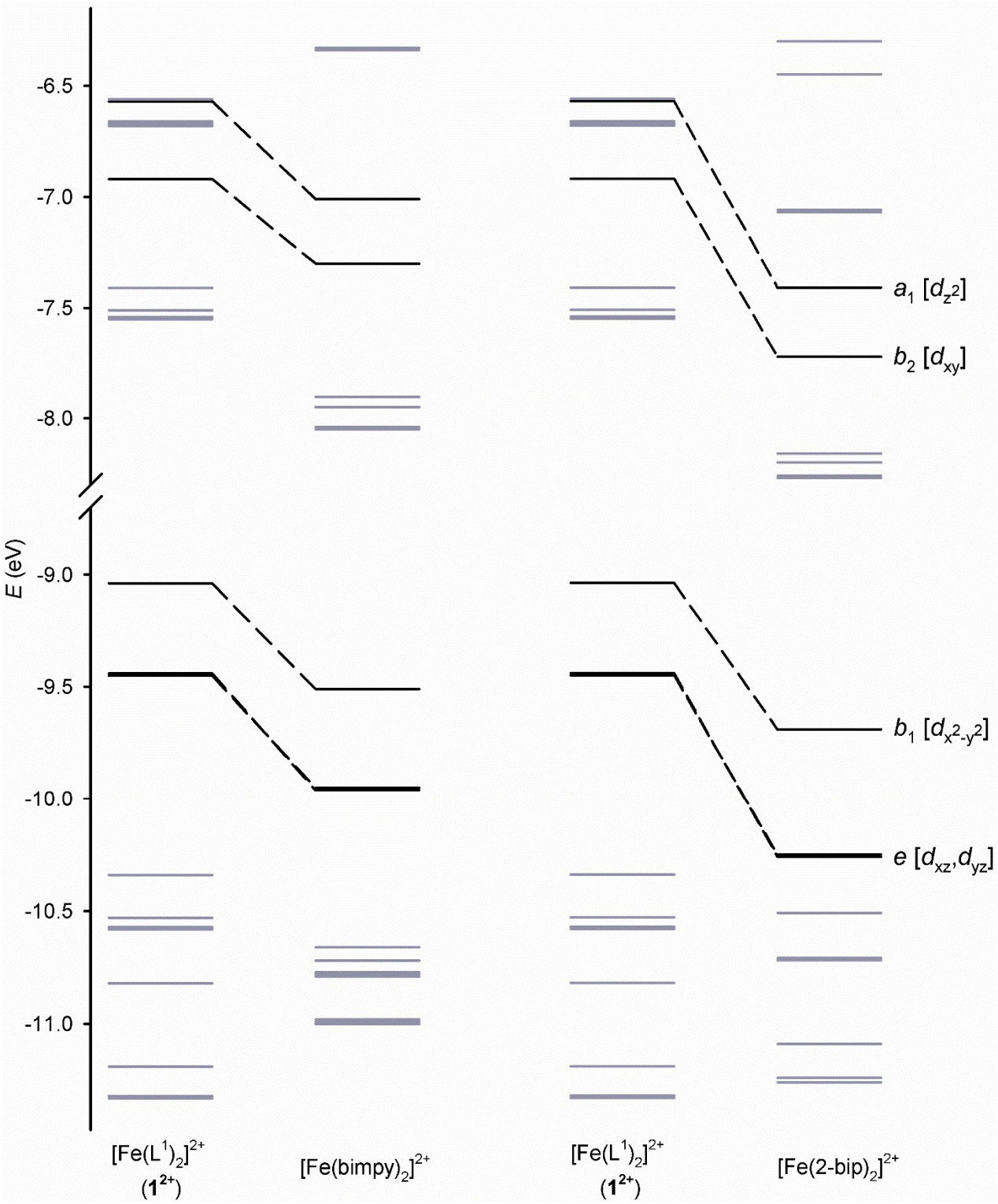

Figure S46 Comparison of the FMO energies of the reference molecule $\mathbf{1}^{2+}$ with its constitutional isomers $[Fe(bimpy)_2]^{2+}$ and $[Fe(2\text{-}bip)_2]^{2+}$. Details as for Figure S45.

The π^*-LUMOs for each complex in the Figures are similar in form (Figure S45), but the shapes of the high-lying π-orbitals show more variation between the complexes reflecting the different heterocycles present.

The interpretation of these data is discussed on the next page.

Discussion of the frontier orbitals in the complexes (Figures S45 and S46)

The following discussion compares each complex against $\mathbf{1}^{2+}$, which is the baseline standard for the ΔE_{rel}{HS–LS} spin state energies (Table 4, main article).

- The π-bonding *d*-orbitals are all less destabilised than the σ-symmetry *d*-orbitals in $\mathbf{2}^{2+}$, compared to $\mathbf{1}^{2+}$ (Figure S45). Hence, the positive ΔE_{rel}{HS–LS} for $\mathbf{2}^{2+}$ reflects a comparatively stronger π-ligand field in that complex. That is consistent with the greater π-acidity of L^2 predicted by the free ligand calculation (page S58).

- The *d*-orbitals of $\mathbf{3}^{2+}$ are all destabilised to a similar degree compared to $\mathbf{1}^{2+}$ (Figure S45), which is consistent with the near-zero ΔE_{rel}{HS–LS} computed for $\mathbf{3}^{2+}$. Hence, although it could not be experimentally confirmed, $[Fe(L^3)_2]^{2+}$ is predicted to have similar spin state properties to $\mathbf{1[BF_4]_2}$.

- The π-symmetry *d*-orbitals in $[Fe(bimpy)_2]^{2+}$ are more stabilised than d_{xy} and d_{z2} in $\mathbf{1}^{2+}$ (Figure S46), implying its positive ΔE_{rel}{HS–LS} is a function of stronger metal-ligand π-back bonding. That cannot be explained in so much detail as the other complexes, however, on the basis of this Figure.

- The *d*-orbitals in $[Fe(2\text{-bip})_2]^{2+}$ are mostly stabilised by similar amounts compared to $\mathbf{1}^{2+}$ (Figure S46). Thus the weaker σ-basicity and greater π-acidity of 2-bip have almost equal but opposite effects on the ligand field of $[Fe(2\text{-bip})_2]^{2+}$. The slightly negative ΔE_{rel}{HS–LS} for that complex reflects its less-stabilised $d_{y2\text{-}y2}$ level, showing the imidazopyridyl groups in L^1 and the indazol-2-yl donors in 2-bip have more similar π-donor character. These aspects are consistent with the free ligand calculations (Figure S42).

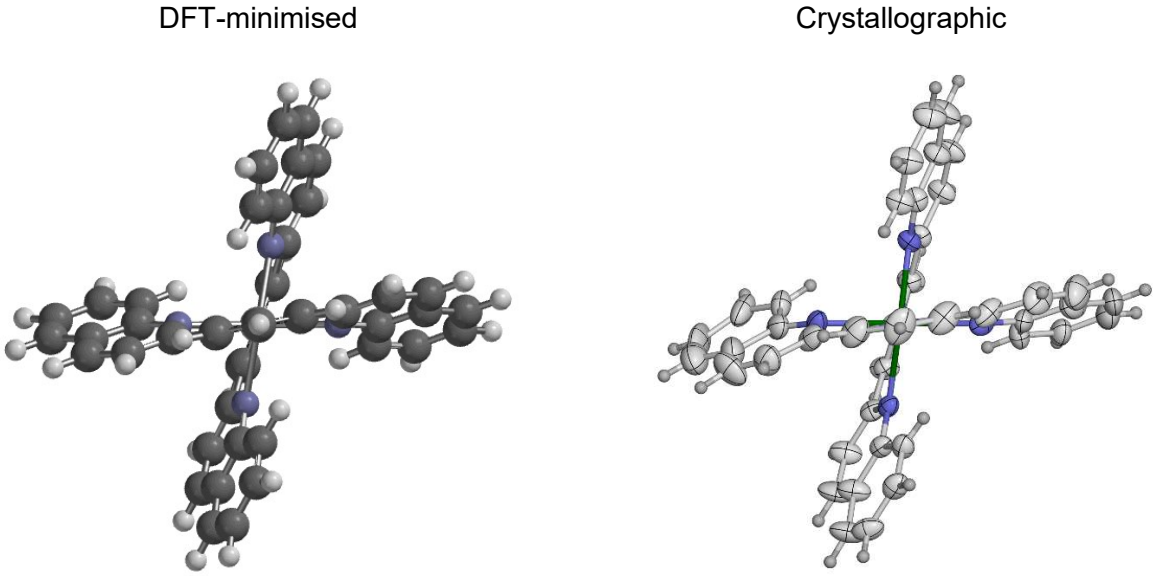

Figure S47 Comparison of the computed and experimental high-spin molecular geometries of $[Fe(L^4)_2]^{2+}$ ($\mathbf{4}^{2+}$). The view is the same as in Figures S26-S27. The crystallographic molecule is molecule D in the structure of $\mathbf{4[BF_4]_2}\cdot 1.39MeCN\cdot 0.125Et_2O\cdot 0.25H_2O$ (Figure S24).

The pitch of the helical ligand conformation is expressed by the θ parameter (page S13), which is 76.0° in the computed structure and 73.38(4)° in the crystallographic molecule shown.

The other molecules in the crystal structure of this complex show $57.75(5) \leq \theta \leq 73.38(4)°$ (Table S7), so experimentally the degree of helical canting in $[Fe(L^4)_2]^{2+}$ influenced by crystal packing. However, the calculation shows the preference for a helical ligand conformation is not a packing effect, and is intrinsic to the molecule.

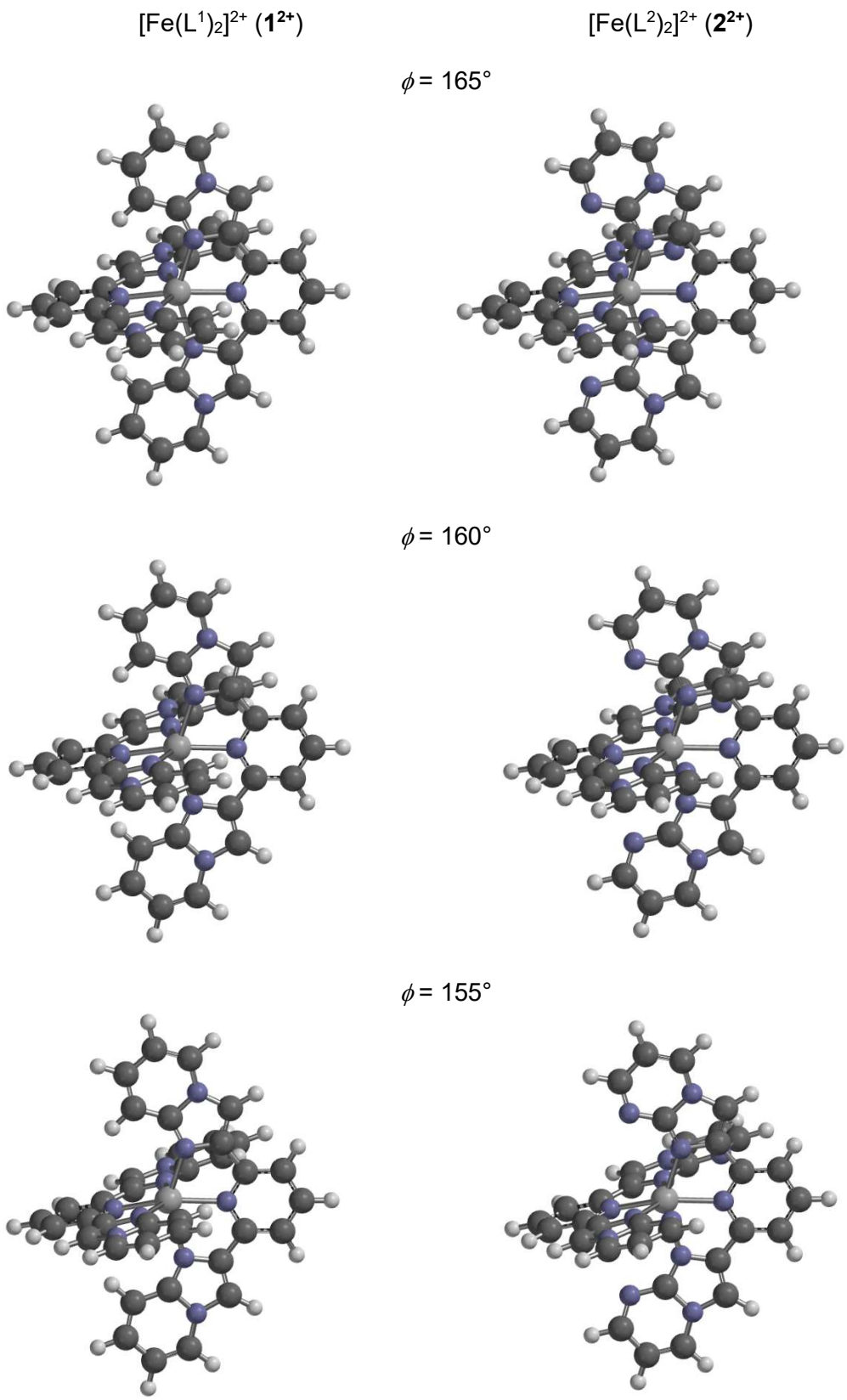

Figure S48 Energy-minimised structures of the distorted coordination geometries of high-spin $\mathbf{1}^{2+}$ and $\mathbf{2}^{2+}$ in the gas phase. The undistorted minimisations of these molecules are shown in Figure S43, and ϕ is defined on page S13.

Colour code: C, dark grey; H, white; N, blue; Fe, pale grey.

Table S13 Computed metric parameters for the distorted coordination geometries of high-spin $\mathbf{1}^{2+}$ and $\mathbf{2}^{2+}$ (Å, deg; Figure S48). The atom numbering is the same as in Table S12 (Figure S43). The undistorted molecules in Table S12 are included again here, to aid comparison. Where available, crystallographic values are also given in square brackets for comparison. α is the average ligand bite angle in the molecule; see page S13 for definitions of ϕ and θ.

	$[Fe(L^1)_2]^{2+}$ ($\mathbf{1}^{2+}$)				$[Fe(L^2)_2]^{2+}$ ($\mathbf{2}^{2+}$)			
ϕ	180	165.0[a]	160.0[a]	155.0[a]	180	165.0[a]	160.0[a]	155.0[a]
Fe–*N*1	2.167 [2.175(3)]	2.164	2.162	2.161	2.164	2.170 [2.148(2)]	2.170	2.173 [2.160(3)]
Fe–*N*2	2.228 [2.199(4)]	2.191	2.177	2.162	2.204	2.175 [2.193(2)]	2.164	2.153 [2.209(3)]
Fe–*N*3	2.228 [2.191(3)]	2.273	2.304	2.334	2.204	2.241 [2.183(2)]	2.259	2.281 [2.203(3)]
Fe–*N*4	2.167 [2.175(3)]	2.164	2.162	2.163	2.164	2.170 [2.154(2)]	2.170	2.173 [2.162(3)]
Fe–*N*5	2.228 [2.199(3)]	2.273	2.304	2.341	2.204	2.241 [2.197(2)]	2.259	2.281 [2.212(3)]
Fe–*N*6	2.228 [2.191(4)]	2.191	2.177	2.162	2.204	2.175 [2.201(2)]	2.164	2.153 [2.196(3)]
Fe–N{pyridyl}$_{av}$	2.167 [2.175(3)]	2.164	2.162	2.162	2.164	2.170 [2.151(3)]	2.170	2.173 [2.161]
Fe–N{distal}$_{av}$	2.228 [2.195(5)]	2.232	2.241	2.248	2.204	2.208 [2.182(4)]	2.212	2.217 [2.205]
*N*1–Fe–*N*2	74.6 [73.84(13)]	75.5	76.0	76.5	74.6	75.2 [74.78(9)]	75.4	75.7 [74.54(12)]
*N*1–Fe–*N*3	74.6 [74.41(12)]	73.9	73.5	72.9	74.6	73.7 [74.57(9)]	73.3	72.8 [74.36(12)]
*N*1–Fe–*N*4	180.0 [176.42(18)]	165.0	160.0	155.0	180.0	165.0 [163.52(9)]	160.0	155.0 [156.26(12)]
*N*1–Fe–*N*5	105.4 [108.75(12)]	95.3	92.2	88.7	105.4	95.5 [120.61(9)]	92.3	89.1 [89.15(12)]
*N*1–Fe–*N*6	105.4 [103.08(12)]	115.5	118.6	121.9	105.4	115.7 [90.12(9)]	119.0	122.4 [122.64(13)]
*N*2–Fe–*N*3	149.2 [148.15(12)]	149.2	149.1	148.8	149.1	148.7 [148.43(9)]	148.5	148.2 [148.29(13)]
*N*2–Fe–*N*4	105.4 [108.75(12)]	115.5	118.6	121.7	105.4	115.7 [110.48(9)]	119.0	122.4 [121.03(13)]
*N*2–Fe–*N*5	95.9 [93.03(19)]	96.5	96.4	97.2	96.2	96.1 [98.12(9)]	96.0	96.2 [91.12(12)]
*N*2–Fe–*N*6	92.2 [94.79(13)]	93.2	94.1	95.2	91.9	94.6 [91.67(9)]	95.5	96.3 [100.68(12)]
*N*3–Fe–*N*4	105.4 [103.08(12)]	95.3	92.2	89.2	105.4	95.5 [101.07(9)]	92.3	89.1 [90.43(13)]
*N*3–Fe–*N*5	92.2 [94.79(13)]	89.9	89.2	87.6	91.9	89.9 [90.99(9)]	89.4	88.4 [94.47(13)]
*N*3–Fe–*N*6	95.9 [94.64(19)]	96.5	96.4	96.2	96.2	96.1 [95.79(9)]	96.0	96.2 [90.88(12)]
*N*4–Fe–*N*5	74.6 [73.84(13)]	73.9	73.5	72.9	74.6	73.7 [74.86(9)]	73.3	72.8 [73.69(12)]
*N*4–Fe–*N*6	74.6 [74.41(12)]	75.5	76.0	76.4	74.6	75.2 [74.35(9)]	75.4	75.7 [74.69(12)]
*N*5–Fe–*N*6	149.2 [148.15(12)]	149.2	149.1	149.0	149.1	148.7 [149.19(9)]	148.5	148.2 [147.95(13)]
α	74.6 [74.13(18)]	74.7	74.8	74.7	74.6	74.5 [74.64(18)]	74.3	74.3 [74.3]
ϕ	180.0 [176.42(18)]	165.0	160.0	155.0	180.0	165.0 [163.52(9)]	160.0	155.0 [156.26(12)]
θ	89.2 [89.66(3)]	86.1	84.8	82.7	89.2	86.8 [87.59(3)]	85.2	82.7 [88.37(2)]

[a]Fixed during the minimisation process.

Table S14 Atomic coordinates for the DFT-minimised molecules.

L^1 (cisoid conformation).

1	H	3.544092	-0.298040	-2.968170
2	C	2.702499	-0.227498	-2.263319
3	N	0.543137	-0.048949	-0.479029
4	C	2.172740	1.021719	-1.913908
5	C	2.141444	-1.386316	-1.711014
6	C	1.053761	-1.251433	-0.810754
7	C	1.079974	1.066982	-1.010549
8	H	2.591154	1.941036	-2.346162
9	H	2.534358	-2.375680	-1.982634
10	C	0.479156	2.364499	-0.610873
11	N	-0.677780	2.443000	0.119496
12	C	-0.914256	3.743644	0.288712
13	N	0.098171	4.537605	-0.334663
14	C	0.980850	3.647408	-0.906004
15	H	1.869347	3.991844	-1.441681
16	C	0.431757	-2.445981	-0.185862
17	C	0.880466	-3.777466	-0.288648
18	N	0.001197	-4.529961	0.458749
19	C	-0.958013	-3.608927	0.984156
20	N	-0.691542	-2.362597	0.594791
21	H	1.728847	-4.237208	-0.802613
22	C	0.078920	5.917100	-0.294113
23	C	-0.951437	6.557665	0.364822
24	C	-1.988714	5.804474	1.000345
25	C	-1.969467	4.417481	0.962393
26	H	0.902613	6.438471	-0.799768
27	H	-0.960007	7.655401	0.392350
28	H	-2.800676	6.332382	1.519708
29	H	-2.743453	3.801028	1.437386
30	C	-1.999342	-4.126434	1.802119
31	C	-2.056500	-5.487125	2.067736
32	C	-1.072423	-6.370742	1.522432
33	C	-0.056012	-5.882948	0.725458
34	H	-2.732711	-3.414230	2.201741
35	H	-2.858341	-5.893312	2.700032
36	H	-1.111286	-7.448343	1.729878
37	H	0.727479	-6.508547	0.277459

L^2 (cisoid conformation).

1	H	4.317780	0.107318	-1.108205
2	C	3.252863	0.081732	-0.834219
3	N	0.539011	0.016629	-0.122018
4	C	2.503370	1.264379	-0.788118
5	C	2.630724	-1.133257	-0.519360
6	C	1.258625	-1.120899	-0.159915
7	C	1.133484	1.185635	-0.428814
8	H	2.977619	2.229206	-1.014923
9	H	3.203723	-2.070301	-0.547798
10	C	0.289230	2.406513	-0.376785
11	N	-0.976943	2.393637	0.141209
12	C	-1.436080	3.635656	0.030151
13	N	-0.436416	4.491559	-0.583635

14	C	0.650584	3.692057	-0.832391
15	H	1.554164	4.081778	-1.310064
16	C	0.553495	-2.378996	0.194694
17	C	1.101453	-3.678987	0.167897
18	N	0.091280	-4.515013	0.570594
19	C	-1.056643	-3.664895	0.833647
20	N	-0.753138	-2.392481	0.600720
21	H	2.090681	-4.059867	-0.101413
22	C	-0.699493	5.820792	-0.802225
23	C	-1.933990	6.307625	-0.417218
24	C	-2.873094	5.412343	0.185798
25	N	-2.633175	4.125024	0.401748
26	H	0.089862	6.423898	-1.272699
27	H	-2.182219	7.365071	-0.574873
28	H	-3.861395	5.792591	0.497536
29	N	-2.224370	-4.187499	1.250941
30	C	-2.294977	-5.502899	1.411615
31	C	-1.203358	-6.395114	1.168153
32	C	0.003052	-5.873950	0.741271
33	H	-3.261989	-5.910194	1.754376
34	H	-1.313881	-7.476979	1.316516
35	H	0.900160	-6.472116	0.527808

L^3 (cisoid conformation).

1	H	4.262404	-0.196122	-1.729901
2	C	3.245138	-0.148448	-1.314113
3	N	0.651921	-0.027075	-0.248811
4	C	2.604747	1.086220	-1.147634
5	C	2.576509	-1.321574	-0.940725
6	C	1.265912	-1.215895	-0.408063
7	C	1.294318	1.103211	-0.604182
8	H	3.114520	2.016478	-1.433453
9	H	3.067781	-2.297540	-1.055627
10	C	0.569531	2.382248	-0.401559
11	N	-0.699182	2.433211	0.123018
12	C	-1.025429	3.721724	0.158584
13	N	0.020755	4.538521	-0.340701
14	C	1.036280	3.674282	-0.697042
15	H	1.979194	4.030516	-1.116174
16	C	0.512163	-2.426599	0.001659
17	C	0.918653	-3.763419	-0.147150
18	N	-0.098902	-4.533260	0.379287
19	C	-1.084419	-3.617704	0.828280
20	N	-0.721316	-2.358646	0.602983
21	H	1.818348	-4.207004	-0.577609
22	C	-0.073202	5.935607	-0.415105
23	C	-1.292273	6.541214	0.040069
24	C	-2.360516	5.712404	0.551896
25	C	-2.230881	4.344309	0.609905
26	H	-3.282946	6.201949	0.895565
27	H	-3.022768	3.688074	0.992794
28	C	-2.273309	-4.127883	1.436842
29	C	-2.444008	-5.485326	1.578948
30	C	-1.437943	-6.415301	1.117563
31	C	-0.239386	-5.923198	0.500301

32	H	-3.018554	-3.396533	1.774640
33	H	-3.353739	-5.888592	2.046301
34	C	-1.397972	7.957107	-0.034091
35	H	-2.329159	8.429200	0.312951
36	C	0.979941	6.734614	-0.917168
37	H	1.910260	6.265966	-1.263498
38	C	0.750014	-6.822351	0.039825
39	H	1.664487	-6.441466	-0.433207
40	C	-1.587733	-7.823036	1.249416
41	H	-2.504045	-8.207511	1.721687
42	C	-0.607144	-8.705478	0.794768
43	H	-0.745386	-9.790245	0.907823
44	C	0.565235	-8.200343	0.186919
45	H	1.340644	-8.891348	-0.174252
46	C	-0.355961	8.740439	-0.531702
47	H	-0.461428	9.833711	-0.579180
48	C	0.837243	8.124122	-0.974208
49	H	1.661602	8.736767	-1.366870

L^4 (cisoid conformation).

1	H	3.610586	-0.628900	-3.704701
2	C	2.847644	-0.496617	-2.923748
3	N	0.912312	-0.160038	-0.938417
4	C	2.256444	0.756594	-2.718881
5	C	2.459307	-1.579874	-2.125087
6	C	1.473422	-1.368140	-1.126660
7	C	1.276611	0.886636	-1.700675
8	H	2.561499	1.605979	-3.342808
9	H	2.918886	-2.562856	-2.287596
10	C	0.595277	2.202447	-1.415224
11	C	-0.704360	4.617165	-0.830866
12	C	0.884152	3.378194	-2.191611
13	N	-0.284045	2.222469	-0.415031
14	C	-0.928697	3.382923	-0.110198
15	C	0.238672	4.567566	-1.898407
16	H	1.607324	3.350313	-3.016424
17	H	0.447260	5.476683	-2.483063
18	C	0.999078	-2.482652	-0.226447
19	C	0.073798	-4.507022	1.477380
20	N	0.046155	-2.182433	0.653915
21	C	1.555359	-3.806176	-0.317832
22	C	1.094215	-4.801546	0.526971
23	C	-0.421371	-3.148001	1.493196
24	H	2.341914	-4.041671	-1.045653
25	H	1.508410	-5.819926	0.472292
26	C	-1.867452	3.379424	0.970203
27	C	-2.546928	4.539793	1.316908
28	C	-2.321818	5.753573	0.604314
29	C	-1.417661	5.792709	-0.450574
30	H	-2.019237	2.428898	1.500117
31	H	-3.266982	4.527615	2.148682
32	H	-2.869288	6.662573	0.893850
33	H	-1.240904	6.728301	-1.003178
34	C	-1.445839	-2.800928	2.430428
35	C	-1.950714	-3.753084	3.306104

36	C	-1.459566	-5.091061	3.286393
37	C	-0.465367	-5.462654	2.388864
38	H	-1.803802	-1.762132	2.421553
39	H	-2.737462	-3.477903	4.024292
40	H	-1.873074	-5.831130	3.987280
41	H	-0.083760	-6.495111	2.370337

bimpy (cisoid conformation; from ref. 24).

1	N	0.000000	0.000000	0.616630
2	C	-1.162256	-0.001972	1.295402
3	C	-1.207796	-0.004410	2.715171
4	C	0.000000	0.000000	3.423601
5	H	0.000000	0.000000	4.523193
6	C	1.207796	0.004410	2.715171
7	H	2.157040	0.010453	3.269501
8	C	1.162256	0.001972	1.295402
9	C	-2.401316	-0.000115	0.484491
10	N	-2.457993	-0.006753	-0.840925
11	C	-3.802588	-0.003695	-1.152830
12	C	-4.597145	0.007517	0.040975
13	N	-3.671817	0.010541	1.067644
14	C	2.401316	0.000115	0.484491
15	N	2.457993	0.006753	-0.840925
16	C	3.802588	0.003695	-1.152830
17	C	4.597145	-0.007517	0.040975
18	N	3.671817	-0.010541	1.067644
19	H	-2.157040	-0.010453	3.269501
20	H	6.606369	-0.022469	0.935553
21	C	6.004024	-0.013576	0.015575
22	C	4.441399	0.009088	-2.414480
23	H	3.839625	0.017665	-3.333746
24	H	7.707593	-0.012782	-1.317976
25	C	6.609758	-0.008104	-1.249760
26	C	5.840774	0.003035	-2.444729
27	H	6.362693	0.006657	-3.412873
28	H	-3.839625	-0.017665	-3.333746
29	C	-4.441399	-0.009088	-2.414480
30	C	-6.004024	0.013576	0.015575
31	H	-6.606369	0.022468	0.935553
32	C	-6.609758	0.008104	-1.249760
33	H	-7.707593	0.012782	-1.317976
34	H	-6.362693	-0.006657	-3.412873
35	C	-5.840774	-0.003035	-2.444729
36	H	-3.890065	0.023954	2.061296
37	H	3.890065	-0.023954	2.061296

2-bip (cisoid conformation).

1	H	0.000000	0.000000	4.685392
2	C	0.000000	0.000000	3.586014
3	N	0.000000	0.000000	0.800580
4	C	1.216129	0.000000	2.888897
5	C	-1.216129	0.000000	2.888897

6	C	-1.148831	0.000000	1.477108
7	C	1.148831	0.000000	1.477108
8	H	2.166354	0.000000	3.434641
9	H	-2.166354	0.000000	3.434641
10	N	-2.345945	0.000000	0.689132
11	N	2.345945	0.000000	0.689132
12	N	-2.258693	0.000000	-0.661896
13	N	2.258693	0.000000	-0.661896
14	C	-3.543396	0.000000	-1.075507
15	C	-3.643177	0.000000	1.168140
16	H	-3.880366	0.000000	2.233859
17	C	-4.474235	0.000000	0.040821
18	C	3.543396	0.000000	-1.075507
19	C	3.643177	0.000000	1.168140
20	H	3.880366	0.000000	2.233859
21	C	4.474235	0.000000	0.040821
22	C	-4.023495	0.000000	-2.419729
23	H	-3.311684	0.000000	-3.256484
24	C	-5.396137	0.000000	-2.615569
25	H	-5.797999	0.000000	-3.639715
26	C	-6.319051	0.000000	-1.513367
27	H	-7.398042	0.000000	-1.727974
28	C	-5.882646	0.000000	-0.196673
29	H	-6.598450	0.000000	0.638325
30	C	4.023495	0.000000	-2.419729
31	H	3.311684	0.000000	-3.256484
32	C	5.396137	0.000000	-2.615569
33	H	5.797999	0.000000	-3.639715
34	C	6.319051	0.000000	-1.513367
35	H	7.398042	0.000000	-1.727974
36	C	5.882646	0.000000	-0.196673
37	H	6.598450	0.000000	0.638325

$[Fe(L^1)_2]^{2+}$ (**1**$^{2+}$), high-spin, $\phi = 180°$.

1	Fe	0.000000	0.000000	0.000001
2	N	0.000000	0.000000	2.167255
3	C	-0.851380	-0.817159	2.841620
4	C	-0.879415	-0.839242	4.251113
5	C	0.000000	0.000000	4.955950
6	H	0.000000	0.000000	6.054996
7	C	0.879415	0.839243	4.251112
8	H	1.573094	1.500665	4.787070
9	C	0.851379	0.817159	2.841620
10	C	-1.691136	-1.638185	1.959825
11	N	-1.544786	-1.492508	0.591061
12	C	-2.406656	-2.360096	0.021791
13	N	-3.107700	-3.061983	1.027165
14	C	-2.654212	-2.601873	2.251782
15	H	-3.043799	-2.992478	3.195486
16	C	1.691136	1.638185	1.959824
17	N	1.544786	1.492508	0.591061
18	C	2.406656	2.360096	0.021791
19	N	3.107701	3.061983	1.027165
20	C	2.654212	2.601874	2.251782
21	H	3.043799	2.992478	3.195486

22	N	0.000000	0.000000	-2.167254
23	C	0.851380	-0.817159	-2.841619
24	C	0.879415	-0.839242	-4.251112
25	H	1.573094	-1.500664	-4.787070
26	C	0.000000	0.000000	-4.955950
27	H	0.000000	0.000000	-6.054996
28	C	-0.879415	0.839242	-4.251112
29	C	-0.851380	0.817159	-2.841619
30	C	1.691136	-1.638185	-1.959824
31	N	1.544786	-1.492508	-0.591061
32	C	2.406657	-2.360097	-0.021791
33	N	3.107701	-3.061983	-1.027165
34	C	2.654211	-2.601873	-2.251782
35	H	3.043798	-2.992478	-3.195486
36	C	-1.691136	1.638185	-1.959824
37	N	-1.544786	1.492508	-0.591061
38	C	-2.406657	2.360097	-0.021790
39	N	-3.107701	3.061983	-1.027165
40	C	-2.654212	2.601874	-2.251782
41	H	-3.043798	2.992478	-3.195486
42	H	-1.573094	-1.500664	4.787071
43	H	-1.573094	1.500665	-4.787070
44	C	-2.691578	-2.649540	-1.336988
45	H	-2.147528	-2.104627	-2.117475
46	C	-4.057727	-4.021336	0.728991
47	H	-4.544495	-4.512634	1.581395
48	C	-3.646363	-3.611830	-1.636883
49	H	-3.879056	-3.848337	-2.684242
50	C	-4.333173	-4.302369	-0.592323
51	H	-5.087448	-5.064919	-0.826287
52	C	2.691579	2.649540	-1.336989
53	H	2.147528	2.104627	-2.117476
54	C	4.057727	4.021336	0.728991
55	H	4.544496	4.512634	1.581394
56	C	3.646364	3.611829	-1.636884
57	H	3.879057	3.848336	-2.684242
58	C	4.333174	4.302368	-0.592324
59	H	5.087449	5.064919	-0.826287
60	C	-2.691579	2.649541	1.336989
61	H	-2.147529	2.104628	2.117476
62	C	-4.057727	4.021336	-0.728992
63	H	-4.544496	4.512634	-1.581395
64	C	4.057727	-4.021336	-0.728992
65	H	4.544495	-4.512635	-1.581396
66	C	2.691579	-2.649541	1.336989
67	H	2.147529	-2.104628	2.117476
68	C	4.333174	-4.302369	0.592323
69	H	5.087449	-5.064920	0.826286
70	C	3.646364	-3.611831	1.636883
71	H	3.879057	-3.848338	2.684241
72	C	-3.646365	3.611830	1.636883
73	H	-3.879058	3.848337	2.684241
74	C	-4.333175	4.302369	0.592323
75	H	-5.087449	5.064920	0.826286

$[Fe(L^1)_2]^{2+}$ (**1**$^{2+}$), high-spin, $\phi = 165°$.

1	Fe	-0.000025	-0.000007	-0.112467
2	N	0.528665	2.079126	0.169992
3	C	1.493513	2.621441	-0.620966
4	C	1.878981	3.970062	-0.481583
5	C	1.244211	4.752898	0.498759
6	H	1.527058	5.806784	0.630154
7	C	0.241610	4.187876	1.302966
8	H	-0.269197	4.790217	2.065694
9	C	-0.103395	2.834454	1.104726
10	C	2.060139	1.668487	-1.585845
11	N	1.545512	0.383101	-1.617243
12	C	2.231170	-0.282246	-2.570159
13	N	3.187892	0.577865	-3.150774
14	C	3.075463	1.811110	-2.528591
15	H	3.713885	2.655411	-2.801575
16	C	-1.149845	2.110334	1.833365
17	N	-1.396579	0.791929	1.496513
18	C	-2.409009	0.383482	2.289608
19	N	-2.808615	1.442753	3.136801
20	C	-2.008771	2.533348	2.845780
21	H	-2.120394	3.486824	3.368463
22	N	-0.528541	-2.079150	0.169937
23	C	-1.493376	-2.621508	-0.621024
24	C	-1.878764	-3.970156	-0.481682
25	H	-2.656349	-4.401651	-1.125957
26	C	-1.243950	-4.753001	0.498625
27	H	-1.526734	-5.806908	0.629980
28	C	-0.241389	-4.187936	1.302848
29	C	0.103541	-2.834489	1.104659
30	C	-2.060068	-1.668563	-1.585865
31	N	-1.545543	-0.383140	-1.617196
32	C	-2.231257	0.282226	-2.570058
33	N	-3.187904	-0.577925	-3.150733
34	C	-3.075375	-1.811204	-2.528625
35	H	-3.713735	-2.655534	-2.801662
36	C	1.149919	-2.110331	1.833356
37	N	1.396595	-0.791913	1.496537
38	C	2.408996	-0.383436	2.289658
39	N	2.808581	-1.442680	3.136895
40	C	2.008786	-2.533299	2.845839
41	H	2.120408	-3.486767	3.368539
42	H	2.656584	4.401549	-1.125844
43	H	0.269456	-4.790262	2.065563
44	C	2.136532	-1.616846	-3.038971
45	H	1.392784	-2.285530	-2.588799
46	C	4.038963	0.159556	-4.156585
47	H	4.749922	0.902742	-4.540078
48	C	2.990201	-2.036781	-4.050730
49	H	2.931969	-3.067612	-4.426434
50	C	3.948957	-1.139232	-4.611414
51	H	4.625382	-1.470438	-5.410093
52	C	-3.088821	-0.857346	2.393666
53	H	-2.787823	-1.680791	1.736955
54	C	-3.832199	1.309560	4.056577
55	H	-4.064489	2.193977	4.663823
56	C	-4.116063	-0.992361	3.317715

57	H	-4.651128	-1.947740	3.407360
58	C	-4.489440	0.101724	4.156138
59	H	-5.302750	-0.002783	4.885916
60	C	3.088792	0.857408	2.393725
61	H	2.787816	1.680836	1.736985
62	C	3.832108	-1.309448	4.056726
63	H	4.064380	-2.193850	4.664002
64	C	-4.039011	-0.159615	-4.156512
65	H	-4.749906	-0.902834	-4.540060
66	C	-2.136738	1.616875	-3.038767
67	H	-1.393047	2.285587	-2.588542
68	C	-3.949120	1.139216	-4.611244
69	H	-4.625577	1.470421	-5.409895
70	C	-2.990446	2.036810	-4.050495
71	H	-2.932307	3.067675	-4.426120
72	C	4.115977	0.992460	3.317833
73	H	4.651017	1.947852	3.407491
74	C	4.489325	-0.101599	4.156300
75	H	5.302592	0.002935	4.886121

$[Fe(L^1)_2]^{2+}$ (**1²⁺**), high-spin, $\phi = 160°$.

1	Fe	0.000000	0.000000	-0.155523
2	N	0.659354	2.024633	0.219929
3	C	1.661270	2.526215	-0.552491
4	C	2.138682	3.839465	-0.369263
5	C	1.555769	4.632704	0.634569
6	H	1.909730	5.659891	0.800503
7	C	0.512334	4.112719	1.416197
8	H	0.038656	4.724966	2.194761
9	C	0.075035	2.793089	1.173501
10	C	2.165471	1.573280	-1.551430
11	N	1.558831	0.331054	-1.638718
12	C	2.200255	-0.343530	-2.616035
13	N	3.221261	0.466946	-3.155736
14	C	3.195165	1.678730	-2.483095
15	H	3.894690	2.484504	-2.720277
16	C	-1.029838	2.127132	1.869087
17	N	-1.379045	0.845745	1.484549
18	C	-2.429782	0.496961	2.256784
19	N	-2.750406	1.557744	3.136326
20	C	-1.860875	2.586899	2.888464
21	H	-1.899072	3.528604	3.441987
22	N	-0.659354	-2.024633	0.219929
23	C	-1.661270	-2.526215	-0.552491
24	C	-2.138681	-3.839465	-0.369263
25	H	-2.945551	-4.236820	-0.999225
26	C	-1.555769	-4.632704	0.634569
27	H	-1.909730	-5.659891	0.800503
28	C	-0.512334	-4.112719	1.416197
29	C	-0.075035	-2.793088	1.173500
30	C	-2.165471	-1.573281	-1.551430
31	N	-1.558832	-0.331054	-1.638718
32	C	-2.200255	0.343531	-2.616035
33	N	-3.221261	-0.466946	-3.155737
34	C	-3.195165	-1.678730	-2.483096

35	H	-3.894689	-2.484505	-2.720278
36	C	1.029838	-2.127132	1.869087
37	N	1.379045	-0.845744	1.484549
38	C	2.429782	-0.496961	2.256784
39	N	2.750406	-1.557744	3.136325
40	C	1.860875	-2.586899	2.888464
41	H	1.899072	-3.528604	3.441987
42	H	2.945550	4.236820	-0.999226
43	H	-0.038655	-4.724965	2.194761
44	C	2.010530	-1.646873	-3.140346
45	H	1.215878	-2.276964	-2.722264
46	C	4.047236	0.029160	-4.174078
47	H	4.813747	0.733227	-4.522788
48	C	2.838959	-2.086243	-4.164692
49	H	2.708058	-3.093536	-4.583450
50	C	3.865388	-1.239524	-4.683089
51	H	4.521708	-1.586636	-5.491690
52	C	-3.211322	-0.686244	2.319260
53	H	-2.973642	-1.513239	1.642008
54	C	-3.789418	1.481141	4.044925
55	H	-3.954111	2.362608	4.678022
56	C	-4.254256	-0.764714	3.231975
57	H	-4.866089	-1.675533	3.288055
58	C	-4.544564	0.329477	4.102377
59	H	-5.370305	0.269583	4.823158
60	C	3.211322	0.686244	2.319260
61	H	2.973642	1.513240	1.642007
62	C	3.789419	-1.481141	4.044924
63	H	3.954111	-2.362608	4.678021
64	C	-4.047236	-0.029160	-4.174079
65	H	-4.813746	-0.733228	-4.522789
66	C	-2.010531	1.646873	-3.140346
67	H	-1.215879	2.276965	-2.722263
68	C	-3.865388	1.239523	-4.683090
69	H	-4.521707	1.586636	-5.491691
70	C	-2.838960	2.086243	-4.164692
71	H	-2.708059	3.093537	-4.583450
72	C	4.254256	0.764714	3.231975
73	H	4.866089	1.675533	3.288055
74	C	4.544564	-0.329477	4.102376
75	H	5.370306	-0.269583	4.823157

$[Fe(L^1)_2]^{2+}$ (**1**$^{2+}$), high-spin, $\phi = 155°$.

1	Fe	0.065221	-0.022488	-0.205286
2	N	0.088753	2.124052	0.056619
3	C	1.157592	2.807477	-0.438464
4	C	1.252275	4.207843	-0.317396
5	C	0.212396	4.898900	0.328778
6	H	0.259974	5.991511	0.437595
7	C	-0.890843	4.188674	0.825387
8	H	-1.717278	4.714755	1.320954
9	C	-0.927579	2.787023	0.661689
10	C	2.166884	1.946273	-1.071489
11	N	1.919672	0.584979	-1.137128
12	C	2.990777	0.025552	-1.738724

13	N	3.926419	1.029790	-2.061297
14	C	3.402484	2.243136	-1.641610
15	H	3.944303	3.182758	-1.777568
16	C	-2.031427	1.920432	1.081686
17	N	-1.970781	0.571859	0.784924
18	C	-3.125232	0.039542	1.240560
19	N	-3.914869	1.048893	1.842527
20	C	-3.218101	2.237774	1.739280
21	H	-3.619437	3.177811	2.126412
22	N	-0.292394	-2.065460	0.400727
23	C	-0.831265	-2.910315	-0.521437
24	C	-1.092791	-4.260687	-0.215254
25	H	-1.521156	-4.933851	-0.969667
26	C	-0.786668	-4.728614	1.074196
27	H	-0.981894	-5.776416	1.342301
28	C	-0.218484	-3.855356	2.014025
29	C	0.031546	-2.518384	1.637459
30	C	-1.107621	-2.271492	-1.816290
31	N	-0.755273	-0.941601	-1.981612
32	C	-1.119891	-0.597415	-3.235252
33	N	-1.706546	-1.707995	-3.875454
34	C	-1.695974	-2.765079	-2.978162
35	H	-2.099694	-3.746590	-3.239916
36	C	0.675399	-1.510438	2.483687
37	N	0.932191	-0.262276	1.948399
38	C	1.569186	0.432454	2.915008
39	N	1.709773	-0.371526	4.071271
40	C	1.140870	-1.600289	3.794095
41	H	1.124308	-2.409310	4.528920
42	H	2.117346	4.749237	-0.722963
43	H	0.039801	-4.210633	3.020377
44	C	3.288504	-1.321517	-2.062214
45	H	2.561705	-2.101287	-1.802794
46	C	5.127285	0.742037	-2.682968
47	H	5.790310	1.592026	-2.889727
48	C	4.494337	-1.611052	-2.687360
49	H	4.745456	-2.649487	-2.943698
50	C	5.418834	-0.568393	-2.999052
51	H	6.373041	-0.795808	-3.491943
52	C	-3.644255	-1.281605	1.206166
53	H	-3.054656	-2.071664	0.730702
54	C	-5.153848	0.792723	2.399599
55	H	-5.681716	1.649991	2.837039
56	C	-4.887825	-1.540316	1.765977
57	H	-5.297904	-2.559373	1.742117
58	C	-5.647974	-0.493365	2.369748
59	H	-6.632669	-0.696540	2.810216
60	C	2.097730	1.749621	2.947733
61	H	2.007512	2.380294	2.057525
62	C	2.331679	0.080751	5.220437
63	H	2.387770	-0.626273	6.058240
64	C	-2.179529	-1.641849	-5.172964
65	H	-2.622969	-2.558661	-5.582269
66	C	-1.006512	0.624652	-3.943515
67	H	-0.552099	1.487460	-3.441132
68	C	-2.070127	-0.453324	-5.863978

69	H	-2.445712	-0.401788	-6.894290
70	C	-1.479654	0.691132	-5.247293
71	H	-1.403200	1.629806	-5.813138
72	C	2.723390	2.204461	4.100338
73	H	3.137990	3.221339	4.134201
74	C	2.839005	1.361841	5.247172
75	H	3.334134	1.719663	6.159219

$[Fe(L^1)_2]^{2+}$ (**1**$^{2+}$), low-spin.

1	Fe	0.000000	0.000000	0.000000
2	N	0.000000	0.000000	1.923404
3	C	-0.839846	-0.839847	2.603432
4	C	-0.860485	-0.860485	4.010672
5	C	0.000000	0.000000	4.716436
6	H	0.000000	0.000000	5.815120
7	C	0.860485	0.860485	4.010672
8	H	1.539456	1.539456	4.543596
9	C	0.839847	0.839846	2.603432
10	C	-1.635704	-1.635704	1.678106
11	N	-1.402844	-1.402844	0.327091
12	C	-2.229814	-2.229814	-0.354105
13	N	-2.987578	-2.987578	0.569597
14	C	-2.611996	-2.611996	1.846172
15	H	-3.057668	-3.057668	2.739108
16	C	1.635704	1.635704	1.678106
17	N	1.402844	1.402844	0.327091
18	C	2.229814	2.229814	-0.354105
19	N	2.987578	2.987578	0.569597
20	C	2.611996	2.611996	1.846172
21	H	3.057668	3.057668	2.739108
22	N	0.000000	0.000000	-1.923404
23	C	0.839847	-0.839847	-2.603432
24	C	0.860485	-0.860485	-4.010672
25	H	1.539456	-1.539456	-4.543596
26	C	0.000000	0.000000	-4.716436
27	H	0.000000	0.000000	-5.815120
28	C	-0.860485	0.860485	-4.010672
29	C	-0.839846	0.839846	-2.603432
30	C	1.635704	-1.635704	-1.678106
31	N	1.402844	-1.402844	-0.327091
32	C	2.229814	-2.229814	0.354105
33	N	2.987578	-2.987578	-0.569597
34	C	2.611996	-2.611996	-1.846172
35	H	3.057668	-3.057668	-2.739108
36	C	-1.635704	1.635704	-1.678106
37	N	-1.402844	1.402844	-0.327091
38	C	-2.229814	2.229814	0.354105
39	N	-2.987578	2.987578	-0.569597
40	C	-2.611996	2.611996	-1.846172
41	H	-3.057668	3.057667	-2.739108
42	H	-1.539456	-1.539456	4.543596
43	H	-1.539456	1.539456	-4.543596
44	C	-2.442742	-2.442742	-1.740920
45	H	-1.862806	-1.862806	-2.465964
46	C	-3.922774	-3.922774	0.163319

47	H	-4.456515	-4.456515	0.960240
48	C	-3.381632	-3.381631	-2.146230
49	H	-3.555313	-3.555313	-3.217030
50	C	-4.127521	-4.127520	-1.183508
51	H	-4.870474	-4.870474	-1.501512
52	C	2.442742	2.442742	-1.740920
53	H	1.862806	1.862806	-2.465964
54	C	3.922774	3.922774	0.163319
55	H	4.456515	4.456515	0.960240
56	C	3.381631	3.381632	-2.146230
57	H	3.555313	3.555313	-3.217030
58	C	4.127520	4.127521	-1.183508
59	H	4.870474	4.870474	-1.501512
60	C	-2.442742	2.442742	1.740920
61	H	-1.862806	1.862806	2.465964
62	C	-3.922774	3.922774	-0.163319
63	H	-4.456515	4.456515	-0.960240
64	C	3.922774	-3.922774	-0.163319
65	H	4.456516	-4.456516	-0.960240
66	C	2.442742	-2.442742	1.740921
67	H	1.862806	-1.862806	2.465964
68	C	4.127521	-4.127521	1.183508
69	H	4.870474	-4.870474	1.501512
70	C	3.381631	-3.381631	2.146230
71	H	3.555313	-3.555313	3.217030
72	C	-3.381632	3.381632	2.146230
73	H	-3.555313	3.555313	3.217029
74	C	-4.127521	4.127521	1.183507
75	H	-4.870474	4.870474	1.501512

$[Fe(L^2)_2]^{2+}$ (**2**$^{2+}$), high-spin, $\phi = 180°$.

1	Fe	0.000000	0.000000	0.000000
2	N	0.000000	0.000000	2.163638
3	C	-0.812959	-0.850707	2.836262
4	C	-0.837220	-0.880141	4.244871
5	C	-0.000001	0.000001	4.950244
6	H	-0.000001	0.000001	6.049183
7	C	0.837219	0.880142	4.244871
8	H	1.497443	1.575296	4.780679
9	C	0.812959	0.850708	2.836262
10	C	-1.632556	-1.690421	1.949908
11	N	-1.471967	-1.531933	0.586589
12	C	-2.327870	-2.378066	-0.007611
13	N	-3.047957	-3.094804	0.994244
14	C	-2.601974	-2.656412	2.225804
15	H	-3.000356	-3.051144	3.164711
16	C	1.632556	1.690421	1.949908
17	N	1.471967	1.531932	0.586589
18	C	2.327870	2.378065	-0.007611
19	N	3.047957	3.094804	0.994245
20	C	2.601975	2.656412	2.225804
21	H	3.000357	3.051144	3.164711
22	N	0.000000	0.000000	-2.163638
23	C	0.812959	-0.850707	-2.836262
24	C	0.837219	-0.880142	-4.244871

25	H	1.497443	-1.575296	-4.780679
26	C	-0.000001	0.000000	-4.950244
27	H	-0.000001	0.000000	-6.049183
28	C	-0.837220	0.880142	-4.244871
29	C	-0.812959	0.850707	-2.836262
30	C	1.632556	-1.690421	-1.949908
31	N	1.471967	-1.531933	-0.586589
32	C	2.327870	-2.378065	0.007611
33	N	3.047957	-3.094804	-0.994244
34	C	2.601974	-2.656412	-2.225804
35	H	3.000356	-3.051144	-3.164711
36	C	-1.632556	1.690421	-1.949907
37	N	-1.471966	1.531932	-0.586589
38	C	-2.327870	2.378065	0.007611
39	N	-3.047957	3.094804	-0.994244
40	C	-2.601975	2.656412	-2.225803
41	H	-3.000357	3.051144	-3.164710
42	H	-1.497444	-1.575295	4.780679
43	H	-1.497444	1.575296	-4.780678
44	N	-2.525290	-2.573625	-1.318395
45	C	-3.993039	-4.026014	0.625933
46	H	-4.526214	-4.551012	1.430312
47	C	-3.439195	-3.477237	-1.666952
48	H	-3.596848	-3.633887	-2.746707
49	C	-4.202821	-4.231135	-0.723346
50	H	-4.947605	-4.964460	-1.058203
51	N	2.525291	2.573624	-1.318395
52	C	3.993039	4.026013	0.625933
53	H	4.526214	4.551012	1.430313
54	C	3.439195	3.477236	-1.666951
55	H	3.596848	3.633887	-2.746706
56	C	4.202821	4.231134	-0.723346
57	H	4.947606	4.964459	-1.058202
58	N	-2.525290	2.573625	1.318395
59	C	-3.993039	4.026013	-0.625933
60	H	-4.526214	4.551012	-1.430312
61	C	3.993039	-4.026013	-0.625933
62	H	4.526214	-4.551012	-1.430313
63	N	2.525291	-2.573624	1.318395
64	C	4.202821	-4.231134	0.723346
65	H	4.947606	-4.964459	1.058202
66	C	3.439195	-3.477236	1.666952
67	H	3.596849	-3.633886	2.746706
68	C	-3.439194	3.477236	1.666951
69	H	-3.596847	3.633887	2.746706
70	C	-4.202820	4.231134	0.723346
71	H	-4.947605	4.964459	1.058203

$[Fe(L^2)_2]^{2+}$ (**2**$^{2+}$), high-spin, $\phi = 165°$.

1	Fe	0.000000	0.000000	-0.125132
2	N	0.705032	2.032218	0.158058
3	C	1.728088	2.480276	-0.610692
4	C	2.242930	3.782324	-0.456489
5	C	1.677925	4.616198	0.523030
6	H	2.061559	5.635927	0.667033

7	C	0.617140	4.144775	1.313160
8	H	0.161636	4.786484	2.079149
9	C	0.146112	2.833747	1.096298
10	C	2.208301	1.482665	-1.578589
11	N	1.577646	0.253103	-1.600673
12	C	2.186714	-0.483704	-2.543544
13	N	3.225207	0.288815	-3.139120
14	C	3.231198	1.528080	-2.526733
15	H	3.940951	2.312057	-2.805280
16	C	-0.973035	2.199183	1.806346
17	N	-1.300592	0.902886	1.460535
18	C	-2.354671	0.555446	2.215675
19	N	-2.709241	1.650796	3.059818
20	C	-1.830744	2.682981	2.796392
21	H	-1.890070	3.645111	3.312887
22	N	-0.705032	-2.032218	0.158058
23	C	-1.728088	-2.480276	-0.610691
24	C	-2.242930	-3.782324	-0.456489
25	H	-3.067868	-4.139843	-1.087007
26	C	-1.677926	-4.616198	0.523031
27	H	-2.061559	-5.635927	0.667033
28	C	-0.617141	-4.144775	1.313160
29	C	-0.146112	-2.833747	1.096298
30	C	-2.208301	-1.482665	-1.578588
31	N	-1.577646	-0.253103	-1.600673
32	C	-2.186714	0.483704	-2.543544
33	N	-3.225207	-0.288815	-3.139119
34	C	-3.231198	-1.528080	-2.526733
35	H	-3.940951	-2.312057	-2.805280
36	C	0.973035	-2.199183	1.806346
37	N	1.300592	-0.902886	1.460535
38	C	2.354671	-0.555446	2.215675
39	N	2.709241	-1.650796	3.059818
40	C	1.830743	-2.682981	2.796392
41	H	1.890069	-3.645111	3.312888
42	H	3.067868	4.139843	-1.087007
43	H	-0.161637	-4.786484	2.079150
44	N	1.912966	-1.741261	-2.914421
45	C	3.998543	-0.258534	-4.138306
46	H	4.790014	0.371343	-4.566651
47	C	2.663696	-2.263868	-3.882009
48	H	2.435973	-3.299205	-4.184314
49	C	3.724447	-1.555093	-4.526368
50	H	4.318059	-2.027892	-5.319253
51	N	-3.017846	-0.609283	2.231805
52	C	-3.771368	1.534477	3.928339
53	H	-4.009871	2.405198	4.554272
54	C	-4.041059	-0.716048	3.076952
55	H	-4.581301	-1.676946	3.085003
56	C	-4.457332	0.336331	3.949498
57	H	-5.309729	0.202776	4.627763
58	N	3.017847	0.609283	2.231805
59	C	3.771368	-1.534477	3.928339
60	H	4.009871	-2.405198	4.554272
61	C	-3.998543	0.258534	-4.138305
62	H	-4.790014	-0.371343	-4.566651

63	N	-1.912966	1.741260	-2.914421
64	C	-3.724447	1.555094	-4.526368
65	H	-4.318059	2.027892	-5.319253
66	C	-2.663696	2.263868	-3.882009
67	H	-2.435972	3.299205	-4.184314
68	C	4.041059	0.716047	3.076952
69	H	4.581301	1.676945	3.085003
70	C	4.457332	-0.336331	3.949498
71	H	5.309729	-0.202776	4.627763

$[Fe(L^2)_2]^{2+}$ (**2**$^{2+}$), high-spin, $\phi = 160°$.

1	Fe	0.000000	0.000000	-0.161902
2	N	0.826418	1.971163	0.214979
3	C	1.886331	2.376931	-0.527262
4	C	2.490483	3.631303	-0.315882
5	C	1.974707	4.464031	0.691253
6	H	2.427772	5.447379	0.879742
7	C	0.872585	4.039207	1.450327
8	H	0.452236	4.681861	2.235380
9	C	0.312772	2.774171	1.176819
10	C	2.303148	1.391783	-1.536194
11	N	1.587709	0.212175	-1.617620
12	C	2.148183	-0.521639	-2.592575
13	N	3.238989	0.203842	-3.151481
14	C	3.329959	1.409356	-2.480819
15	H	4.092567	2.154753	-2.723175
16	C	-0.861617	2.197216	1.844625
17	N	-1.278630	0.943351	1.443188
18	C	-2.372716	0.652148	2.164985
19	N	-2.659582	1.739733	3.044987
20	C	-1.699474	2.709544	2.837266
21	H	-1.695967	3.653725	3.388945
22	N	-0.826418	-1.971163	0.214979
23	C	-1.886330	-2.376931	-0.527262
24	C	-2.490482	-3.631303	-0.315882
25	H	-3.345312	-3.954160	-0.924905
26	C	-1.974707	-4.464031	0.691254
27	H	-2.427772	-5.447379	0.879742
28	C	-0.872585	-4.039207	1.450327
29	C	-0.312772	-2.774171	1.176819
30	C	-2.303148	-1.391784	-1.536194
31	N	-1.587709	-0.212175	-1.617620
32	C	-2.148183	0.521639	-2.592575
33	N	-3.238989	-0.203842	-3.151481
34	C	-3.329959	-1.409356	-2.480819
35	H	-4.092567	-2.154754	-2.723175
36	C	0.861617	-2.197215	1.844625
37	N	1.278630	-0.943351	1.443188
38	C	2.372716	-0.652148	2.164985
39	N	2.659582	-1.739733	3.044987
40	C	1.699474	-2.709544	2.837266
41	H	1.695967	-3.653725	3.388944
42	H	3.345312	3.954160	-0.924905
43	H	-0.452236	-4.681861	2.235380
44	N	1.789407	-1.739264	-3.019422

45	C	3.975184	-0.349321	-4.175253
46	H	4.809930	0.242797	-4.574319
47	C	2.504973	-2.267941	-4.010177
48	H	2.207998	-3.270654	-4.358776
49	C	3.613248	-1.604808	-4.622117
50	H	4.175193	-2.080585	-5.436054
51	N	-3.127123	-0.455304	2.123647
52	C	-3.744425	1.675134	3.890221
53	H	-3.927121	2.538131	4.544980
54	C	-4.172473	-0.512503	2.946072
55	H	-4.787056	-1.426825	2.906110
56	C	-4.522418	0.535126	3.852742
57	H	-5.395953	0.443521	4.510716
58	N	3.127123	0.455304	2.123647
59	C	3.744425	-1.675134	3.890221
60	H	3.927121	-2.538131	4.544980
61	C	-3.975184	0.349321	-4.175253
62	H	-4.809930	-0.242797	-4.574319
63	N	-1.789407	1.739264	-3.019422
64	C	-3.613248	1.604808	-4.622117
65	H	-4.175194	2.080585	-5.436054
66	C	-2.504973	2.267941	-4.010176
67	H	-2.207999	3.270654	-4.358776
68	C	4.172473	0.512503	2.946073
69	H	4.787056	1.426825	2.906110
70	C	4.522418	-0.535126	3.852742
71	H	5.395953	-0.443521	4.510716

$[Fe(L^2)_2]^{2+}$ (**2**$^{2+}$), high-spin, $\phi = 155°$.

1	Fe	0.000000	0.000000	-0.204736
2	N	0.913592	1.914532	0.265554
3	C	1.999597	2.291539	-0.454737
4	C	2.668211	3.502445	-0.192065
5	C	2.187951	4.324869	0.840761
6	H	2.689902	5.275768	1.068025
7	C	1.056959	3.932680	1.574220
8	H	0.661146	4.569254	2.376788
9	C	0.433385	2.709735	1.250534
10	C	2.368973	1.330271	-1.504486
11	N	1.591544	0.195920	-1.641756
12	C	2.111434	-0.518624	-2.653185
13	N	3.241177	0.171978	-3.176765
14	C	3.396997	1.336751	-2.447990
15	H	4.198684	2.051240	-2.654954
16	C	-0.779070	2.175845	1.884246
17	N	-1.264294	0.965618	1.429924
18	C	-2.382663	0.714032	2.129522
19	N	-2.613513	1.781893	3.050222
20	C	-1.595161	2.699269	2.889307
21	H	-1.542266	3.619751	3.477236
22	N	-0.913592	-1.914532	0.265553
23	C	-1.999596	-2.291539	-0.454739
24	C	-2.668208	-3.502446	-0.192069
25	H	-3.543975	-3.801387	-0.783301
26	C	-2.187949	-4.324871	0.840757

27	H	-2.689899	-5.275770	1.068020
28	C	-1.056958	-3.932682	1.574217
29	C	-0.433385	-2.709735	1.250533
30	C	-2.368973	-1.330271	-1.504487
31	N	-1.591544	-0.195920	-1.641756
32	C	-2.111434	0.518624	-2.653185
33	N	-3.241177	-0.171977	-3.176764
34	C	-3.396996	-1.336751	-2.447991
35	H	-4.198682	-2.051240	-2.654956
36	C	0.779067	-2.175844	1.884247
37	N	1.264291	-0.965616	1.429926
38	C	2.382665	-0.714035	2.129518
39	N	2.613509	-1.781890	3.050226
40	C	1.595156	-2.699265	2.889314
41	H	1.542258	-3.619745	3.477245
42	H	3.543978	3.801385	-0.783297
43	H	-0.661145	-4.569255	2.376786
44	N	1.684111	-1.690607	-3.139331
45	C	3.947003	-0.371869	-4.226818
46	H	4.814814	0.190597	-4.597179
47	C	2.370164	-2.210133	-4.155694
48	H	2.016697	-3.175587	-4.553229
49	C	3.515699	-1.581875	-4.734203
50	H	4.051899	-2.048062	-5.570798
51	N	-3.203004	-0.342832	2.039114
52	C	-3.708420	1.750448	3.883991
53	H	-3.845369	2.596950	4.570684
54	C	-4.258154	-0.368268	2.850670
55	H	-4.926221	-1.241502	2.770138
56	C	-4.553536	0.662329	3.795403
57	H	-5.437571	0.598299	4.442531
58	N	3.203013	0.342823	2.039099
59	C	3.708414	-1.750443	3.883997
60	H	3.845357	-2.596940	4.570698
61	C	-3.947004	0.371870	-4.226817
62	H	-4.814815	-0.190595	-4.597178
63	N	-1.684111	1.690608	-3.139330
64	C	-3.515700	1.581877	-4.734201
65	H	-4.051900	2.048064	-5.570797
66	C	-2.370164	2.210134	-4.155693
67	H	-2.016698	3.175588	-4.553228
68	C	4.258162	0.368260	2.850658
69	H	4.926234	1.241489	2.770119
70	C	4.553535	-0.662329	3.795402
71	H	5.437569	-0.598298	4.442531

$[Fe(L^2)_2]^{2+}$ (**2**$^{2+}$), low-spin.

1	Fe	0.000000	0.000000	0.000000
2	N	0.000000	0.000000	1.923959
3	C	-0.837482	-0.837482	2.600453
4	C	-0.859807	-0.859807	4.006036
5	C	0.000000	0.000000	4.711247
6	H	0.000000	0.000000	5.809865
7	C	0.859807	0.859807	4.006036
8	H	1.538708	1.538708	4.539243

9	C	0.837482	0.837482	2.600453
10	C	-1.632500	-1.632500	1.669594
11	N	-1.384195	-1.384195	0.325482
12	C	-2.193816	-2.193816	-0.382711
13	N	-2.970640	-2.970640	0.528533
14	C	-2.613217	-2.613217	1.813312
15	H	-3.067948	-3.067948	2.697683
16	C	1.632500	1.632500	1.669594
17	N	1.384195	1.384195	0.325482
18	C	2.193816	2.193816	-0.382711
19	N	2.970640	2.970640	0.528533
20	C	2.613217	2.613217	1.813312
21	H	3.067948	3.067948	2.697683
22	N	0.000000	0.000000	-1.923959
23	C	0.837482	-0.837482	-2.600453
24	C	0.859807	-0.859807	-4.006036
25	H	1.538708	-1.538708	-4.539243
26	C	0.000000	0.000000	-4.711247
27	H	0.000000	0.000000	-5.809865
28	C	-0.859807	0.859807	-4.006036
29	C	-0.837482	0.837482	-2.600453
30	C	1.632500	-1.632500	-1.669594
31	N	1.384195	-1.384195	-0.325482
32	C	2.193816	-2.193816	0.382711
33	N	2.970640	-2.970640	-0.528533
34	C	2.613217	-2.613217	-1.813312
35	H	3.067948	-3.067948	-2.697683
36	C	-1.632500	1.632500	-1.669594
37	N	-1.384195	1.384195	-0.325482
38	C	-2.193816	2.193816	0.382711
39	N	-2.970640	2.970640	-0.528533
40	C	-2.613217	2.613217	-1.813312
41	H	-3.067948	3.067948	-2.697683
42	H	-1.538708	-1.538708	4.539243
43	H	-1.538708	1.538708	-4.539243
44	N	-2.306326	-2.306326	-1.711534
45	C	-3.882079	-3.882079	0.040252
46	H	-4.458799	-4.458799	0.776080
47	C	-3.188903	-3.188903	-2.175024
48	H	-3.276848	-3.276848	-3.270157
49	C	-4.004255	-4.004255	-1.329130
50	H	-4.719404	-4.719404	-1.755279
51	N	2.306326	2.306326	-1.711534
52	C	3.882079	3.882079	0.040252
53	H	4.458799	4.458799	0.776080
54	C	3.188903	3.188903	-2.175024
55	H	3.276848	3.276848	-3.270157
56	C	4.004255	4.004255	-1.329130
57	H	4.719404	4.719404	-1.755279
58	N	-2.306326	2.306326	1.711534
59	C	-3.882079	3.882079	-0.040252
60	H	-4.458799	4.458799	-0.776080
61	C	3.882079	-3.882079	-0.040252
62	H	4.458799	-4.458799	-0.776080
63	N	2.306326	-2.306326	1.711534
64	C	4.004255	-4.004255	1.329130

65	H	4.719404	-4.719404	1.755279
66	C	3.188903	-3.188903	2.175024
67	H	3.276848	-3.276848	3.270157
68	C	-3.188903	3.188903	2.175024
69	H	-3.276848	3.276848	3.270157
70	C	-4.004255	4.004255	1.329130
71	H	-4.719404	4.719404	1.755279

$[Fe(L^3)_2]^{2+}$ (**3**$^{2+}$), high-spin.

1	Fe	-0.000727	0.004589	0.000086
2	N	2.167940	0.003812	-0.009342
3	C	2.838648	-0.851683	-0.825561
4	C	4.248457	-0.875217	-0.856368
5	C	4.955417	0.012114	-0.027745
6	H	6.054448	0.015363	-0.035189
7	C	4.254444	0.895871	0.809983
8	H	4.792852	1.595850	1.462652
9	C	2.844691	0.864155	0.797519
10	C	1.954116	-1.698995	-1.632277
11	N	0.584387	-1.547661	-1.491178
12	C	0.016559	-2.421063	-2.343718
13	N	1.008307	-3.135398	-3.031446
14	C	2.234710	-2.680177	-2.578926
15	H	3.182282	-3.071310	-2.953208
16	C	1.964511	1.707476	1.613404
17	N	0.594428	1.555954	1.475971
18	C	0.027881	2.427645	2.330810
19	N	1.020696	3.139093	3.019419
20	C	2.246588	2.685398	2.563159
21	H	3.194773	3.075594	2.936934
22	N	-2.169062	-0.042938	-0.019015
23	C	-2.853961	0.793333	-0.843909
24	C	-4.262514	0.765620	-0.904094
25	H	-4.807711	1.445547	-1.572099
26	C	-4.953282	-0.151930	-0.094705
27	H	-6.051082	-0.195036	-0.124672
28	C	-4.237757	-1.015035	0.751983
29	C	-2.829887	-0.932751	0.768283
30	C	-1.983594	1.676818	-1.627120
31	N	-0.612831	1.568054	-1.460539
32	C	-0.056484	2.470361	-2.290035
33	N	-1.056622	3.160158	-2.990091
34	C	-2.276684	2.659526	-2.568506
35	H	-3.228733	3.025820	-2.956382
36	C	-1.936708	-1.752207	1.594158
37	N	-0.569725	-1.559621	1.478830
38	C	0.008527	-2.417684	2.339730
39	N	-0.973768	-3.161580	3.009349
40	C	-2.204994	-2.741641	2.535892
41	H	-3.147188	-3.160725	2.893175
42	H	4.782271	-1.571004	-1.517190
43	H	-4.763506	-1.738544	1.389093
44	C	-1.359965	-2.686228	-2.610375
45	H	-2.117621	-2.116142	-2.060636
46	C	0.709327	-4.119471	-3.994896

47	C	-1.689421	-3.642070	-3.545026
48	H	-2.744175	-3.859627	-3.765304
49	C	-0.674794	-4.378758	-4.257893
50	C	-1.348440	2.693542	2.596302
51	H	-2.105488	2.125935	2.042989
52	C	0.722183	4.120490	3.985843
53	C	-1.677418	3.646449	3.534068
54	H	-2.731983	3.864911	3.754338
55	C	-0.661971	4.379271	4.249887
56	C	1.387504	-2.644803	2.627231
57	H	2.136790	-2.048360	2.094231
58	C	-0.662422	-4.140068	3.974560
59	C	-0.769349	4.164576	-3.936024
60	C	1.315854	2.784326	-2.521562
61	H	2.079145	2.236089	-1.957466
62	C	0.611067	4.470259	-4.167273
63	C	1.633897	3.760120	-3.439302
64	H	2.685370	4.015855	-3.632597
65	C	1.729041	-3.597501	3.560764
66	H	2.785919	-3.787910	3.795496
67	C	0.724300	-4.365408	4.254437
68	C	-1.788529	4.847417	-4.633185
69	H	-2.846450	4.615141	-4.456194
70	C	-1.443212	5.832454	-5.563088
71	H	-2.237613	6.363681	-6.106180
72	C	-0.086448	6.150533	-5.808897
73	H	0.168833	6.927973	-6.542360
74	C	0.922347	5.479712	-5.119590
75	H	1.978669	5.722752	-5.304502
76	C	1.058798	-5.352498	5.223210
77	H	2.120157	-5.534854	5.445490
78	C	0.066282	-6.075624	5.882417
79	H	0.340063	-6.834595	6.628427
80	C	-1.296249	-5.833162	5.591885
81	H	-2.077748	-6.403516	6.113599
82	C	-1.664743	-4.873628	4.644198
83	H	-2.727488	-4.699729	4.432520
84	C	1.735044	4.826978	4.670718
85	H	2.795556	4.630206	4.468060
86	C	1.379037	5.789280	5.620200
87	H	2.167763	6.339014	6.153004
88	C	0.018341	6.059975	5.899522
89	H	-0.245614	6.819075	6.648974
90	C	-0.983842	5.366449	5.223096
91	H	-2.043019	5.572983	5.434296
92	C	1.721512	-4.828294	-4.677382
93	H	2.782147	-4.631124	-4.475801
94	C	1.364961	-5.793790	-5.623395
95	H	2.153504	-6.345469	-6.154480
96	C	0.004403	-6.065545	-5.901236
97	H	-0.259721	-6.827396	-6.647821
98	C	-0.997465	-5.369374	-5.227147
99	H	-2.056735	-5.576449	-5.437263

$[Fe(L^3)_2]^{2+}$ (**3**$^{2+}$), low-spin.

1	Fe	0.000000	0.000000	0.000000
2	N	0.000000	0.000000	1.925668
3	C	0.840064	-0.840061	2.604282
4	C	0.860687	-0.860685	4.011836
5	C	0.000000	0.000000	4.716913
6	H	0.000000	0.000000	5.815624
7	C	-0.860688	0.860685	4.011836
8	H	-1.539603	1.539598	4.544697
9	C	-0.840064	0.840061	2.604282
10	C	1.634022	-1.634016	1.678495
11	N	1.403935	-1.403928	0.325191
12	C	2.231444	-2.231434	-0.350256
13	N	2.985945	-2.985935	0.564460
14	C	2.609424	-2.609417	1.840149
15	H	3.044901	-3.044894	2.740831
16	C	-1.634022	1.634016	1.678495
17	N	-1.403935	1.403928	0.325191
18	C	-2.231444	2.231434	-0.350256
19	N	-2.985945	2.985935	0.564460
20	C	-2.609424	2.609417	1.840149
21	H	-3.044901	3.044894	2.740831
22	N	0.000000	0.000000	-1.925668
23	C	0.840059	0.840066	-2.604282
24	C	0.860683	0.860690	-4.011836
25	H	1.539594	1.539607	-4.544697
26	C	0.000000	0.000000	-4.716913
27	H	0.000000	0.000000	-5.815625
28	C	-0.860683	-0.860690	-4.011836
29	C	-0.840059	-0.840066	-2.604282
30	C	1.634012	1.634026	-1.678495
31	N	1.403926	1.403936	-0.325191
32	C	2.231430	2.231448	0.350256
33	N	2.985926	2.985954	-0.564460
34	C	2.609407	2.609434	-1.840149
35	H	3.044881	3.044914	-2.740831
36	C	-1.634012	-1.634026	-1.678494
37	N	-1.403926	-1.403936	-0.325191
38	C	-2.231430	-2.231448	0.350256
39	N	-2.985926	-2.985954	-0.564460
40	C	-2.609407	-2.609434	-1.840149
41	H	-3.044881	-3.044914	-2.740831
42	H	1.539603	-1.539598	4.544697
43	H	-1.539594	-1.539607	-4.544697
44	C	2.427920	-2.427905	-1.750202
45	H	1.837758	-1.837741	-2.457622
46	C	3.941874	-3.941862	0.162611
47	C	3.353665	-3.353646	-2.176798
48	H	3.514671	-3.514649	-3.252128
49	C	4.130886	-4.130870	-1.243637
50	C	-2.427920	2.427905	-1.750202
51	H	-1.837757	1.837741	-2.457622
52	C	-3.941874	3.941862	0.162612
53	C	-3.353665	3.353647	-2.176798
54	H	-3.514671	3.514649	-3.252128
55	C	-4.130886	4.130870	-1.243637
56	C	-2.427905	-2.427921	1.750202

57	H	-1.837746	-1.837752	2.457622
58	C	-3.941847	-3.941889	-0.162611
59	C	3.941847	3.941889	-0.162612
60	C	2.427905	2.427921	1.750202
61	H	1.837747	1.837752	2.457622
62	C	4.130858	4.130899	1.243637
63	C	3.353642	3.353669	2.176798
64	H	3.514647	3.514673	3.252128
65	C	-3.353642	-3.353669	2.176798
66	H	-3.514647	-3.514673	3.252128
67	C	-4.130858	-4.130899	1.243637
68	C	-5.091341	-5.091396	1.666827
69	H	-5.244337	-5.244391	2.744967
70	C	-4.687995	-4.688051	-1.099497
71	H	-4.544820	-4.544878	-2.178068
72	C	4.687995	4.688051	-1.099497
73	H	4.544820	4.544878	-2.178068
74	C	5.091341	5.091396	1.666827
75	H	5.244337	5.244391	2.744967
76	C	5.827068	5.827138	0.739026
77	H	6.565421	6.565501	1.081289
78	C	5.623207	5.623277	-0.645603
79	H	6.203341	6.203423	-1.376986
80	C	-5.827068	-5.827138	0.739026
81	H	-6.565421	-6.565500	1.081289
82	C	-5.623207	-5.623277	-0.645603
83	H	-6.203341	-6.203423	-1.376986
84	C	-4.688028	4.688019	1.099497
85	H	-4.544852	4.544846	2.178068
86	C	-5.091378	5.091360	-1.666827
87	H	-5.244375	5.244353	-2.744967
88	C	4.688028	-4.688019	1.099497
89	H	4.544851	-4.544846	2.178068
90	C	5.091378	-5.091360	-1.666827
91	H	5.244375	-5.244353	-2.744967
92	C	5.623247	-5.623237	0.645603
93	H	6.203386	-6.203378	1.376986
94	C	5.827111	-5.827095	-0.739026
95	H	6.565469	-6.565452	-1.081289
96	C	-5.623247	5.623237	0.645603
97	H	-6.203386	6.203378	1.376986
98	C	-5.827111	5.827095	-0.739026
99	H	-6.565469	6.565452	-1.081289

$[Fe(L^4)_2]^{2+}$ (**4**$^{2+}$), high-spin.

1	Fe	0.000000	0.000001	0.000000
2	N	0.000000	0.000001	-2.103203
3	C	1.025379	0.590270	-2.771461
4	C	1.058644	0.592566	-4.181415
5	C	0.000000	0.000002	-4.886673
6	H	-0.000001	0.000003	-5.985747
7	C	-1.058645	-0.592562	-4.181415
8	H	-1.881884	-1.070092	-4.726071
9	C	-1.025379	-0.590268	-2.771461
10	C	2.034240	1.268147	-1.915477

11	N	1.694252	1.433030	-0.619644
12	C	2.506647	2.189515	0.197660
13	C	3.264591	1.750993	-2.448277
14	H	3.527642	1.566906	-3.496715
15	C	-2.034240	-1.268146	-1.915477
16	N	-1.694251	-1.433029	-0.619644
17	C	-2.506646	-2.189515	0.197659
18	C	-3.264590	-1.750993	-2.448278
19	H	-3.527641	-1.566906	-3.496715
20	N	0.000000	0.000001	2.103203
21	C	1.025379	-0.590268	2.771462
22	C	1.058645	-0.592561	4.181415
23	H	1.881884	-1.070091	4.726071
24	C	0.000001	0.000003	4.886673
25	H	0.000002	0.000005	5.985747
26	C	-1.058643	0.592566	4.181415
27	C	-1.025379	0.590271	2.771461
28	C	2.034239	-1.268146	1.915477
29	N	1.694251	-1.433029	0.619644
30	C	2.506645	-2.189515	-0.197659
31	C	3.264590	-1.750994	2.448278
32	H	3.527641	-1.566906	3.496715
33	C	-2.034240	1.268147	1.915477
34	N	-1.694252	1.433030	0.619644
35	C	-2.506647	2.189515	-0.197660
36	C	-3.264591	1.750993	2.448277
37	H	-3.527642	1.566906	3.496715
38	H	1.881883	1.070097	-4.726071
39	H	-1.881882	1.070098	4.726071
40	C	4.140488	-2.435648	1.621943
41	H	5.106250	-2.794222	2.007647
42	C	3.777441	-2.702736	0.272469
43	C	-4.140491	2.435646	1.621943
44	H	-5.106252	2.794218	2.007646
45	C	-3.777444	2.702734	0.272468
46	C	-4.598423	3.466140	-0.609323
47	H	-5.564482	3.842777	-0.242983
48	C	-2.090815	2.516797	-1.521308
49	H	-1.102715	2.184646	-1.856612
50	C	-4.172067	3.749401	-1.900100
51	H	-4.802317	4.349032	-2.571912
52	C	-2.904214	3.283417	-2.347805
53	H	-2.559576	3.544272	-3.359034
54	C	2.090812	-2.516797	-1.521308
55	H	1.102713	-2.184645	-1.856612
56	C	4.598420	-3.466143	-0.609322
57	H	5.564478	-3.842781	-0.242981
58	C	4.172063	-3.749403	-1.900099
59	H	4.802313	-4.349036	-2.571911
60	C	2.904211	-3.283418	-2.347805
61	H	2.559573	-3.544273	-3.359033
62	C	-4.140489	-2.435648	-1.621944
63	H	-5.106250	-2.794221	-2.007647
64	C	3.777444	2.702735	-0.272468
65	C	4.140491	2.435646	-1.621943
66	H	5.106252	2.794219	-2.007646

67	C	-3.777441	-2.702736	-0.272469
68	C	-2.090813	-2.516797	1.521308
69	H	-1.102714	-2.184644	1.856612
70	C	-4.598420	-3.466144	0.609321
71	H	-5.564478	-3.842781	0.242981
72	C	-2.904211	-3.283419	2.347804
73	H	-2.559573	-3.544273	3.359033
74	C	-4.172063	-3.749404	1.900098
75	H	-4.802313	-4.349036	2.571910
76	C	2.090815	2.516797	1.521309
77	H	1.102715	2.184646	1.856613
78	C	4.598423	3.466140	0.609323
79	H	5.564482	3.842777	0.242983
80	C	4.172067	3.749401	1.900100
81	H	4.802317	4.349032	2.571912
82	C	2.904214	3.283417	2.347806
83	H	2.559576	3.544272	3.359034

$[Fe(L^4)_2]^{2+}$ (**4**$^{2+}$), low-spin.

1	Fe	0.000000	0.000000	0.000000
2	N	0.000000	0.000000	-1.896682
3	C	1.029507	0.590158	-2.564948
4	C	1.063422	0.588480	-3.973067
5	C	-0.000001	0.000001	-4.678076
6	H	-0.000001	0.000001	-5.776849
7	C	-1.063423	-0.588480	-3.973067
8	H	-1.893982	-1.059357	-4.513523
9	C	-1.029507	-0.590159	-2.564948
10	C	1.967108	1.267991	-1.660299
11	N	1.535276	1.367925	-0.371330
12	C	2.263900	2.171226	0.496461
13	C	3.200945	1.807168	-2.112755
14	H	3.509431	1.662167	-3.155258
15	C	-1.967108	-1.267991	-1.660299
16	N	-1.535276	-1.367925	-0.371330
17	C	-2.263899	-2.171226	0.496462
18	C	-3.200945	-1.807168	-2.112755
19	H	-3.509431	-1.662168	-3.155258
20	N	0.000000	0.000000	1.896683
21	C	1.029507	-0.590159	2.564948
22	C	1.063422	-0.588480	3.973067
23	H	1.893981	-1.059358	4.513524
24	C	-0.000001	0.000000	4.678076
25	H	-0.000001	0.000000	5.776850
26	C	-1.063423	0.588480	3.973067
27	C	-1.029507	0.590159	2.564948
28	C	1.967108	-1.267991	1.660299
29	N	1.535277	-1.367925	0.371330
30	C	2.263900	-2.171226	-0.496461
31	C	3.200945	-1.807168	2.112755
32	H	3.509431	-1.662168	3.155259
33	C	-1.967108	1.267991	1.660299
34	N	-1.535277	1.367925	0.371329
35	C	-2.263900	2.171226	-0.496462
36	C	-3.200945	1.807168	2.112755

37	H	-3.509432	1.662168	3.155258
38	H	1.893981	1.059358	-4.513524
39	H	-1.893982	1.059358	4.513523
40	C	4.015506	-2.480391	1.220756
41	H	4.994555	-2.870948	1.533777
42	C	3.554436	-2.710286	-0.104807
43	C	-4.015507	2.480391	1.220756
44	H	-4.994555	2.870949	1.533776
45	C	-3.554436	2.710286	-0.104807
46	C	-4.304665	3.494562	-1.030222
47	H	-5.286872	3.878286	-0.718804
48	C	-1.749759	2.546291	-1.771157
49	H	-0.736468	2.245775	-2.041987
50	C	-3.791087	3.798677	-2.282778
51	H	-4.368244	4.415674	-2.985655
52	C	-2.492761	3.342095	-2.636667
53	H	-2.060425	3.636250	-3.603932
54	C	1.749759	-2.546291	-1.771157
55	H	0.736469	-2.245775	-2.041987
56	C	4.304666	-3.494561	-1.030222
57	H	5.286873	-3.878285	-0.718803
58	C	3.791088	-3.798676	-2.282778
59	H	4.368245	-4.415672	-2.985655
60	C	2.492762	-3.342095	-2.636667
61	H	2.060426	-3.636249	-3.603932
62	C	-4.015506	-2.480391	-1.220756
63	H	-4.994555	-2.870949	-1.533777
64	C	3.554436	2.710286	0.104807
65	C	4.015507	2.480391	-1.220756
66	H	4.994555	2.870949	-1.533777
67	C	-3.554435	-2.710286	0.104807
68	C	-1.749759	-2.546291	1.771157
69	H	-0.736468	-2.245775	2.041988
70	C	-4.304665	-3.494562	1.030222
71	H	-5.286872	-3.878286	0.718804
72	C	-2.492762	-3.342095	2.636667
73	H	-2.060425	-3.636250	3.603933
74	C	-3.791087	-3.798677	2.282778
75	H	-4.368244	-4.415673	2.985655
76	C	1.749759	2.546291	1.771157
77	H	0.736468	2.245775	2.041988
78	C	4.304666	3.494562	1.030221
79	H	5.286872	3.878285	0.718803
80	C	3.791088	3.798676	2.282777
81	H	4.368245	4.415673	2.985654
82	C	2.492762	3.342095	2.636667
83	H	2.060426	3.636249	3.603932

$[Fe(bimpy)_2]^{2+}$, high-spin (from ref. 24).

1	Fe	-0.000017	-0.000028	0.003395
2	N	-2.160871	-0.007777	-0.016768
3	C	-2.828845	0.795211	-0.883617
4	C	-4.238828	0.808592	-0.931271
5	C	-4.946712	-0.025677	-0.048494
6	H	-6.045499	-0.033082	-0.061417

7	C	-4.248583	-0.850356	0.851096
8	H	-4.799442	-1.501496	1.543344
9	C	-2.838325	-0.818183	0.836085
10	C	-1.915817	1.599846	-1.698696
11	N	-0.584445	1.486418	-1.547800
12	C	-0.014552	2.388731	-2.435767
13	C	-1.056873	3.063847	-3.147360
14	N	-2.239755	2.531719	-2.650427
15	C	-1.933407	-1.608584	1.673877
16	N	-0.600778	-1.476174	1.553032
17	C	-0.037931	-2.364247	2.459344
18	C	-1.085931	-3.051398	3.150567
19	N	-2.265045	-2.540513	2.622900
20	N	2.160861	0.007486	-0.016664
21	C	2.828792	-0.795656	-0.883394
22	C	4.238779	-0.809302	-0.930863
23	H	4.782014	-1.453740	-1.635257
24	C	4.946700	0.024872	-0.048025
25	H	6.045490	0.032065	-0.060798
26	C	4.248609	0.849728	0.851431
27	C	2.838344	0.817820	0.836230
28	C	1.915722	-1.600151	-1.698572
29	N	0.584351	-1.486524	-1.547831
30	C	0.014431	-2.388723	-2.435898
31	C	1.056736	-3.063971	-3.147390
32	N	2.239636	-2.532041	-2.650295
33	C	1.933463	1.608453	1.673845
34	N	0.600825	1.476248	1.552885
35	C	0.038035	2.364545	2.459009
36	C	1.086079	3.051623	3.150240
37	N	2.265161	2.540464	2.622769
38	H	-4.782087	1.452897	-1.635767
39	H	4.799499	1.500794	1.543722
40	H	-1.644162	-4.544653	4.663182
41	C	-0.833838	-4.020521	4.138311
42	C	1.311870	-2.650335	2.762653
43	H	2.129112	-2.133320	2.243089
44	H	0.759035	-5.037614	5.184064
45	C	0.511166	-4.287330	4.420083
46	C	1.565628	-3.613551	3.744098
47	H	2.604517	-3.860840	4.004189
48	H	2.151028	2.194574	-2.169151
49	C	1.337134	2.699323	-2.705596
50	C	-0.797689	4.042961	-4.123334
51	H	-1.604105	4.557234	-4.663747
52	C	0.548909	4.332966	-4.372457
53	H	0.802272	5.091746	-5.126178
54	H	2.638482	3.938459	-3.909140
55	C	1.597956	3.672399	-3.675460
56	H	-3.179796	2.799629	-2.942713
57	H	-3.207491	-2.819875	2.896109
58	H	3.179671	-2.800067	-2.942493
59	H	3.207625	2.819728	2.896017
60	C	0.797526	-4.043005	-4.123438
61	H	1.603932	-4.557378	-4.663771
62	C	-1.337269	-2.699094	-2.705917

63	H	-2.151158	-2.194230	-2.169571
64	H	-0.802469	-5.091503	-5.126528
65	C	-0.549084	-4.332793	-4.372743
66	H	-2.638655	-3.937974	-3.909683
67	C	-1.598118	-3.672090	-3.675853
68	C	0.834045	4.020935	4.137815
69	H	1.644402	4.545008	4.662694
70	C	-1.311750	2.650911	2.762128
71	H	-2.129024	2.133972	2.242538
72	H	-2.604323	3.861822	4.003343
73	C	-1.565449	3.614312	3.743405
74	H	-0.758768	5.038448	5.183250
75	C	-0.510944	4.288009	4.419406

$[Fe(bimpy)_2]^{2+}$, low-spin (from ref. 24).

1	Fe	0.000000	0.000001	0.000000
2	N	0.000000	0.000000	1.919619
3	C	-0.839132	-0.839132	2.600432
4	C	-0.861769	-0.861769	4.009171
5	C	0.000000	0.000000	4.712597
6	H	0.000000	0.000000	5.811214
7	C	0.861769	0.861769	4.009172
8	H	1.537500	1.537500	4.550689
9	C	0.839132	0.839132	2.600432
10	C	-1.614522	-1.614521	1.649932
11	N	-1.397274	-1.397273	0.333428
12	C	-2.252771	-2.252771	-0.354499
13	C	-3.005668	-3.005668	0.604121
14	N	-2.571465	-2.571464	1.849926
15	C	1.614521	1.614522	1.649932
16	N	1.397273	1.397274	0.333428
17	C	2.252771	2.252771	-0.354499
18	C	3.005667	3.005668	0.604121
19	N	2.571464	2.571465	1.849926
20	N	0.000000	0.000000	-1.919619
21	C	0.839132	-0.839132	-2.600432
22	C	0.861769	-0.861769	-4.009172
23	H	1.537499	-1.537500	-4.550690
24	C	-0.000001	0.000000	-4.712597
25	H	-0.000001	-0.000001	-5.811214
26	C	-0.861770	0.861769	-4.009172
27	C	-0.839132	0.839132	-2.600432
28	C	1.614521	-1.614521	-1.649932
29	N	1.397274	-1.397274	-0.333428
30	C	2.252771	-2.252771	0.354499
31	C	3.005668	-3.005667	-0.604121
32	N	2.571465	-2.571465	-1.849926
33	C	-1.614521	1.614521	-1.649932
34	N	-1.397273	1.397273	-0.333428
35	C	-2.252770	2.252771	0.354499
36	C	-3.005667	3.005667	-0.604121
37	N	-2.571465	2.571464	-1.849926
38	H	-1.537500	-1.537500	4.550689
39	H	-1.537500	1.537499	-4.550689
40	H	4.534906	4.534906	0.976778

41	C	3.964481	3.964481	0.231052
42	C	2.466689	2.466689	-1.735092
43	H	1.906062	1.906062	-2.491861
44	H	4.896745	4.896745	-1.480816
45	C	4.157605	4.157605	-1.141329
46	C	3.420091	3.420090	-2.106837
47	H	3.607186	3.607185	-3.173622
48	H	-1.906062	-1.906062	-2.491861
49	C	-2.466689	-2.466689	-1.735093
50	C	-3.964481	-3.964481	0.231052
51	H	-4.534907	-4.534906	0.976777
52	C	-4.157605	-4.157605	-1.141329
53	H	-4.896745	-4.896745	-1.480817
54	H	-3.607186	-3.607186	-3.173622
55	C	-3.420090	-3.420090	-2.106838
56	H	-2.908887	-2.908887	2.751506
57	H	2.908886	2.908887	2.751507
58	H	2.908887	-2.908887	-2.751506
59	H	-2.908887	2.908886	-2.751506
60	C	3.964481	-3.964481	-0.231052
61	H	4.534906	-4.534906	-0.976777
62	C	2.466689	-2.466688	1.735092
63	H	1.906062	-1.906061	2.491861
64	H	4.896745	-4.896745	1.480816
65	C	4.157605	-4.157605	1.141329
66	H	3.607186	-3.607185	3.173622
67	C	3.420091	-3.420090	2.106838
68	C	-3.964481	3.964480	-0.231052
69	H	-4.534906	4.534906	-0.976777
70	C	-2.466688	2.466689	1.735092
71	H	-1.906061	1.906062	2.491861
72	H	-3.607185	3.607186	3.173622
73	C	-3.420090	3.420090	2.106838
74	H	-4.896745	4.896745	1.480816
75	C	-4.157604	4.157605	1.141329

$[Fe(2\text{-bip})_2]^{2+}$, high-spin.

1	Fe	-0.007329	0.002544	0.022586
2	N	0.029983	2.157219	-0.211137
3	C	1.098459	2.759233	-0.770083
4	C	1.177714	4.152391	-0.938189
5	C	0.084012	4.917463	-0.496498
6	H	0.105532	6.010435	-0.608708
7	C	-1.037685	4.301201	0.085302
8	H	-1.890264	4.899516	0.427208
9	C	-1.013911	2.901029	0.204686
10	N	2.106529	1.850380	-1.166360
11	N	1.884972	0.512386	-0.957547
12	C	2.995739	-0.108846	-1.440601
13	C	3.937811	0.863929	-1.959182
14	C	3.315766	2.104597	-1.761267
15	H	3.643619	3.120164	-1.999726
16	N	-2.060535	2.131571	0.764044
17	N	-1.892790	0.771487	0.839027
18	C	-3.040281	0.305244	1.403784

19	C	-3.950268	1.398704	1.684064
20	C	-3.270825	2.547851	1.256562
21	H	-3.561796	3.601860	1.268745
22	N	-0.066202	-2.145708	0.270501
23	C	-0.549537	-2.931264	-0.712694
24	C	-0.639867	-4.328043	-0.586859
25	H	-1.034302	-4.960386	-1.390871
26	C	-0.204228	-4.895827	0.622956
27	H	-0.260218	-5.984400	0.762772
28	C	0.302059	-4.088267	1.656036
29	C	0.352401	-2.703037	1.424593
30	N	-0.944486	-2.208574	-1.861557
31	N	-0.802596	-0.843392	-1.844817
32	C	-1.248131	-0.427678	-3.061996
33	C	-1.684436	-1.559090	-3.857375
34	C	-1.465407	-2.676653	-3.040693
35	H	-1.639512	-3.741683	-3.217296
36	N	0.836268	-1.757658	2.358236
37	N	0.796873	-0.430135	2.011109
38	C	1.331268	0.229424	3.075250
39	C	1.717058	-0.707602	4.112305
40	C	1.374699	-1.967488	3.601678
41	H	1.480278	-2.968784	4.028487
42	H	2.050852	4.634425	-1.393569
43	H	0.640453	-4.533293	2.599191
44	C	3.292493	-1.498258	-1.489619
45	H	2.584555	-2.242803	-1.104339
46	C	4.509051	-1.873014	-2.047641
47	H	4.768776	-2.940127	-2.103356
48	C	5.446509	-0.914127	-2.557924
49	H	6.392790	-1.274489	-2.984911
50	C	5.181216	0.446149	-2.521785
51	H	5.899704	1.180403	-2.911003
52	C	-3.401751	-1.032480	1.720565
53	H	-2.720471	-1.867097	1.512796
54	C	-4.648472	-1.238951	2.299860
55	H	-4.958615	-2.262023	2.557531
56	C	-5.553403	-0.160376	2.575936
57	H	-6.525683	-0.389109	3.034203
58	C	-5.224688	1.152887	2.277568
59	H	-5.917686	1.978603	2.489310
60	C	1.532663	1.625329	3.253472
61	H	1.245776	2.343425	2.474801
62	C	2.108797	2.041003	4.448282
63	H	2.279193	3.114080	4.618056
64	C	2.494126	1.117370	5.476497
65	H	2.945919	1.509546	6.398272
66	C	2.307663	-0.248298	5.327549
67	H	2.603675	-0.956103	6.113803
68	C	-1.318642	0.892099	-3.586438
69	H	-0.989281	1.755433	-2.994315
70	C	-1.819718	1.042671	-4.874289
71	H	-1.887578	2.049869	-5.310524
72	C	-2.255277	-0.073807	-5.663493
73	H	-2.642315	0.111785	-6.675129
74	C	-2.196247	-1.370145	-5.175965

75	H	-2.530819	-2.224693	-5.779866

$[Fe(2\text{-bip})_2]^{2+}$, low-spin.

1	Fe	-0.002291	0.001703	0.000649
2	N	0.037213	1.890346	-0.210819
3	C	1.123407	2.486633	-0.761942
4	C	1.196599	3.876177	-0.940949
5	C	0.090421	4.643139	-0.527939
6	H	0.111233	5.734435	-0.653815
7	C	-1.043085	4.032411	0.041764
8	H	-1.906183	4.629300	0.360117
9	C	-1.024150	2.636587	0.183033
10	N	2.102796	1.542598	-1.103126
11	N	1.799683	0.219777	-0.834741
12	C	2.889401	-0.485363	-1.249586
13	C	3.893050	0.418046	-1.785976
14	C	3.340774	1.700024	-1.669172
15	H	3.730134	2.685169	-1.941535
16	N	-2.038686	1.832195	0.720727
17	N	-1.789382	0.471210	0.758828
18	C	-2.904034	-0.077704	1.319062
19	C	-3.867935	0.963113	1.632955
20	C	-3.266366	2.162307	1.231685
21	H	-3.615488	3.197970	1.274136
22	N	-0.045561	-1.884701	0.215085
23	C	-0.548635	-2.666035	-0.772561
24	C	-0.608314	-4.063031	-0.657009
25	H	-1.017701	-4.688539	-1.459374
26	C	-0.121073	-4.637954	0.532020
27	H	-0.151618	-5.729082	0.657542
28	C	0.404716	-3.835868	1.562278
29	C	0.421812	-2.448066	1.357097
30	N	-0.973157	-1.894889	-1.863256
31	N	-0.813432	-0.524414	-1.748195
32	C	-1.284027	-0.013761	-2.921406
33	C	-1.746970	-1.089032	-3.782158
34	C	-1.526878	-2.267552	-3.059414
35	H	-1.719368	-3.315618	-3.305952
36	N	0.895679	-1.474149	2.246865
37	N	0.799974	-0.159336	1.825548
38	C	1.308350	0.580054	2.851277
39	C	1.732720	-0.293635	3.932110
40	C	1.445943	-1.593202	3.495766
41	H	1.590142	-2.566371	3.973690
42	H	2.079071	4.351013	-1.386532
43	H	0.784724	-4.283445	2.488608
44	C	3.131018	-1.887428	-1.219035
45	H	2.387583	-2.588792	-0.823459
46	C	4.347396	-2.342335	-1.712957
47	H	4.559992	-3.421112	-1.701498
48	C	5.341798	-1.453692	-2.241370
49	H	6.284500	-1.875052	-2.617292
50	C	5.132322	-0.085160	-2.285504
51	H	5.891004	0.598193	-2.691022
52	C	-3.203685	-1.438832	1.606774

53	H	-2.494565	-2.242453	1.378925
54	C	-4.433718	-1.718809	2.189392
55	H	-4.690076	-2.762417	2.422466
56	C	-5.388139	-0.693931	2.499553
57	H	-6.344234	-0.980435	2.959198
58	C	-5.123439	0.638661	2.230361
59	H	-5.850962	1.427206	2.466791
60	C	1.456707	1.990295	2.972175
61	H	1.143092	2.669842	2.171770
62	C	2.014891	2.481455	4.145966
63	H	2.140230	3.567345	4.265507
64	C	2.436982	1.621838	5.214127
65	H	2.872016	2.071537	6.117474
66	C	2.303902	0.246073	5.123852
67	H	2.624904	-0.415746	5.939899
68	C	-1.366065	1.337434	-3.361108
69	H	-1.025162	2.166489	-2.730934
70	C	-1.897715	1.573426	-4.623122
71	H	-1.972836	2.608421	-4.986907
72	C	-2.354571	0.513942	-5.475503
73	H	-2.763929	0.766186	-6.463545
74	C	-2.287371	-0.809760	-5.073536
75	H	-2.635376	-1.624851	-5.722824

References

1. K. Li, J.-L. Niu, M.-Z. Yang, Z. Li, L.-Y. Wu, X.-Q. Hao and M.-P. Song, *Organometallics*, 2015, **34**, 1170−1176.
2. E. Largy, F. Hamon, F. Rosu, V. Gabelica, E. De Pauw, A. Guédin, J.-L. Mergny and M.-P. Teulade-Fichou, *Chem. − Eur. J.*, 2011, **17**, 13274–13283.
3. G. M. Sheldrick, *Acta Cryst. Sect. A: Found. Adv.*, 2015, **71**, 3–8.
4. G. M. Sheldrick, *Acta Cryst. Sect. C.: Struct. Chem.*, 2015, **71**, 3–8.
5. L. J. Barbour, *J. Appl. Crystallogr.*, 2020, **53**, 1141–1146.
6. O. V. Dolomanov, L. J. Bourhis, R. J. Gildea, J. A. K. Howard and H. Puschmann, *J. Appl. Crystallogr.*, 2009, **42**, 339–341.
7. A. L. Spek, Acta Cryst. Sect. C.: Struct. Chem., 2015, **71**, 9–18.
8. P. Guionneau, M. Marchivie, G. Bravic, J.-F. Létard and D. Chasseau, *Top. Curr. Chem.*, 2004, **234**, 97–128.
9. I. Capel Berdiell, R. Kulmaczewski and M. A. Halcrow, *Inorg. Chem.*, 2017, **56**, 8817 − 8828.
10. J. K. McCusker, A. L. Rheingold and D. N. Hendrickson, *Inorg. Chem.*, 1996, **35**, 2100–2112.
11. J. M. Holland, J. A. McAllister, C. A. Kilner, M. Thornton-Pett, A. J. Bridgeman and M. A. Halcrow, *J. Chem. Soc. Dalton Trans.*, 2002, 548–554.
12. a) L. J. Kershaw Cook, F. L. Thorp-Greenwood, T .P. Comyn, O. Cespedes, G. Chastanet and M. A. Halcrow, *Inorg. Chem.*, 2015, **54**, 6319−6330;
    b) I. Capel Berdiell, R. Kulmaczewski, N. Shahid, O. Cespedes and M.A. Halcrow, *Chem. Commun.*, 2021, **57**, 6566–6569;
    c) N. Suryadevara, A. Mizuno L. Spieker S. Salamon, S. Sleziona, A. Maas, E. Pollmann, B. Heinrich, M. Schleberger, H. Wende, S. K. Kuppusamy and M. Ruben, *Chem. – Eur. J.*, 2022, **28**, e202103853;
    d) R. Kulmaczewski, L. J. Kershaw Cook, C. M. Pask, O. Cespedes and M. A. Halcrow, *Cryst. Growth Des.*, 2022, **22**, 1960–1971.
13. S. Vela, J. J. Novoa and J. Ribas-Arino, *Phys. Chem. Chem. Phys.*, 2014, **16**, 27012–27024.
14. M. A. Halcrow, *Coord. Chem. Rev.*, 2009, **253**, 2493–2514.
15. L. J. Kershaw Cook, R. Mohammed, G. Sherborne, T.D. Roberts, S. Alvarez and M. A. Halcrow, *Coord. Chem. Rev.*, 2015, **289–290**, 2–12.
16. G. A. Craig, O. Roubeau and G. Aromí, *Coord. Chem. Rev.*, 2014, **269**, 13–31.
17. P. J. van Koningsbruggen, J. G. Haasnoot, R. A. G. de Graaff and J. Reedijk, *J. Chem. Soc. Dalton Trans.*, 1993, 483–484.
18. A. J. Gordon and R. A. Ford, The Chemists Companion – A Handbook of Practical Data, Techniques and References, John Wiley, Chichester, 1972, p. 109.
19. R. Pritchard, C. A. Kilner and M. A. Halcrow, *Chem. Commun.*, 2007, 577–579.
20. A. Santoro, L. J. Kershaw Cook, R. Kulmaczewski, S. A. Barrett, O. Cespedes and M. A. Halcrow, *Inorg. Chem.*, 2015, **54**, 682–693.
21. C. R. Martinez and B. L. Iverson, *Chem. Sci.*, 2012, **3**, 2191–2201.
22. C. M. Harris, H. R. H. Patil and E. Sinn, *Inorg. Chem.*, 1969, **8**, 101−104.
23. a) D. M. Klassen, C. W. Hudson and E. L. Shaddix, *Inorg. Chem.* 1975, **14**, 2733–2736;
    b) M. L. Stone and G. A. Crosby, *Chem. Phys. Lett.*, 1981, **79**, 169–173;
    c) S. Aroua, T. K. Todorova, P. Hommes, L.-M. Chamoreau, H.-U. Reissig, V. Mougel and M. Fontecave, *Inorg. Chem.*, 2017, **56**, 5930–5940.
24. N. Shahid, K. E. Burrows, C. M. Pask, O. Cespedes, M. J. Howard, P. C. McGowan and M. A. Halcrow, *Dalton Trans.*, 2022, **51**, 4262–4274.

25. R. Boča, P. Baran, L. Dlháň, H. Fuess, W. Haase, F. Renz, W. Linert, I. Svoboda and R. Werner, *Inorg. Chim. Acta*, 1997, **260**, 129−136.

26. a) J. Catalan, J. L. M. Abboud and J. Elguero, *Adv. Heterocycl. Chem.*, 1987, **41**, 187−274;
b) A. C. Humphries, E. Gancia, M. T. Gilligan, S. Goodacre, D. Hallett, K. J. Merchant and S. R. Thomas, *Bioorg. Med. Chem. Lett.*, 2006, **16**, 1518−1522.